

University of Groningen

Molecular motors with new topologies

Caroli, Giuseppe

IMPORTANT NOTE: You are advised to consult the publisher's version (publisher's PDF) if you wish to cite from it. Please check the document version below.

Document Version

Publisher's PDF, also known as Version of record

Publication date:

2010

[Link to publication in University of Groningen/UMCG research database](#)

Citation for published version (APA):

Caroli, G. (2010). *Molecular motors with new topologies*. s.n.

Copyright

Other than for strictly personal use, it is not permitted to download or to forward/distribute the text or part of it without the consent of the author(s) and/or copyright holder(s), unless the work is under an open content license (like Creative Commons).

The publication may also be distributed here under the terms of Article 25fa of the Dutch Copyright Act, indicated by the "Taverne" license. More information can be found on the University of Groningen website: <https://www.rug.nl/library/open-access/self-archiving-pure/taverne-amendment>.

Take-down policy

If you believe that this document breaches copyright please contact us providing details, and we will remove access to the work immediately and investigate your claim.

Downloaded from the University of Groningen/UMCG research database (Pure): <http://www.rug.nl/research/portal>. For technical reasons the number of authors shown on this cover page is limited to 10 maximum.

CHAPTER 6

MOLECULAR MOTORS WITH AROMATIC GROUPS AT THE STEREOGENIC CENTERS

In this chapter, four new first generation five-five membered rings molecular motors are presented, where aromatic groups have been installed at the stereogenic centers. Synthesis, modeling and ¹H-NMR and UV/Vis spectroscopic studies are discussed.

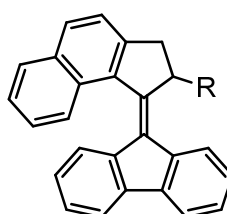
This work not only extends the knowledge on the possible functionalizations of molecular motors, but also offers the possibility for a better understanding of the relationship between their structure and rate of thermal isomerizations.

Moreover, due to their aromatic groups at the stereogenic centers, these newly prepared molecular motors can be considered good candidates to be studied as chiral dopants in liquid crystals.

Parts of this chapter will be submitted for publication: G. Caroli, B. L. Feringa, manuscript in preparation.

6.1 Introduction

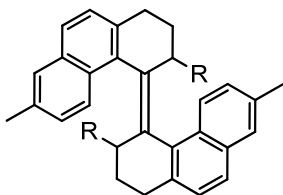
Molecular motors are potential tools fundamental tool in molecular nanotechnology, in particular for future construction of mechanical molecular devices. It is therefore important to develop molecular motors that can perform their unidirectional rotation at different speeds, in order to have a wider range of applicability. Moreover, it is important to explore the possibilities arising from derivatization of the basic structure of molecular motors, and study, for example, how substitution of the methyl group at the stereogenic center affects the performance of the motor. In a recent investigation,¹ this has been done with second generation molecular motors. It has been shown that by changing the substituent at the stereogenic center, the half life of the unstable form changes significantly (Table 1).



R	$t_{1/2}^{20^\circ\text{C}}$ (s)
Ph	587
Me	190
<i>i</i> -Pr	95
<i>t</i> -Bu	0.0057

Table 1: Half lives at 20°C of second generation molecular motors derivatized with different groups at the stereogenic center (ref. 1).

Similar studies have been carried out for analogous first generation molecular motors. In Table 2 the half lives of first generation molecular motors with two 6-membered rings connected to the axle of the rotor are reported.² It can be seen that changing the methyl substituent for an ethyl moiety, the half lives of the two thermal steps of the rotary cycle are both decreased, although the order of magnitude remains the same. With an isopropyl, instead, much larger differences are observed: the unstable *cis* seems to convert to the stable *cis* too quickly to be observed even at -60°C, while the thermal step from unstable to stable *trans* was found to be so slow that the two-step nature of the process could be observed experimentally for the first time.

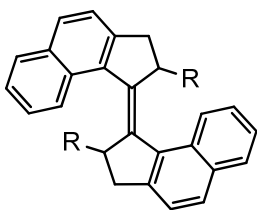


R	$t_{1/2}^{20^\circ\text{C}}$ (unstable to stable <i>trans</i>)	$t_{1/2}^{20^\circ\text{C}}$ (unstable to stable <i>cis</i>)
Me	439 h	32 min
Et	317 h	18 min
<i>i</i> -Pr	very slow	presumably too fast

Table 2: Half lives of first generation six-six membered rings molecular motors derivatized with different groups at the stereogenic center (ref. 2).

In the case of five-five membered ring first generation molecular motors, changing the methyl with a longer alkyl chain decreases slightly the half life of the two thermal steps of the rotary cycle^{3, 4} (Table 3). With a *tert*-butyl group, instead, a distinctly different mechanism was reported.⁵

These results are consistent with those reported for the six-six membered ring motors: a methyl group slows down the thermal isomerization steps compared with those of motors with longer linear alkyl groups, while with more bulky substituents, more significant deviations from the usual rotary behavior are observed.



R	$t_{1/2}^{20^\circ\text{C}}$ (unstable to stable <i>trans</i>)	$t_{1/2}^{20^\circ\text{C}}$ (unstable to stable <i>cis</i>)
Me	18 s	74 min
C ₁₆ H ₃₃	16 s	37 min
<i>t</i> -Bu	/	/

Table 3: Half lives of first generation five-five membered rings molecular motors derivatized with different groups at the stereogenic center (see ref. 3, 4 and 5).

Additionally, in our group, molecular motors have been studied as dopants in liquid crystal (LC) matrices. In liquid crystals, chiral switchable molecules can be used as dopants: the two helical configurations of a switch affect the LC phase differently, resulting in an externally addressable LC phase.⁶ It has been demonstrated that the unidirectional light driven molecular motors can be used as chiral dopants, and that under irradiation of the sample the LC phase can be changed.⁷

To date, several second generation molecular motors have been tested in liquid crystals matrixes,⁸ but similar studies have not been reported for first generation examples. It is important to consider for LC technology also the use of first generation molecular motors. In Chapter 5 an example is reported of a molecular motor that has been functionalized with two mesogenic moieties, to be tested as a chiral switchable dopant for liquid crystals, albeit enantioresolution could not be achieved with the chiral HPLC columns available. The

incorporation of aromatic moieties in the design of molecular motors can indeed be expected to provide insight into the mechanism of interaction between the dopant molecular motor and the mesogens.

In this chapter, the synthesis, photochemical and thermal behavior of a new family of first generation molecular motors is presented. These motors are derivatized with an aromatic group connected to the stereogenic center, comprising one or two benzene rings, connected to the five membered ring directly or using a methylene linker (Chart 1).

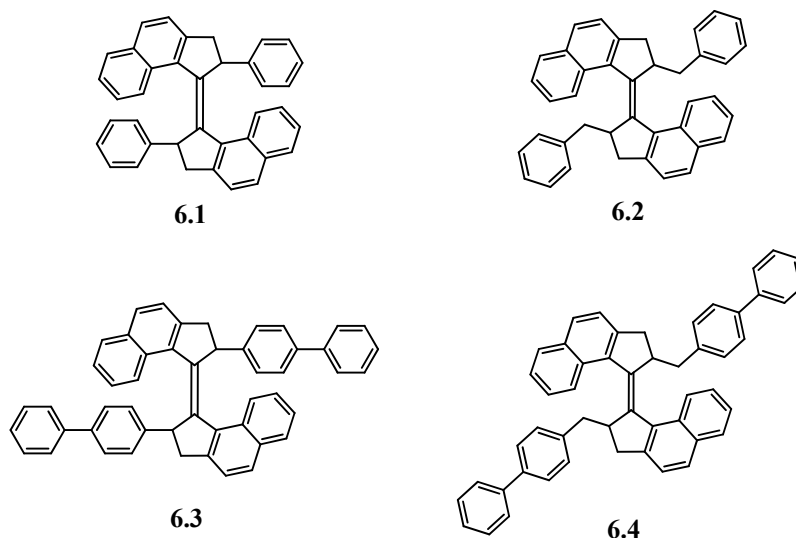


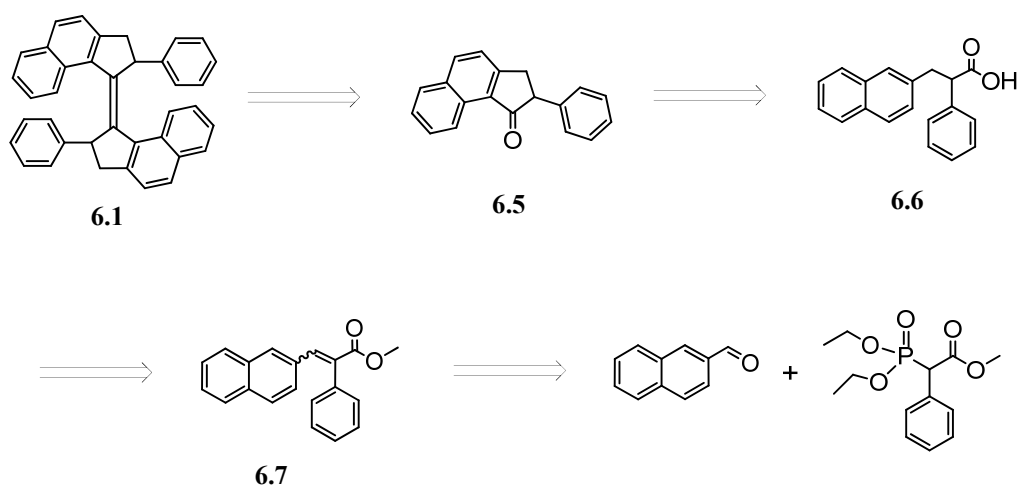
Chart 1: Molecular motors presented in this chapter.

Motors **6.1** and **6.3** present, respectively, a benzyl and a biphenyl group directly attached to the stereogenic center of the 5 membered rings. Motors **6.2** and **6.4**, instead, have attached to the stereogenic center a benzyl and a *p*-phenylbenzyl group, respectively. These motors not only add to the molecular motors toolbox broadening the spectrum of features and topologies available to be used in future applications, but are also good candidates as dopants for LC studies. Indeed, their new aromatic moiety might give a stronger interaction with the mesogens (molecules of liquid crystals), and lead to doped LC with new interesting properties.

6.2 Aryl motor

6.2.1 Retrosynthetic analysis

The retrosynthesis of motor **6.1** is shown in Scheme 1. Motor **6.1** can be obtained by McMurry coupling of ketone **6.5**, which can be obtained by ring closure of acid **6.6**. The ester of acid **6.6** is prepared in a racemic fashion from alkene **6.7**, which can be obtained with a Horner–Wadsworth–Emmons reaction of 2-naphthaldehyde and (diethoxyphosphoryl)-phenyl-acetic acid methyl ester.

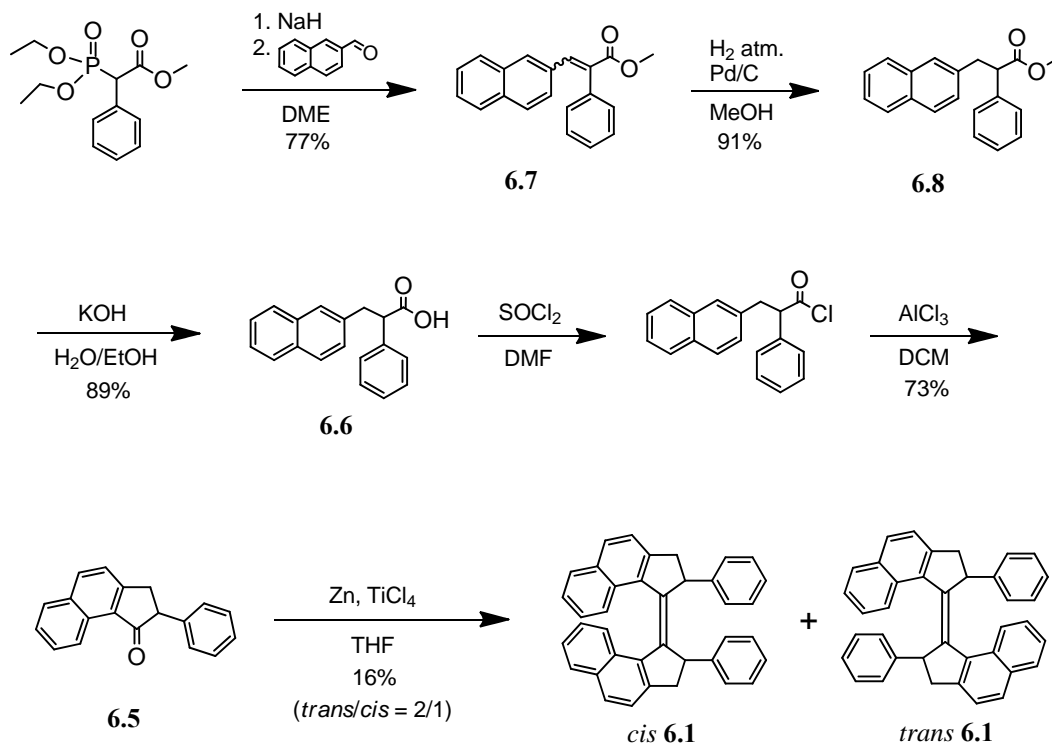


Scheme 1: Retrosynthesis of motor **6.1**.

6.2.2 Synthesis

The synthesis of motor **6.1** is shown in Scheme 2⁹. The first step of the synthesis was a Horner–Wadsworth–Emmons reaction of (diethoxyphosphoryl)-phenyl-acetic acid methyl ester with 2-naphthaldehyde to obtain the alkene **6.7** in a 1:3 *Z/E* ratio. The product was then hydrogenated with palladium to compound **6.8** in high yields, and the ester group was hydrolyzed to provide acid **6.6**. Subsequently, the acid was activated with thionyl chloride, and the obtained acyl chloride was immediately reacted with aluminium trichloride to perform an intramolecular Friedel–Crafts acylation. The ketone **6.5** obtained was then allowed to react with a low valence titanium reagent in a McMurry coupling. Motor **6.1** was obtained as a mixture of *trans* and *cis* isomers in a 2:1 ratio, in a total yield of 16%.

Isomers separation was achieved with flash column chromatography. The two isomers were distinguished on the basis of their $^1\text{H-NMR}$ spectra in the aromatic region, as in the *cis* isomer, due to the interaction between the two naphthalene moieties, the shifts are upfield compared with the *trans* isomer (ranging 7.8-6.4 and 7.9-6.8 ppm for the *cis* and the *trans* isomer, respectively).



Scheme 2: Synthesis of motor **6.1**.

6.2.3 Molecular modeling

To obtain a better insight into the molecular structure of motor **6.1**, computer modeling was performed on all the four isomers involved in the rotary cycle.

The structures were calculated at the DFT B3-LYP 6-31G(d,p) level of theory, with the Gaussian 03W software package.¹⁰ The optimized structures are shown in Figure 1. It should be noted that in the two *cis* isomers the phenyl groups are predicted to be parallel to each other, and perpendicular to the naphthalene moieties. In the unstable *trans* isomer, instead, they are parallel to the naphthalene moieties to minimize the steric hindrance.

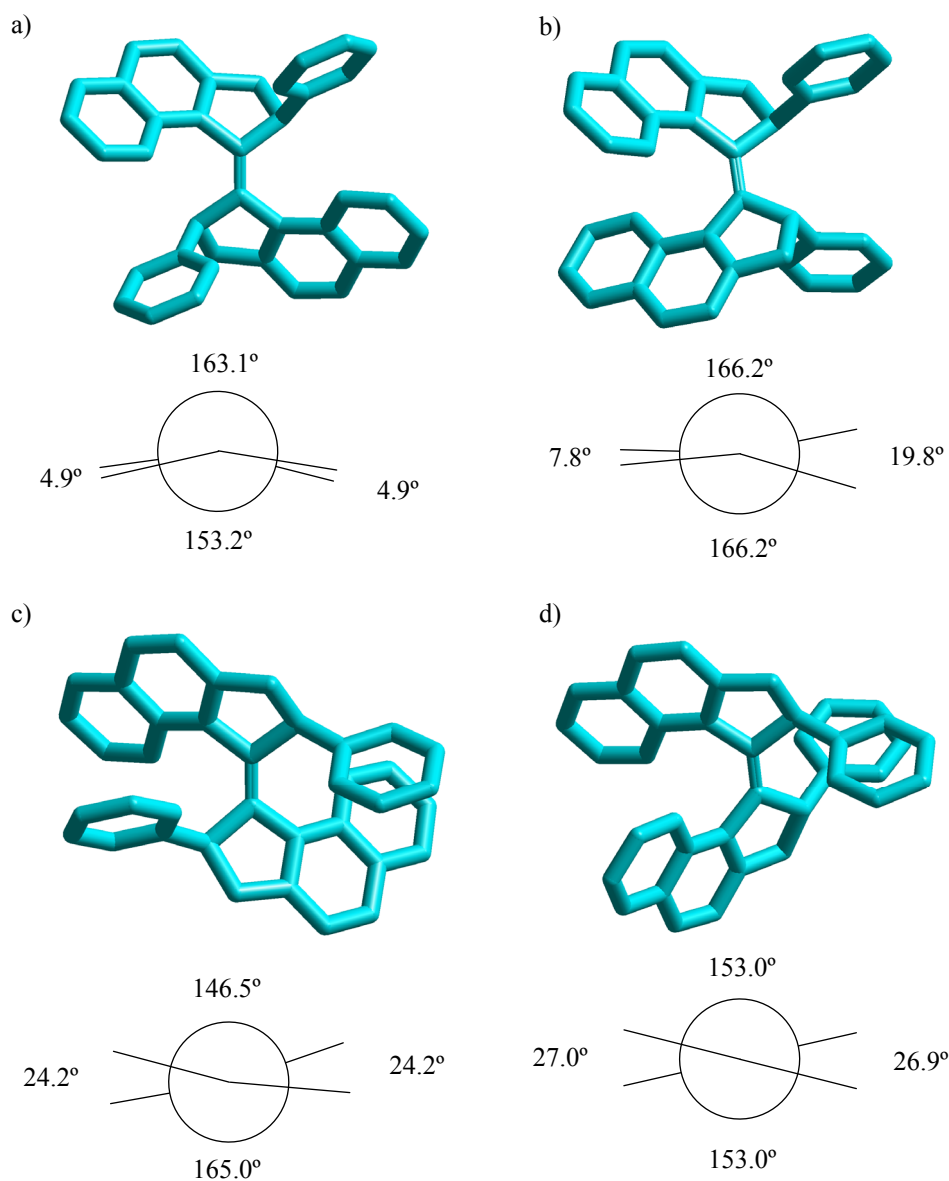
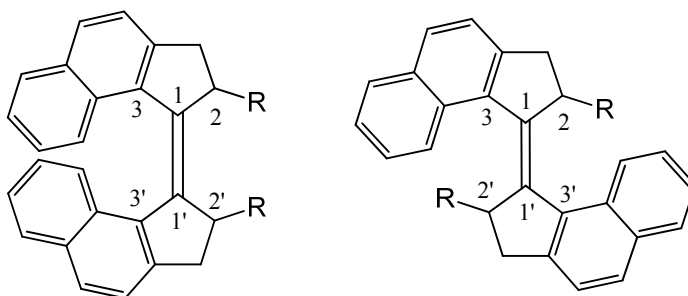


Figure 1: Structures and Newman projections of **6.1** calculated at the DFT B3LYP 6-31G(d,p) level of theory. a) stable *trans*; b) stable *cis*; c) unstable *trans*; d) unstable *cis*.

In Table 4 the most important geometrical features of motor **6.1** and the 5-5 membered ring methyl motor (see Chapter 2) are summarized for comparison. Specifically, the double bond length, and the four dihedral torsion angles formed by the two olefinic carbons and the four carbons connected to them are reported; an average of the deviation from ideality (0° or 180°) of these four dihedral angles is also indicated.



stable <i>trans</i>	R=-C₆H₅ (6.1)	R=Me
211'2'	153.2	152.8
311'3'	163.1	159.9
211'3'	4.9	3.5
311'2'	4.9	3.5
average	13.4	13.6
1-1'	1.36	1.36

stable <i>cis</i>	R=-C₆H₅ (6.1)	R=Me
211'2'	19.8	17.2
311'3'	7.8	4.2
211'3'	166.2	169.3
311'2'	166.2	169.3
average	13.8	10.7
1-1'	1.36	1.36

unstable <i>trans</i>	R=-C₆H₅ (6.1)	R=Me
211'2'	146.5	142.2
311'3'	165.0	162.5
211'3'	24.2	27.7
311'2'	24.2	27.7
average	24.2	27.7
1-1'	1.37	1.37

unstable <i>cis</i>	R=-C₆H₅ (6.1)	R=Me
211'2'	26.9	31.4
311'3'	27.0	25.3
211'3'	153.0	151.7
311'2'	153.0	151.7
average	27.0	28.3
1-1'	1.37	1.37

Table 4: Geometrical parameters calculated for the four isomers of motor **6.1** and for the five-five membered ring methyl analogous. (dihedral angles in degrees and lengths in Angstroms).

The length of the central double bond is invariant between the two molecules over each set of the four isomers. Moreover, the average torsion around the double bond is lower in motor **6.1** in three of four cases (stable *trans*, unstable *trans* and unstable *cis*). This could be rationalized considering that the phenyl group, albeit larger, is flatter than a methyl; therefore it offers less steric hindrance in the direction perpendicular to the aromatic ring.¹¹

Additionally, DFT thermochemical analysis at 25°C was performed to calculate the energies of all the four stable isomers of motor **6.1**. Their relative values after zero point energy correction are shown in Figure 2.

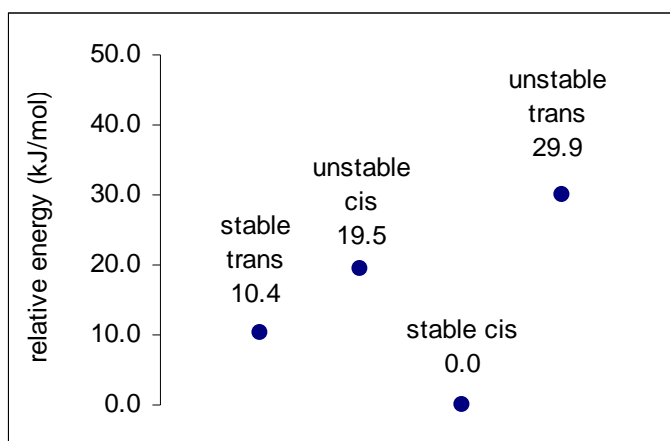


Figure 2: Relative energies (kJ/mol) of the four isomers of motor **6.1**, calculated by DFT thermochemical analysis at 25°C.

However, calculations of transition states were not performed. Therefore, no conclusions on the expected half life-times of the two unstable forms can be drawn.

6.2.4 ¹H-NMR measurements

¹H-NMR spectroscopy is a powerful tool for the study of molecular motors, in that each of the four isomers is characterized by different chemical shifts. The rotary cycle can therefore easily be followed with this method, in order to verify that it occurs in the expected unidirectional fashion.

Stable cis

In Figure 3a the region between 9 and 2.5 ppm of the ¹H-NMR spectrum of a sample of motor *cis* **6.1** in DCM-*d*₂ at -50°C is shown. All the absorptions in the aromatic region can be assigned by comparison with the data reported in chapter 2 for the five-five membered

ring motor. In order to assign the absorptions in the region between 5 and 2.5 ppm, it has to be considered that, as supported by molecular modeling (*vide supra*), the H_rCCH_p dihedral is almost 90° (calculated 94.08°), and only a little or neglectable coupling constant is expected between H_r and H_p . Therefore, the absorption at 3.9 ppm is assigned as H_q .¹² The absorption at 3 ppm and the absorption at 4.5 ppm present very different coupling constants: 15.4 and 6.86 Hz, respectively. As the coupling constant for geminal protons is typically larger than the one for vicinal protons, it can be deduced that the absorption at 2.9 ppm is related to H_r and the absorption at 4.5 is related to H_p . This assignment has been verified by a quantum mechanical 1H -NMR calculations^{13, 14, 15}; the results are shown in Table 5.

Unstable trans

The sample was irradiated with a 365 nm lamp for 4 h, while kept at $-75^\circ C$ in an ethanol bath, and its color changed from pale yellow to more intense yellow. The 1H -NMR spectrum was then measured at $-50^\circ C$ (Figure 3b). Every absorption shifted, and the new isomer, obtained in a 90/10 isomeric ratio with the stable *cis*, can be identified as the unstable *trans* by considering that the aromatic protons of the naphthalene moieties absorb in the range of 7.1-8.0 ppm. Interestingly, all five protons (for each half of the molecule) of the phenyl group absorb at a different chemical shift (four in the region 6.4-6.7 ppm and one at 7.25 ppm), indicating that the phenyl is not rotating freely anymore. This is in agreement with that observed in molecular modeling: due to the torsion of the central double bond, the phenyl groups are pushed against the naphthalene moieties, which cause steric hindrance and limit the rotation around the single bond connecting the phenyl groups to the stereogenic centers. Therefore, the photochemical switch between stable *cis* **6.1** and unstable *trans* **6.1** can be seen as a rotation-on-rotation-off switching system¹⁶ (Scheme 4).¹⁷

Support for this conclusion is provided by a comparison between the proposed proton assignments of the experimental 1H -NMR spectrum with the results of a quantum mechanical 1H -NMR calculation.^{13,14,15} The results are shown in Figure 4. It is noticeable that the calculated chemical shifts, although not accurate,¹⁸ fit qualitatively with the experimental data. In fact, in the aromatic region, in both the experimental and the calculated 1H -NMR spectra of unstable *trans* **6.1**, three groups can be identified: the first, at higher field, is constituted by H_a only; the second includes H_b , H_c , H_d , H_e , H_f and a proton of the phenyl group (H_v according to the calculation); the third group, at higher field, includes the remaining four protons of the phenyl rings. This qualitative agreement between the calculated and the experimental spectra suggests the proposed interpretation of the experimental 1H -NMR reported in Figure 3b to be correct.

The assignment of the absorptions in the region 5-2.5 ppm is aided by the coupling constants. The two double doublets at 3.3 and 3.5 ppm have coupling constants of 8.0 and 15.4 Hz, and 8.8 and 15.4 Hz, respectively. The fact that one of the coupling constants is 15.4 Hz indicates that these absorptions belong to H_r and H_q (vicinal protons) and consequently, the absorption at 4.7 ppm must be assigned as H_p . Considering the calculated dihedral angles H_rCCH_p and H_qCCH_p , the Karplus equation has been tested¹⁹ in an attempt to distinguish H_r and H_q . The calculated coupling constants are, respectively, 10.5 Hz

($H_rCCH_p = 154.7^\circ$) and 6.8 Hz ($H_qCCH_p = 36.3^\circ$). Compared with the experimental results of 8.0 and 8.8 Hz, these result can not be considered reliable, and no clear assignment of H_r and H_q can be made. Also, from the quantum mechanical 1H -NMR calculation illustrated in Figure 4, the assignment of H_p could be confirmed, but no distinction between H_r and H_q was possible due to the low accuracy of the calculation.

Based on the integrals of the absorptions at the photostationary state (PSS), the stable *cis*/unstable *trans* ratio was calculated to be 8:92. Moreover, minor absorptions of the stable *trans* isomer are also visible (see for instance absorptions at 2.8, 4.3, 6.85 and 7.9 ppm) showing that this isomer is present in 4%. On the basis of the thermodynamic parameters calculated from kinetic analysis (see section 6.2.6), the half life at the temperature of acquisition (-50°C) was calculated to be ca. 21 h. This value is too high to explain the formation of the stable *trans* isomer by thermal isomerization of the newly obtained unstable *trans*, which can therefore have been formed only photochemically while irradiating from the unstable *trans* or, perhaps, directly from the stable *cis*.

Stable *trans*

Subsequently, the temperature of the sample was increased to 30°C for ca. 15 min, and the solution became colorless. The 1H -NMR spectrum was then measured again at -50°C (Figure 3c). All the absorptions shifted once again. A comparison with previous results on the five-five membered ring motor measured in the same solvent (chapter 2) indicates that this new isomer is the stable *trans* (range of the absorptions of the aromatic protons from about 6 to 8 ppm). However, few differences are visible in this case: due to the presence of the phenyl group, protons H_a and H_b are shifted upfield in comparison to those in the dimethyl five-five membered ring motor. From the molecular modeling, indeed, it can be clearly seen that these two protons are close to the phenyl group, and therefore, due to the π electrons, H_a and H_b experience greater shielding. The other protons are much less affected.

In order to add support to this interpretation, a quantum mechanical 1H -NMR calculation^{13,14,15} was performed. The results are shown in Figure 5. As before, it is notable that the calculated chemical shifts, although not accurate,¹⁸ fit the experimental data in a qualitative way and the relative positions of the absorptions are, indeed, closely comparable. It should be pointed out here that the chemical shifts of the protons H_x - H_v and H_y - H_w in the calculated spectrum have been averaged to mimic free rotation of the phenyl group.

For the assignment of the absorptions in the region 5-2.5 ppm, the same considerations as for Figure 3a are made. Moreover, these assignments are supported by the calculated values of the chemical shifts (Figure 5).

The absorptions of the residual *cis* stable isomer remain unchanged.

Unstable *cis*

A second irradiation experiment was performed on the same sample using a 365 nm light for 4 h at -75°C in an ethanol bath. The solution became yellow, and the 1H -NMR spectrum was measured at -50°C (Figure 3d). Again, a shift of all the absorptions of the

Chapter 6

motor moiety was observed, implying full conversion to a new isomer, which can be identified as the unstable *cis* by considering the absorption range of the aromatic protons (6.6-7.8 ppm) and comparing with previous results (chapter 2). A lower range of absorption of the naphthalene protons, indeed, is consistent with a *cis* conformation, where the two naphthalene moieties are in close proximity.

For the assignment of the absorptions in the region 5-2.5 ppm, the same considerations as for Figure 3b are made.

No residual stable *trans* isomer is visible in this spectrum, indicating full conversion.

Stable cis

The sample was then warmed to 30°C for ca. 30 min, and subsequently another ¹H-NMR spectrum was acquired at -50°C (Figure 3e). This spectrum proved to be identical to the one in Figure 3a (stable *cis* **6.1**), indicating that the second thermal step has occurred, and a full 360° cycle around the central double bond has been performed.

In the spectrum in Figure 3e also an amount of about 10% of the stable *trans* isomer is visible (see for example the peaks at 2.8, 3.5 and 4.3 ppm), attributed to the photoconversion of the residual stable *cis* of the first irradiation step (Figure 3c).

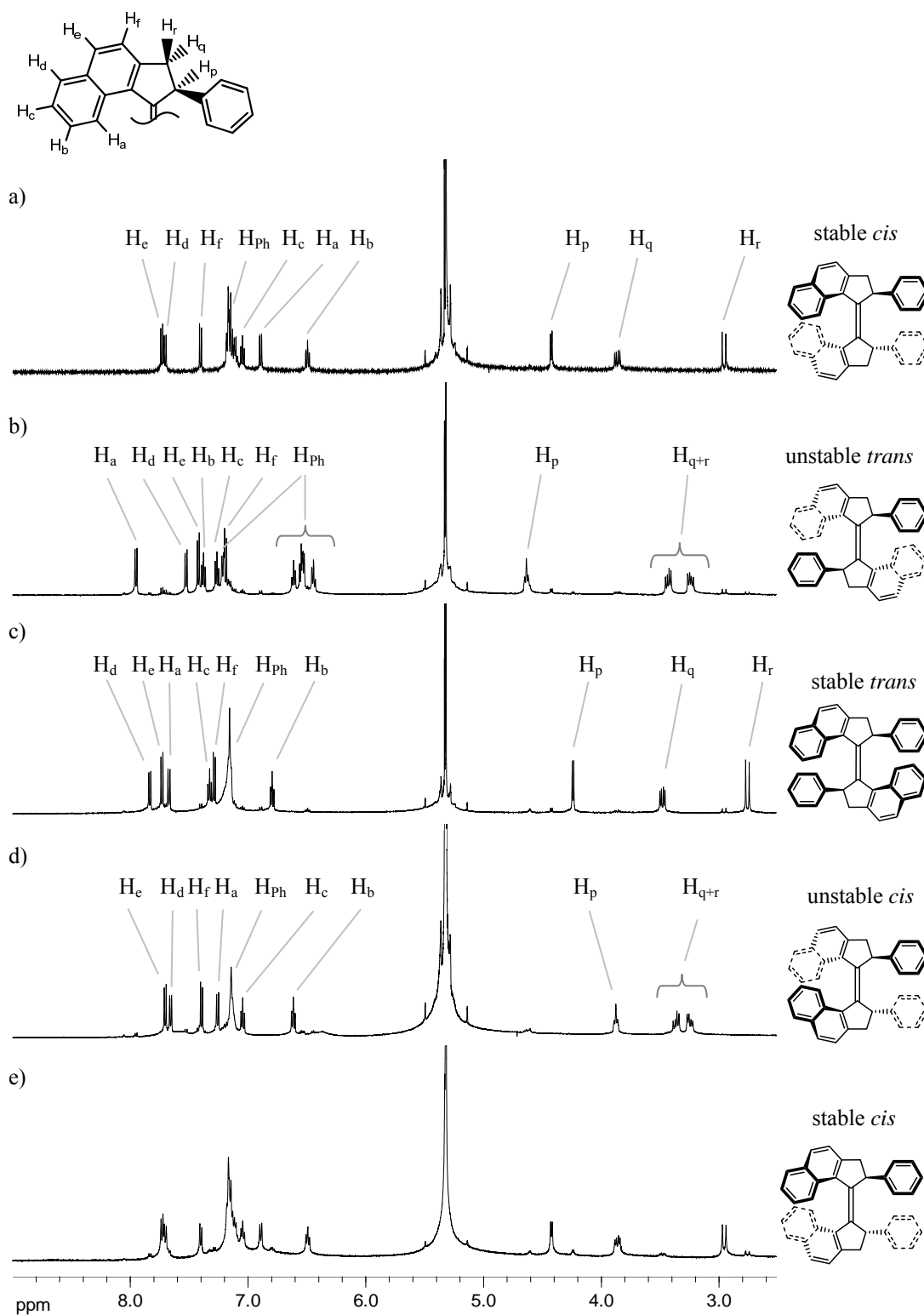


Figure 3: $^1\text{H-NMR}$ spectra of motor **6.1** in DCM-d_2 . a) stable *cis*; b) PSS after first irradiation ($\lambda = 365$ nm): unstable *trans*; c) first thermal step: stable *trans*; d) PSS after second irradiation ($\lambda = 365$ nm): unstable *cis*; e) second thermal step: stable *cis*. (all the spectra were acquired at -50°C).

	H _p	H _q	H _r
experimental	4.42	3.86	2.96
calculated	4.53	3.91	2.78

Table 5: Experimental and calculated chemical shifts (in ppm) in the ¹H-NMR of protons H_p, H_q and H_r of stable *cis* **6.1**.

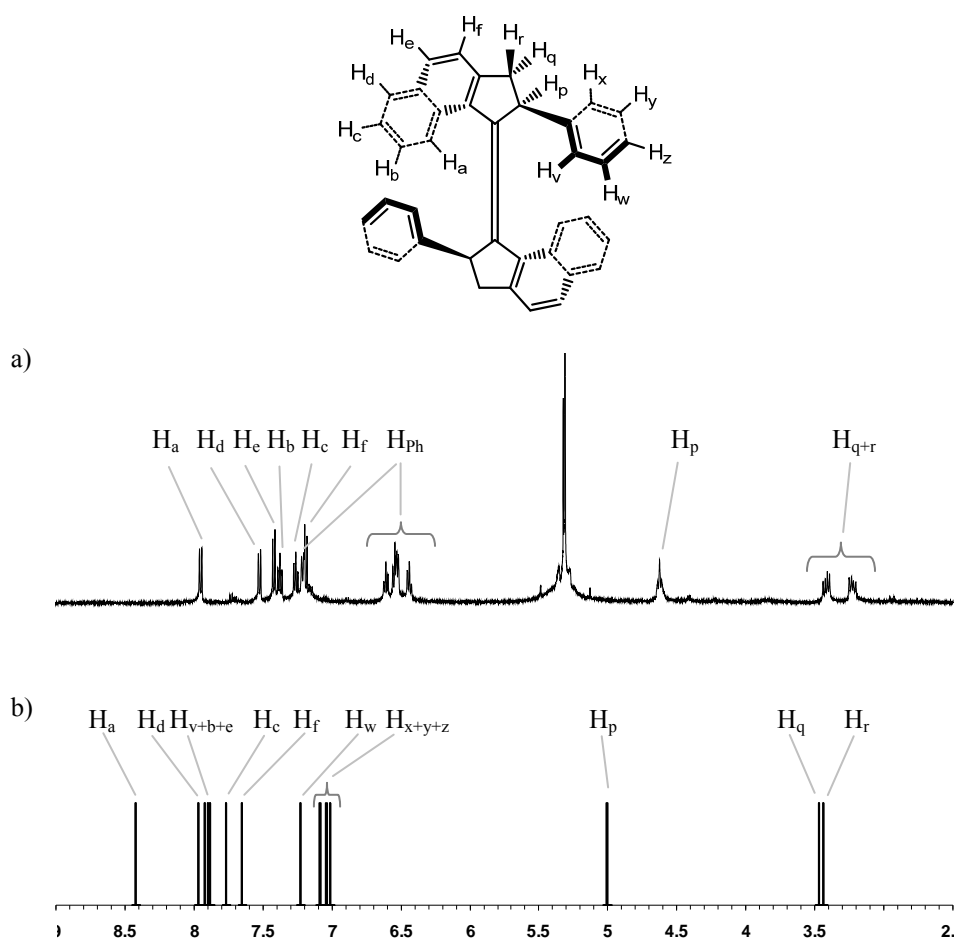


Figure 4: a) Experimental and b) calculated (see ref. 13) ¹H-NMR spectra of unstable *trans* **6.1**.

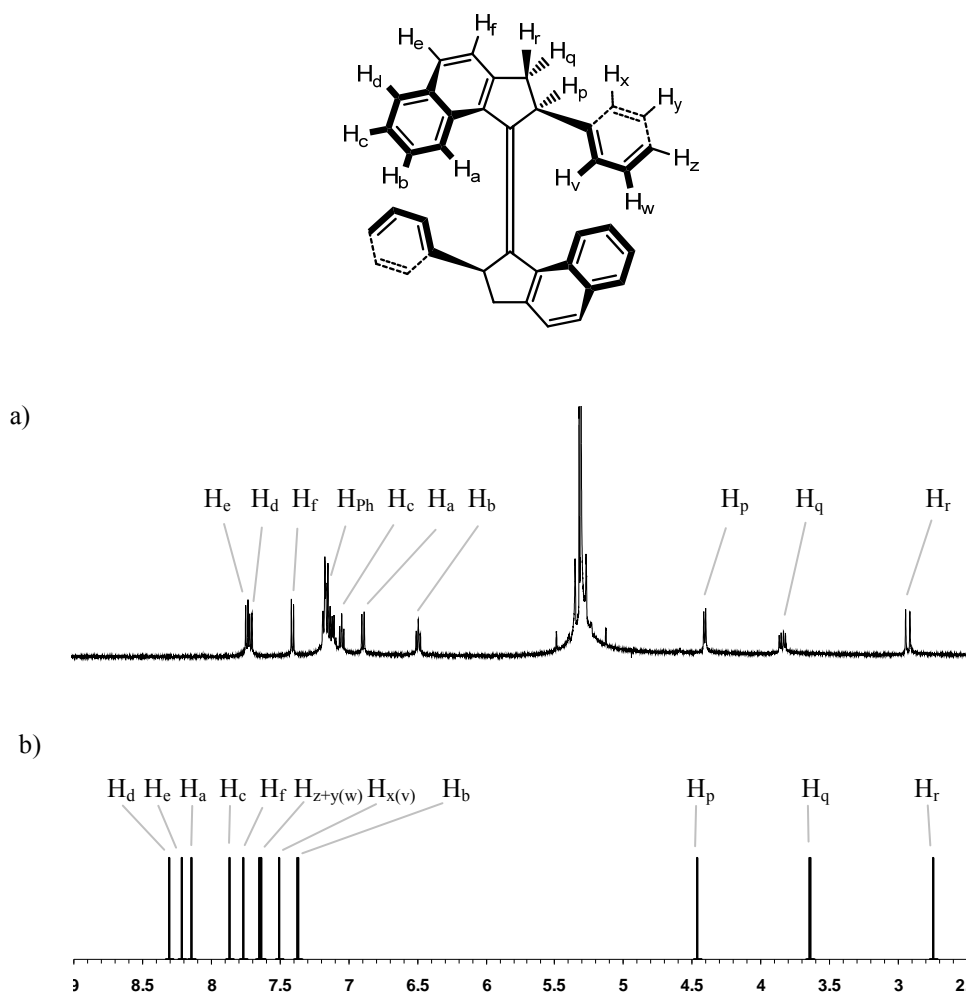
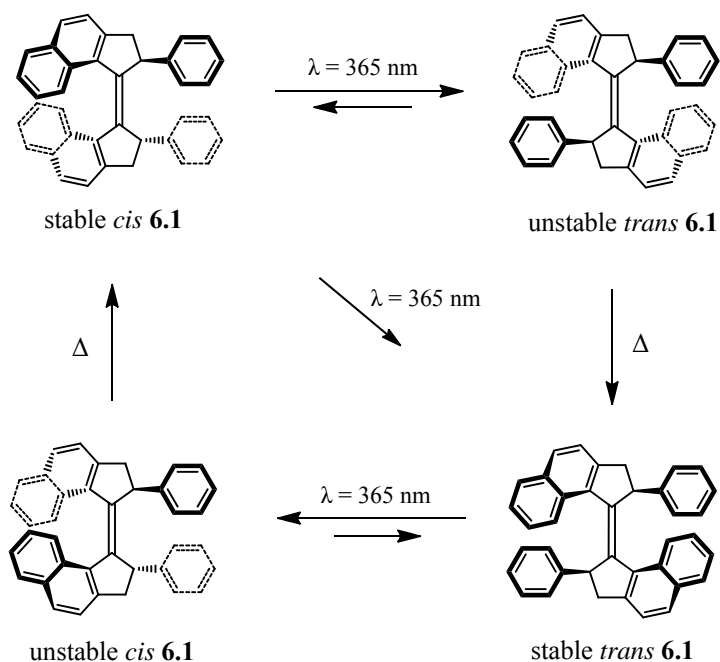


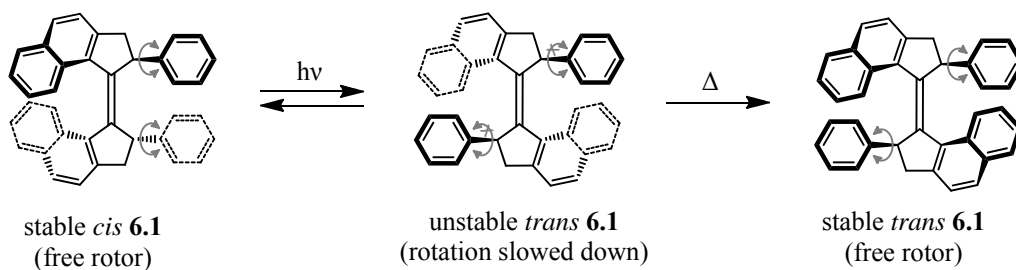
Figure 5: a) Experimental and b) calculated (see ref. 13) ^1H -NMR spectra of stable *trans* **6.1**.

Based upon the photochemical and thermal isomerizations analyzed by ^1H -NMR, we can conclude that molecule **6.1** functions as a controllable unidirectional rotor. The full rotary cycle is shown in Scheme 3.



Scheme 3: Rotary cycle of motor **6.1**.

In Scheme 4 the switchable function of motor **6.1** as a rotation-on–rotation-off system, as deduced from the $^1\text{H-NMR}$ study reported in Figure 3a, b and c is represented.¹⁷



Scheme 4: Rotation-on–rotation-off switchable function of motor **6.1**.

6.2.5 UV/Vis measurements

A $7.4 \cdot 10^{-5}$ M solution of motor *cis* **6.1** in dichloromethane was used for UV/Vis spectroscopic measurements. The UV/Vis spectra of the isomers during the first half of the cycle are shown in Figure 6a. The spectrum of stable *cis* **6.1** at -50°C was acquired,

presenting a maximum at 378 nm. The sample was kept at this temperature and irradiated with a 365 nm light until the PSS was reached. As in the NMR experiments, almost complete conversion of stable *cis* **6.1** was observed after irradiation, and considering that the solvent and the light used were the same employed in this experiment, the same conversion can be expected here. This means that the UV/Vis spectrum at the PSS is representative (within the experimental error of 5% for $^1\text{H-NMR}$) of the unstable *trans* **6.1**. A bathochromic and hyperchromic effect was observed, with two maxima at 390 and 408 nm. This red-shift is consistent with the generation of a higher energy isomer, due to the increased strain on the central double bond. Increasing the temperature to 0°C for 10 min resulted in a change of the UV/Vis spectrum to give two maxima at 358 and 375 nm. This UV/Vis spectrum is characteristic of a stable *trans* isomer, and suggests therefore that the expected thermal rearrangement occurs.

The same sample was used for the study of the second half of the cycle; UV/Vis spectra are shown in Figure 6b. Light at 365 nm was used to irradiate at -40°C the previously obtained sample of *trans* **6.1**. When the PSS was reached, a UV/Vis spectrum was acquired at -40°C. Also in this case a bathochromic effect (maximum at 408 nm) is clearly visible (indicating the formation of a higher energy isomer), together with a decrease of absorption. After performing the second thermal step by means of an increase of temperature (up to 30°C), the resulting UV/Vis spectrum obtained was acquired, and was found to be similar to the spectrum of the initial stable *cis* **6.1** isomer. The slight difference in the UV/Vis of stable *cis* **6.1** in the final spectrum after one cycle compared with the initial stable *cis* **6.1** is expected since the two PSS are not quantitative, and after completing one cycle the amount of *cis* is <100%, with some of the sample being in the *trans* state.

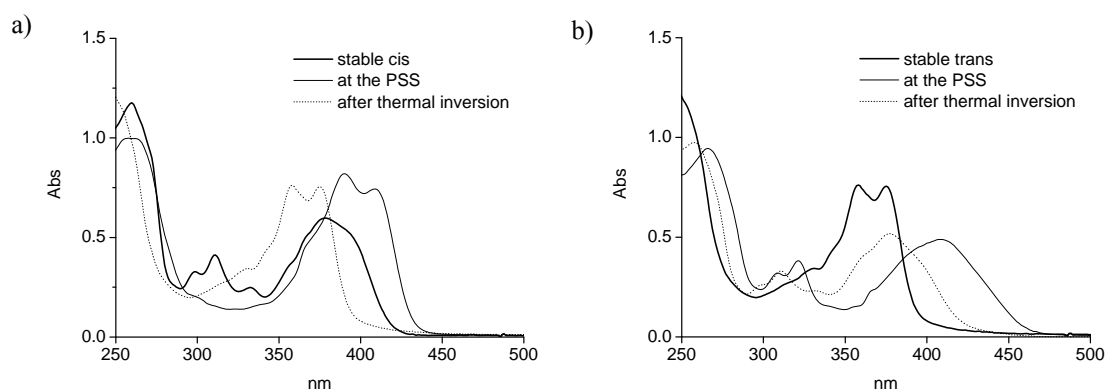


Figure 6: UV/Vis study of molecule **6.1** ($7.4 \cdot 10^{-5}$ M in DCM). a) first half of the cycle: stable *cis* (thick line), PSS after irradiation (main product: unstable *trans*, thin line), after thermal inversion (main product: stable *trans*, dotted line); b) second half of the cycle: sample after the first thermal inversion (main product: stable *trans*, thick line), PSS after irradiation (main product: unstable *cis*, thin line), after thermal inversion (main product: stable *cis*, dotted line).

In order to demonstrate the unimolecularity of each of the four steps of the cycle and confirm the unidirectional rotation ability of the motor, the presence of isosbestic points was verified for each of the four steps. The results are shown in Figure 7. Figure 7a and Figure 7c refer to the photochemical steps, and were obtained at regular intervals during irradiation; Figure 7b and Figure 7d refer to the thermal steps, and were obtained at regular intervals during the thermal inversion.

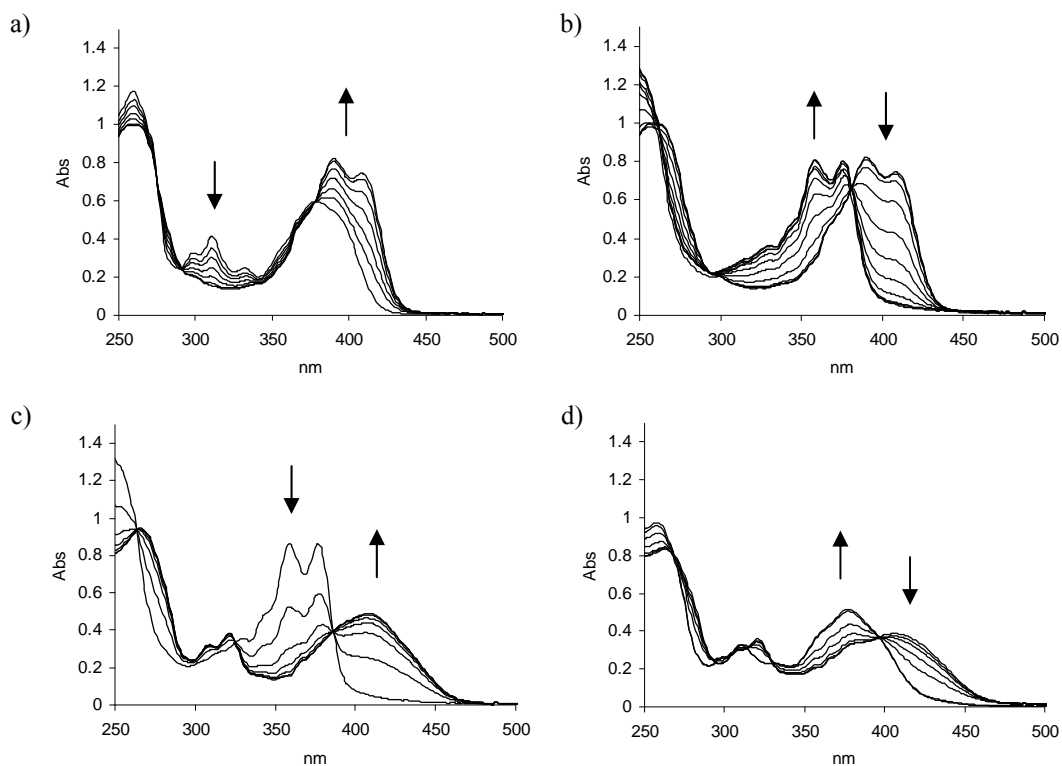


Figure 7: UV/Vis irradiation and thermal inversion experiments for **6.1** ($7.4 \cdot 10^{-5}$ M in DCM). a) photochemical step from stable *cis* to unstable *trans* ($\lambda = 365$ nm); b) thermal step from unstable *trans* to stable *trans* ($-20^{\circ}\text{C} < T < 0^{\circ}\text{C}$); c) photochemical step from stable *trans* to unstable *cis* ($\lambda = 365$ nm); d) thermal step from unstable *cis* to stable *cis* ($20^{\circ}\text{C} < T < 30^{\circ}\text{C}$).

6.2.6 Kinetic analysis

UV/Vis spectroscopic measurements were also performed to study the kinetics of the two thermal steps. A 300 nm high-pass filter was mounted on the exit of the UV/Vis light source to cut off high energy light that might otherwise induce unwanted photochemistry

during the thermal conversion. The changes in UV/Vis absorption spectrum as a function of time due to the thermal inversion at the specific wavelengths at different temperatures (-15, -10, -5 and 0°C for the thermal step of unstable *trans* **6.1** to stable *trans* **6.1** and 25, 35, 45, 55 and 65°C for the thermal step of unstable *cis* **6.1** to stable *cis* **6.1**) were measured. From these data the rate constants (k) for the first-order thermal helix inversion processes at the different temperatures were obtained. The enthalpy of activation ($\Delta^\ddagger H^\circ$) and entropy of activation ($\Delta^\ddagger S^\circ$) were determined from the rate constant by means of the Eyring plot, and from this, the Gibbs free energy of activation ($\Delta^\ddagger G_{20^\circ\text{C}}$) and the half life ($t_{1/2}^{20^\circ\text{C}}$) at room temperature (20°C) were calculated. The Eyring plots of the first thermal step (unstable *trans* to stable *trans*) and of the second thermal step (unstable *cis* to stable *cis*) are shown in Figure 8a and Figure 8b, respectively. The thermodynamic data are shown in Table 6.

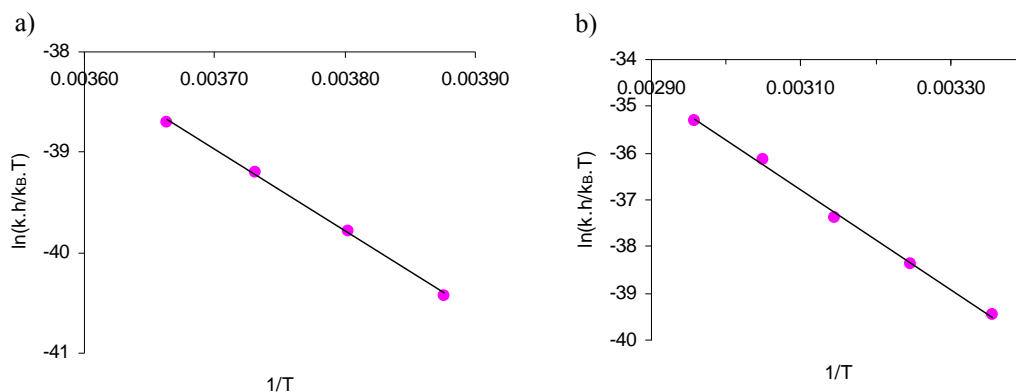


Figure 8: Eyring plot of motor **6.1**, relative to: a) the first thermal step (unstable to stable *trans*), and b) the second thermal step (unstable to stable *cis*).

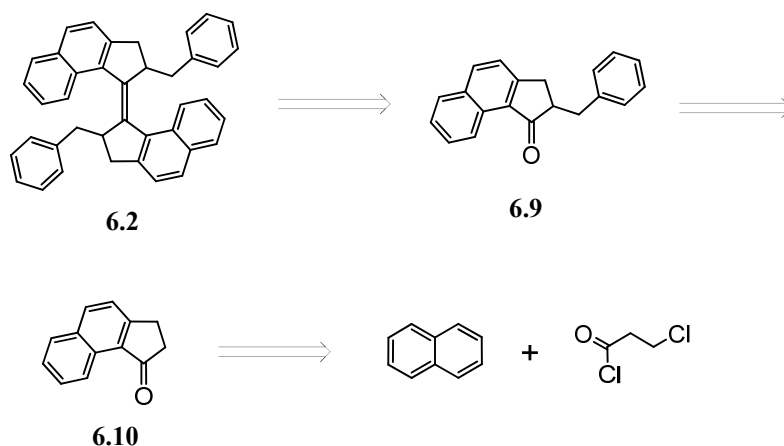
	unstable to stable <i>trans</i>	unstable to stable <i>cis</i>
$k^{20^\circ\text{C}}$	$7.4 \cdot 10^{-2} \text{ s}^{-1}$	$2.3 \cdot 10^{-5} \text{ s}^{-1}$
$\Delta^\ddagger H^\circ$	$67 \text{ kJ} \cdot \text{mol}^{-1}$	$89 \text{ kJ} \cdot \text{mol}^{-1}$
$\Delta^\ddagger S^\circ$	$-35 \text{ J} \cdot \text{K}^{-1} \cdot \text{mol}^{-1}$	$-29 \text{ J} \cdot \text{K}^{-1} \cdot \text{mol}^{-1}$
$\Delta^\ddagger G_{20^\circ\text{C}}$	$78 \text{ kJ} \cdot \text{mol}^{-1}$	$98 \text{ kJ} \cdot \text{mol}^{-1}$
$t_{1/2}^{20^\circ\text{C}}$	9.4 s	8.2 h

Table 6: Thermodynamic data for motor **6.1**.

6.3 Benzyl motor

6.3.1 Retrosynthetic analysis

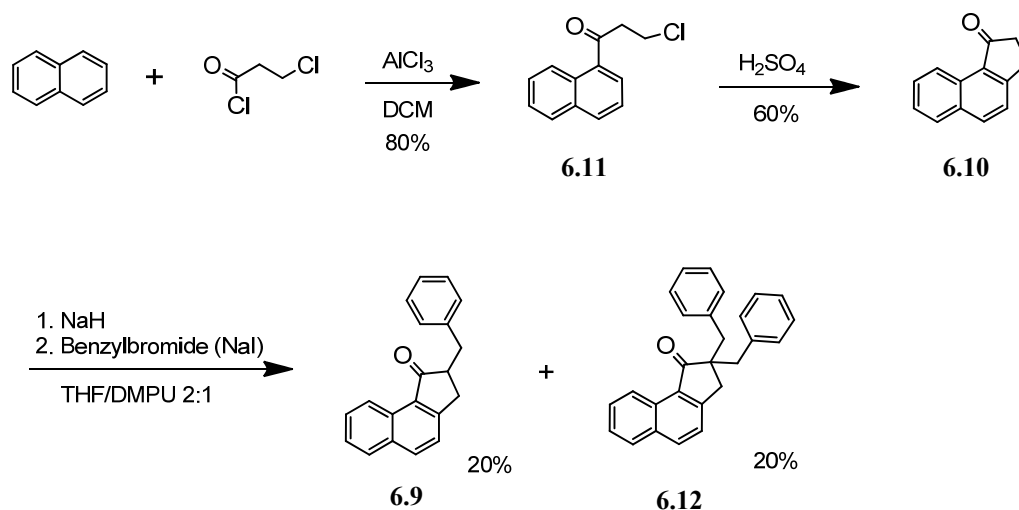
The retrosynthesis of motor **6.2** is shown in Scheme 5. Motor **6.2** can be obtained by McMurry coupling of ketone **6.9**, which can be obtained by α -benzylation of ketone **6.10**. Ketone **6.10** can be prepared in large scale in two steps (namely an acylation followed by an intramolecular alkylation) from inexpensive naphthalene and 3-chloropropanoyl chloride, according to published procedures^{20, 21}.



Scheme 5: Retrosynthesis of motor **6.2**.

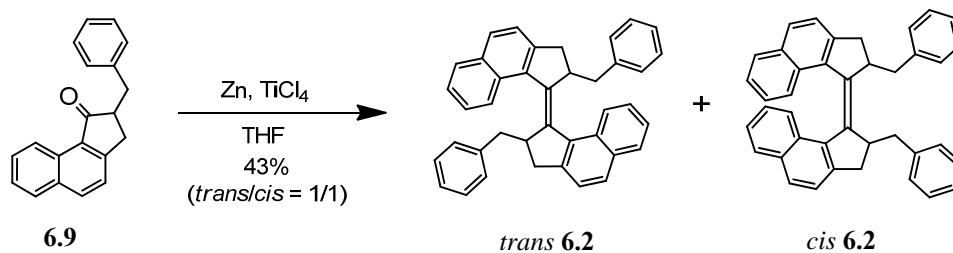
6.3.2 Synthesis

The synthesis starts with the Friedel-Crafts acylation of naphthalene with 3-chloropropanoyl chloride in the presence of AlCl_3 ²⁰ to form **6.11** (Scheme 6). Subsequent ring closure reaction with concentrated sulfuric acid²¹ led to ketone **6.10** in 48% yield over two steps. Sodium hydroxide was used to generate the enolate of **6.10** at 0°C in a mixture of THF and N, N'-dimethyl-N, N'-propylene urea (DMPU)²², which was then allowed to react with freshly distilled benzylbromide in presence of a catalytic amount (5 mol%) of iodide. A mixture of the monoalkylated (**6.9**) and the dialkylated (**6.12**) products resulted in a yield of 20% each, which were separated with column chromatography.



Scheme 6: Synthesis of ketone **6.9**.

Next (Scheme 7), ketone **6.9** was coupled in the presence of low valent titanium (McMurry coupling) in refluxing THF overnight, leading to overcrowded alkene **6.2** in an overall yield of 43%, as a mixture of *cis* and *trans* isomers in 1:1 ratio, as determined by ^1H NMR.



Scheme 7: Preparation of motor **6.2** from ketone **6.9**.

Use of in the silica gel impregnated with silver nitrate²³ 5% was necessary to make the flash column chromatography effective for the separation of the *trans* **6.2** and *cis* **6.2** isomers. The two isomers were distinguished on the basis of their ^1H -NMR spectra in the aromatic region, as in the *cis* isomer, due to the interaction between the two naphthalene moieties, the shifts are more upfield than in the *trans* isomer.

6.3.3 Molecular modeling

Molecular modeling was performed on all the four isomers of the rotary cycle in order to gain a better insight of the molecular structure of motor **6.2**

The structures were first optimized at the PM3 level of theory, using the Hyperchem software package²⁴. For each isomer, the optimization was performed for all the possible stable conformations of the benzyl groups (always maintaining the pseudo-C₂ symmetry of the molecule); their energies were compared, and the conformation with the lowest energy was further optimized at the DFT B3-LYP 6-31G(d,p) level of theory with the Gaussian 03W software package.¹⁰ The final DFT optimized structures of the four isomers are shown in Figure 9.

In Table 7 the most important geometrical features of motor **6.2** and the 5-5 membered ring methyl motor (see Chapter 2) are reported for comparison. Specifically, the double bond length, and the four dihedral torsion angles formed by the two doubly bonded carbons and the four carbons connected to them are reported; an average of the deviation from ideality (0° or 180°) of these four dihedral angles is also indicated.

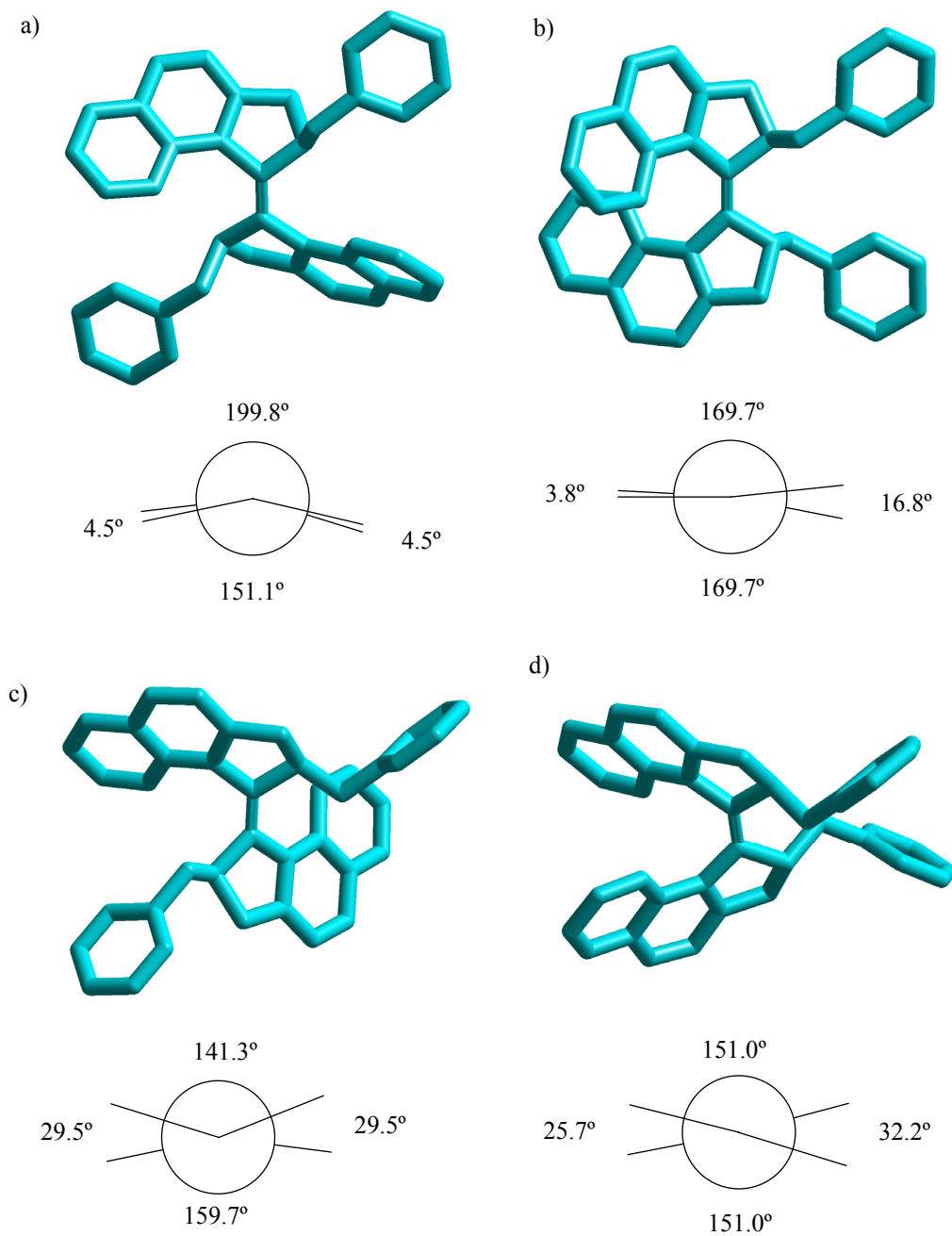
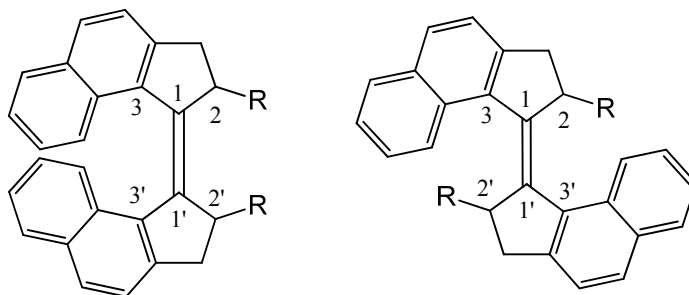


Figure 9: Structures and Newman projections of **6.2** calculated at the DFT B3LYP 6-31G(d,p) level of theory. a) stable *trans*; b) stable *cis*; c) unstable *trans*; d) unstable *cis*.



stable <i>trans</i>	R=-CH₂-C₆H₅ (6.2)	R=Me
211'2'	151.1	152.8
311'3'	160.2	159.9
211'3'	4.5	3.5
311'2'	4.5	3.5
average	14.4	13.6
1-1'	1.36	1.36

stable <i>cis</i>	R=-CH₂-C₆H₅ (6.2)	R=Me
211'2'	16.8	17.2
311'3'	3.8	4.2
211'3'	169.7	169.3
311'2'	169.7	169.3
average	10.3	10.7
1-1'	1.36	1.36

unstable <i>trans</i>	R=-CH₂-C₆H₅ (6.2)	R=Me
211'2'	141.3	142.2
311'3'	159.7	162.5
211'3'	29.5	27.7
311'2'	29.5	27.7
average	29.5	27.7
1-1'	1.37	1.37

unstable <i>cis</i>	R=-CH₂-C₆H₅ (6.2)	R=Me
211'2'	32.2	31.4
311'3'	25.7	25.3
211'3'	151.0	151.7
311'2'	151.0	151.7
average	29.0	28.3
1-1'	1.37	1.37

Table 7: Geometrical parameters calculated for the four isomers of motor **6.2** and for the five-five membered ring methyl motor. (dihedral angles in degrees and lengths in Angstroms).

It should be noted that the length of the central double bond does not present any difference between the two molecules in any of the four isomers. Moreover, the average torsion around the double bond is higher in motor **6.2** in three of the four cases (stable *trans*, unstable *trans* and unstable *cis*). This can be rationalized considering that a benzyl group is larger than a methyl group; therefore it offers more steric hindrance increasing torsional strain.

Additionally, DFT thermochemical analysis at 25°C was performed to calculate the energies of all the four stable isomers of motor **6.2**. Their relative values after zero point energy correction are shown in Figure 10.

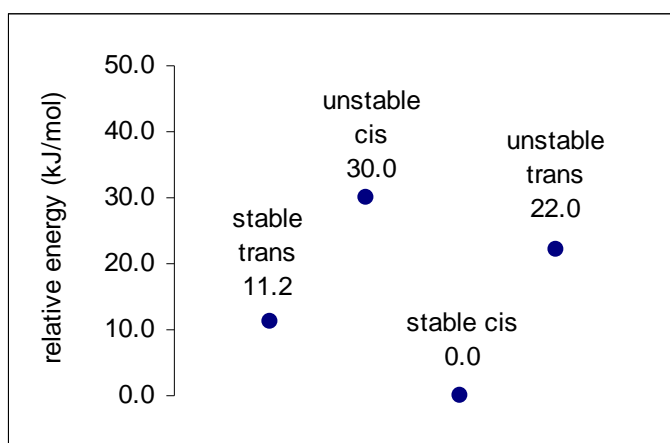


Figure 10: Relative energies (kJ/mol) of the four isomers of motor **6.2**, calculated by DFT thermochemical analysis at 25°C.

However, calculations of transition states were not performed. Therefore, no conclusions on the expected half lives of the two unstable forms can be drawn.

6.3.4 ¹H-NMR measurements

The region between 9 and 6 ppm of the ¹H-NMR spectrum of a sample of motor *trans* **6.2** in DCM-*d*₂ at -50°C is shown in Figure 11a. All the absorptions in the aromatic region can be assigned by comparison with the data reported in Chapter 2 for the five-five membered ring motor.

The sample was then irradiated with a 365 nm lamp for 4 h, while kept at -70°C in an ethanol bath. The color of the solution changed from light yellow to more intense yellow, and its ¹H-NMR spectrum was measured again at -50°C (Figure 11b). A shift of every absorption was observed. The new compound obtained can be identified as the unstable *cis*

isomer by considering that the aromatic protons of the naphthalene moieties absorb in the range of 6.4-7.7 ppm. This lower range is indeed indicative of a *cis* geometry, due to the closer proximity of the naphthalene groups. The absence of residual peaks of the stable *cis* indicates a conversion higher than 95%.

Subsequently, the temperature of the sample was increased to 30°C for about 15 min, and the solution appeared now colorless. Its ¹H-NMR spectrum was then measured again at -50°C (Figure 11c). All the absorptions shifted once again. A comparison with previous results on the five-five membered ring motor measured in the same solvent (chapter 2) indicates that this new quantitatively formed isomer is the stable *cis* (range of the absorptions of the aromatic protons from about 6.3 to 7.8 ppm).

A second irradiation experiment was performed irradiating the same sample with a 365 nm lamp for 4 h, while kept at -75°C in an ethanol bath. The color changed once again to yellow. Its ¹H-NMR spectrum was then measured at -50°C (Figure 11d). Again, a shift of all the absorptions of the motor moiety was observed, implying a conversion to a new isomer, which can be identified as the unstable *trans* by considering the absorption range of the aromatic protons of the naphthalene moiety (7.3-8.2 ppm) and comparing with previous results (chapter 2). The absence of residual peaks of the stable *trans* indicates a conversion higher than 95%

The sample was then warmed to 30°C for ca. 10 min, and subsequently another ¹H-NMR spectrum was acquired at -50°C (Figure 11e). This spectrum was identical to that shown in Figure 11a (stable *trans* **6.2**), indicating that the second thermal step has occurred, and a full 360° cycle around the central double bond has been performed.

It is remarkable that in both photochemical steps, at the PSS the conversion to the unstable isomer appears to be complete within the resolution limit of ¹H-NMR spectroscopy.

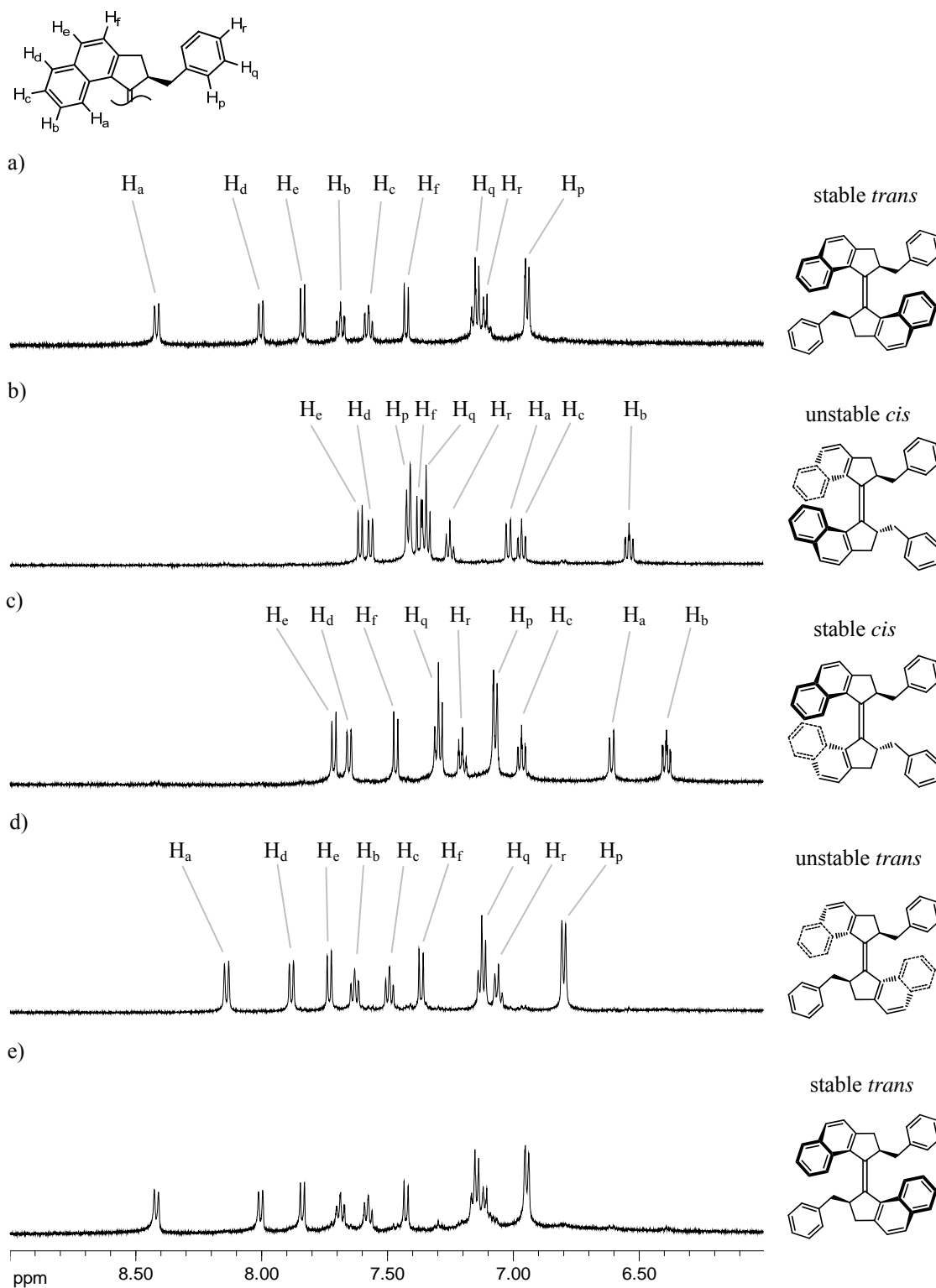
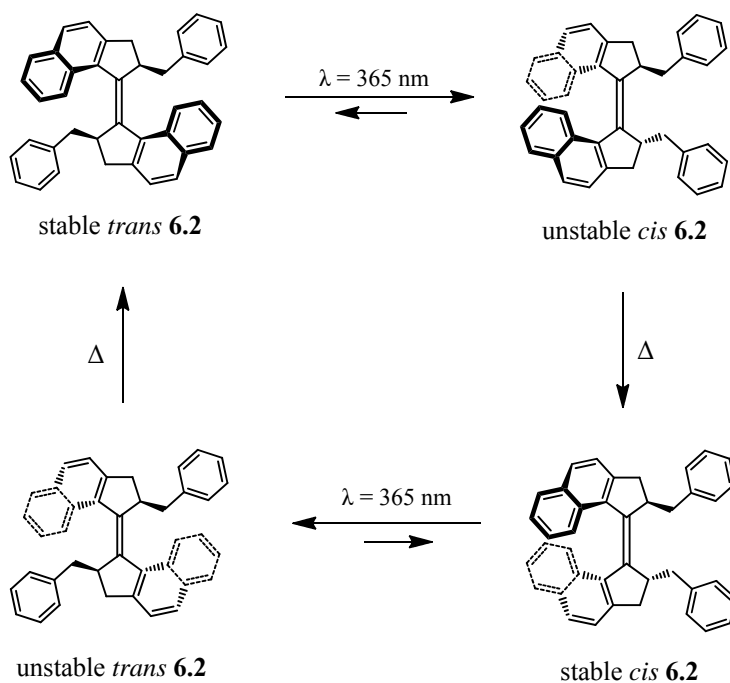


Figure 11: $^1\text{H-NMR}$ spectra of motor **6.2** in DCM-d_2 . a) stable *cis*; b) PSS after first irradiation ($\lambda = 365$ nm): unstable *trans*; c) first thermal step: stable *trans*; d) PSS after second irradiation ($\lambda = 365$ nm): unstable *cis*; e) second thermal step: stable *cis*. (all the spectra were acquired at -50°C).

Based on the $^1\text{H-NMR}$ analysis of photochemical and thermal isomerization steps, we can conclude that molecule **6.2** functions as a controllable unidirectional rotor. The full rotary cycle is shown in Scheme 8. Moreover, the aromatic ring of the benzylic group has been observed to be free to rotate in all the four isomers.



Scheme 8: Rotary cycle of motor **6.2**.

6.3.5 UV/Vis measurements

A $8.0 \cdot 10^{-5}$ M solution of motor *trans* **6.2** in dichloromethane was used for UV/Vis spectroscopic measurements. The UV/Vis spectra of the first half of the cycle are shown in Figure 12a. The spectrum at -30°C was acquired, presenting two maxima at 356 nm and 373 nm. The sample was kept at this temperature and irradiated with a 365 nm light until the PSS was reached. As in the $^1\text{H-NMR}$ experiments a conversion of stable *trans* **6.2** higher than 95% was observed after irradiation, and considering that the solvent and the wavelength of light used in this UV/Vis experiments were the same (DCM and 365 nm), the same conversion can be expected. This means that the UV/Vis spectrum at the PSS is representative of the unstable *cis* **6.2** isomer. A bathochromic and hypochromic effect was

observed, which showed a maximum at 404 nm and a shoulder at about 420 nm. This red-shift is consistent with the generation of a higher energy isomer (ground state/HOMO destabilization) due to the increased strain on the central double bond (in agreement with calculated energies in section 6.3.3 and electrochemical measurements in ref. 25). Increasing the temperature to 30°C for 30 min resulted in the UV/Vis spectrum changing to give a maximum at 373 nm. This UV/Vis spectrum is characteristic of a stable *cis* isomer, and suggests therefore that the expected thermal rearrangement did occur.

For the study of the second half of the rotary cycle with UV/Vis spectroscopic measurements, a $8.0 \cdot 10^{-5}$ M solution of motor *cis* **6.2** in dichloromethane was prepared. The data are shown in Figure 12b. The spectrum at -50°C of the solution was acquired, presenting a maximum at 373 nm. The sample was kept at this temperature and irradiated with 365 nm light until the PSS was reached. As in the NMR experiments a conversion of stable *cis* **6.2** higher than 95% was observed after irradiation, and considering that the solvent and the wavelength of light used in this UV/Vis experiments were the same (DCM and 365 nm), the same conversion can be expected. This means that the UV/Vis spectrum at the PSS is representative of the unstable *trans* **6.2** isomer. A bathochromic and hyperchromic effect was observed, which showed a maximum at 401 nm. As before, this red-shift is consistent with the generation of a higher energy isomer, due to the increased strain on the central double bond (see calculated energies in section 6.3.3 and electrochemical analysis in ref. 25). Increasing the temperature to 20°C for 10 min led the UV/Vis spectrum to change to give two maxima at 356 and 373 nm. This UV/Vis spectrum was found to be similar to the spectrum of the initial isomer stable *trans* **6.2** (Figure 12a). The slight difference in the UV/Vis of stable *trans* **6.2** in the final spectrum after one cycle compared with the one of the initial stable *trans* **6.2** can be expected since the conversion at the two PSS is higher than 95% but might be less than 100%. Therefore, after completing one cycle of rotation, the amount of motor present as the *trans* isomer is nearly 100%, with a small amount of the sample being in the *cis* configuration.

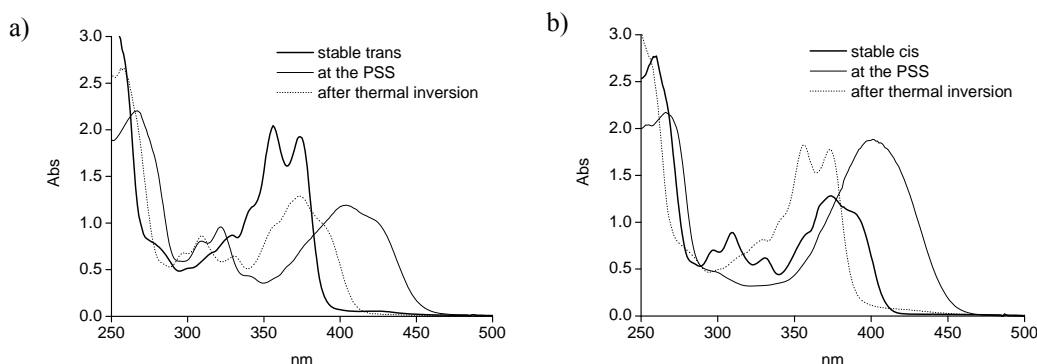


Figure 12: UV/Vis spectra of compound **6.2** ($8.0 \cdot 10^{-5}$ M in DCM). a) first half of the cycle (all the spectra at -30°C): stable *trans* (thick line), PSS after irradiation (main product: unstable *cis*, thin line), after thermal inversion (main product: stable *cis*, dotted line); b) second half of the cycle (all the spectra at -50°C): sample after the first thermal inversion (thick line, main product: stable *cis*), PSS after irradiation (main product: unstable *trans*, thin line), after thermal inversion (main product: stable *trans*, dotted line).

In order to demonstrate the unimolecularity of each of the four steps of the cycle and reinforce the evidence for the unidirectional rotation of the motor, the presence of isosbestic points was verified for each of the four steps. The results are shown in Figure 13. Figure 13a and Figure 13c refer to the photochemical steps, and were obtained at regular intervals during irradiation; Figure 13b and Figure 13d refer to the thermal steps, and were obtained at intervals of few minutes during the thermal inversion.

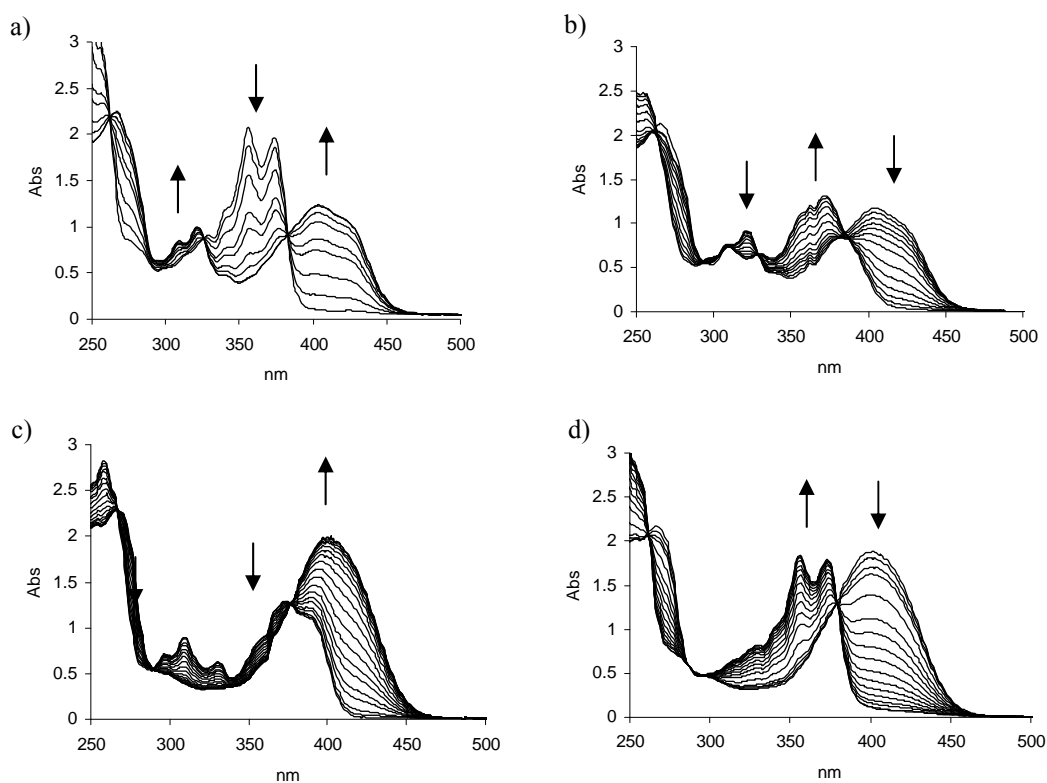


Figure 13: UV/Vis irradiation and thermal inversion experiments for **6.2** ($8.0 \cdot 10^{-5}$ M in DCM). a) photochemical step from stable *trans* to unstable *cis* ($\lambda = 365$ nm); b) thermal step from unstable *cis* to stable *cis* ($0^\circ\text{C} < T < 20^\circ\text{C}$); c) photochemical step from stable *cis* to unstable *trans* ($\lambda = 365$ nm); d) thermal step from unstable *trans* to stable *trans* ($-20^\circ\text{C} < T < 0^\circ\text{C}$).

6.3.6 Kinetic study

UV/Vis spectroscopic measurements were also performed to study the kinetics of the two thermal steps.

A 300 nm filter was mounted on the exit of the UV/Vis light source to cut off high energy light that might otherwise induce unwanted photochemistry during the thermal conversion. The changes in UV/Vis absorption spectrum as a function of time due to the thermal inversion at the specific wavelengths at different temperatures (10, 20, 25 and 30°C for the thermal step of unstable *cis* **6.2** to stable *cis* **6.2** and -10, 0, 10, and 20°C for the thermal step of unstable *trans* **6.2** to stable *trans* **6.2**) were measured. From these data the rate constants (k) for the first-order thermal helix inversion processes at the different temperatures were obtained. The enthalpy of activation ($\Delta^\ddagger H^\circ$) and entropy of activation ($\Delta^\ddagger S^\circ$) were determined from the rate constant by means of the Eyring plot, and from this, the Gibbs free energy of activation ($\Delta^\ddagger G_{20^\circ\text{C}}$) and the half life ($t_{1/2}^{20^\circ\text{C}}$) at room temperature (20°C) were calculated. The Eyring plots of the first thermal step (unstable *cis* to stable *cis*) and of the second thermal step (unstable *trans* to stable *trans*) are shown in Figure 14a and Figure 14b, respectively. The thermodynamic data are shown in Table 8.

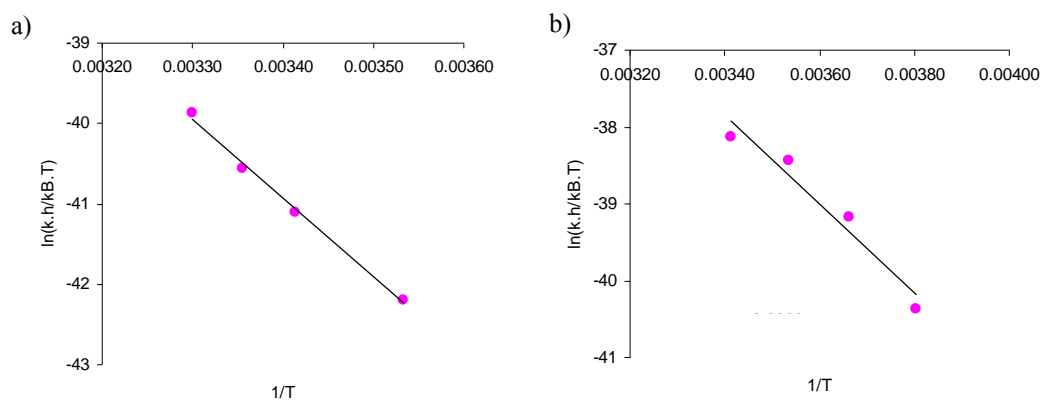


Figure 14: Eyring plot of motor **6.2**, relative to: a) the first thermal step (unstable to stable *cis*), and b) the second thermal step (unstable to stable *trans*).

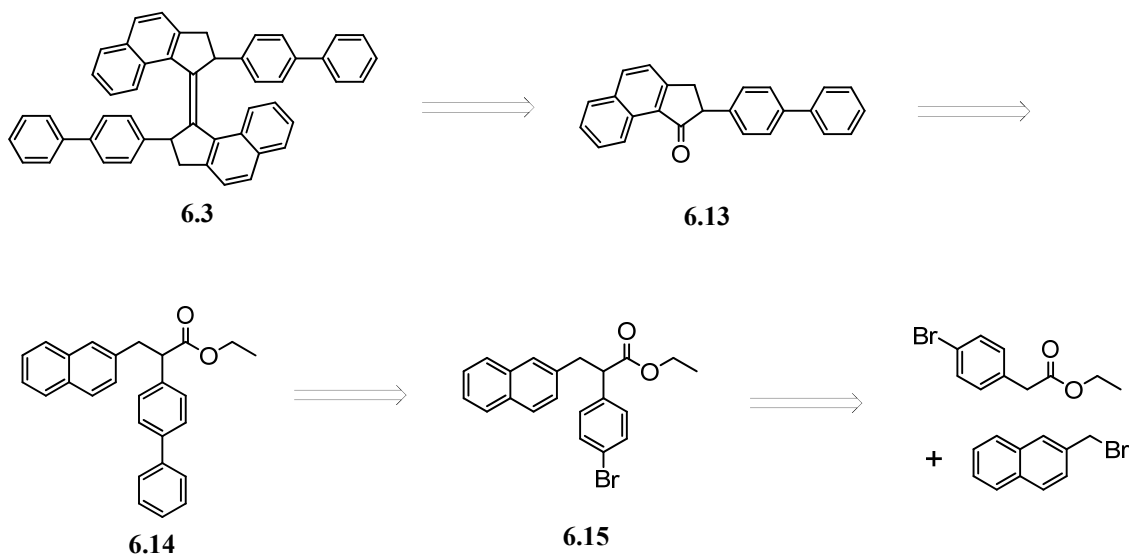
	unstable to stable <i>trans</i>	unstable to stable <i>cis</i>
$k^{20^\circ\text{C}}$	$1.9 \cdot 10^{-2} \text{ s}^{-1}$	$8.6 \cdot 10^{-4} \text{ s}^{-1}$
$\Delta^\ddagger H^\circ$	$48 \text{ kJ} \cdot \text{mol}^{-1}$	$72 \text{ kJ} \cdot \text{mol}^{-1}$
$\Delta^\ddagger S^\circ$	$-115 \text{ J} \cdot \text{K}^{-1} \cdot \text{mol}^{-1}$	$-59 \text{ J} \cdot \text{K}^{-1} \cdot \text{mol}^{-1}$
$\Delta^\ddagger G_{20^\circ\text{C}}$	$81 \text{ kJ} \cdot \text{mol}^{-1}$	$89 \text{ kJ} \cdot \text{mol}^{-1}$
$t_{1/2}^{20^\circ\text{C}}$	37 s	13 min

Table 8: Thermodynamic data for motor **6.2**.

6.4 Biphenyl motor

6.4.1 Retrosynthetic analysis

The retrosynthesis of motor **6.3** is shown in Scheme 9. Motor **6.3** can be obtained by McMurry coupling of ketone **6.13**, which can be obtained by ring closure of the acid of ester **6.14**. The biphenyl group can be obtained via Suzuki coupling of bromide **6.15** with arylboronic acid. Finally, bromide **6.15** can be prepared from the commercially available ethyl 2-(4-bromophenyl)acetate and 2-(bromomethyl)naphthalene.

Scheme 9: Retrosynthesis of motor **6.3**.

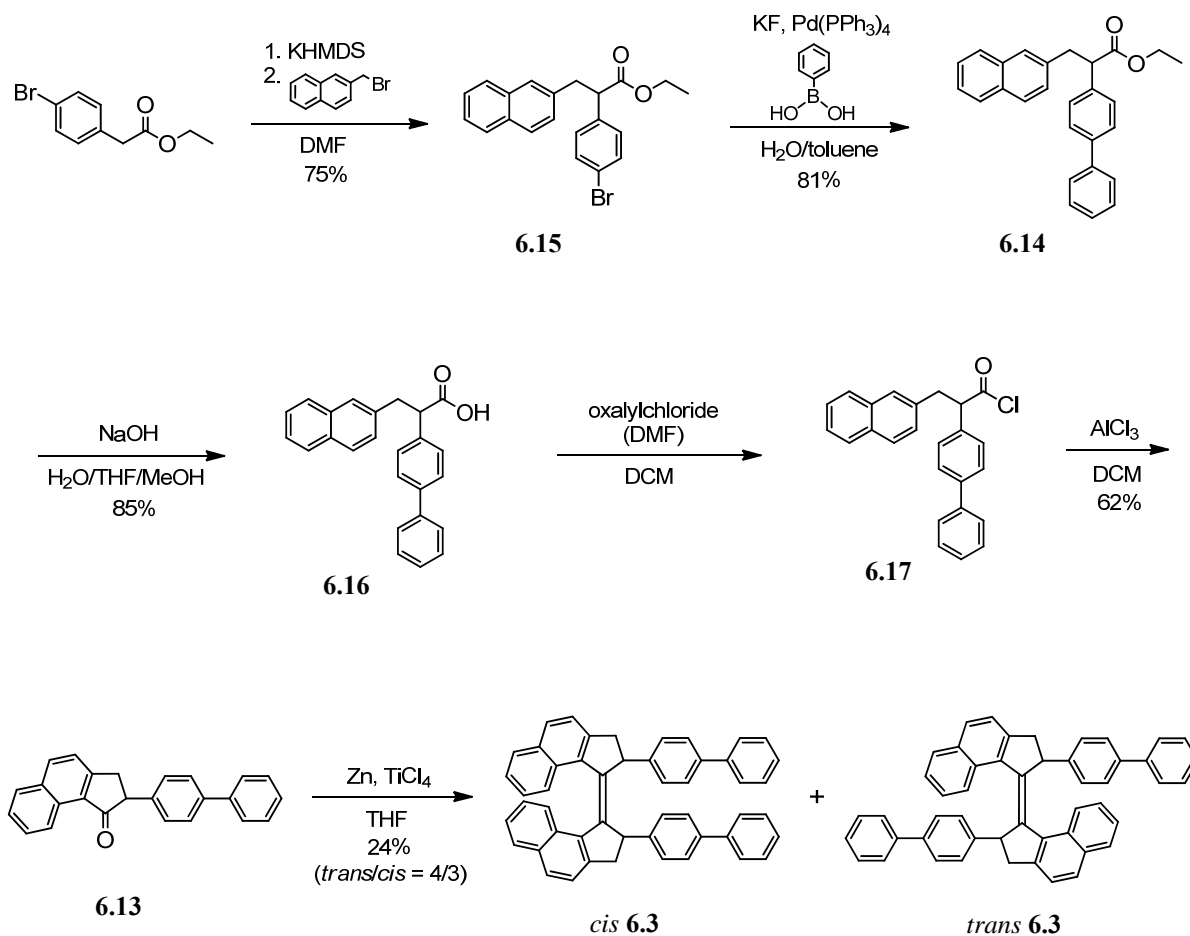
6.4.2 Synthesis

The synthesis of motor **6.3** is shown in Scheme 10. Ethyl 2-(4-bromophenyl)acetate was deprotonated with potassium hexamethyldisilazane (KHMDs) and alkylated with 2-(bromomethyl)naphthalene according to a literature procedure.²⁶ Subsequently, product **6.15** was reacted with arylboronic acid in a palladium catalyzed Suzuki coupling,²⁷ giving the biphenyl in high yield. Next, the ester group was hydrolyzed with sodium hydroxide, and the obtained acid (**6.16**) was activated with oxalylchloride (**6.17**) and treated with aluminium trichloride to give ring-closure to ketone **6.13**, with an overall yield of 62% from acid **6.16**. The key step in the synthesis is the McMurry coupling of ketone **6.13** which resulted in a mixture of *trans* and *cis* isomers in an approximate ratio of 4:3 (calculated on the basis of the ¹H-NMR integrals), in an overall yield of 24%. The two isomers were distinguished on the basis of their ¹H-NMR in the aromatic region, as in the *cis* isomer the interaction between the two naphthalene moieties causes their protons to shift to higher field than in the *trans* isomer (see ¹H-NMR experiments, section 6.4.4). Flash column chromatography was not successful for the separation of the two isomers. With slow recrystallization, instead, crystals of pure *trans* **6.3** could be obtained, which were used for further measurements.

6.4.3 Molecular modeling

For a better insight into the molecular structure of motor **6.3**, computer modeling was performed on all the four isomers of the rotary cycle. The structures were drawn adding an aryl group to the previously calculated structures of motor **6.1**. The optimizations were performed at the DFT B3-LYP 6-31G(d,p) level of theory with the Gaussian 03W software package.¹⁰ The final DFT optimized structures of the four isomers are shown in Figure 15.

Chapter 6



Scheme 10: Synthesis of motor **6.3**.

In Table 9 the most important geometrical features of motor **6.3** are reported, together with those of motor **6.1** and of the 5-5 membered ring methyl motor (see Chapter 2) for comparison. Specifically, the double bond length, and the four dihedral torsion angles formed by the two doubly bonded carbons and the four carbons connected to them are reported; an average of the deviation from ideality (0° or 180°) of these four dihedral angles is also indicated.

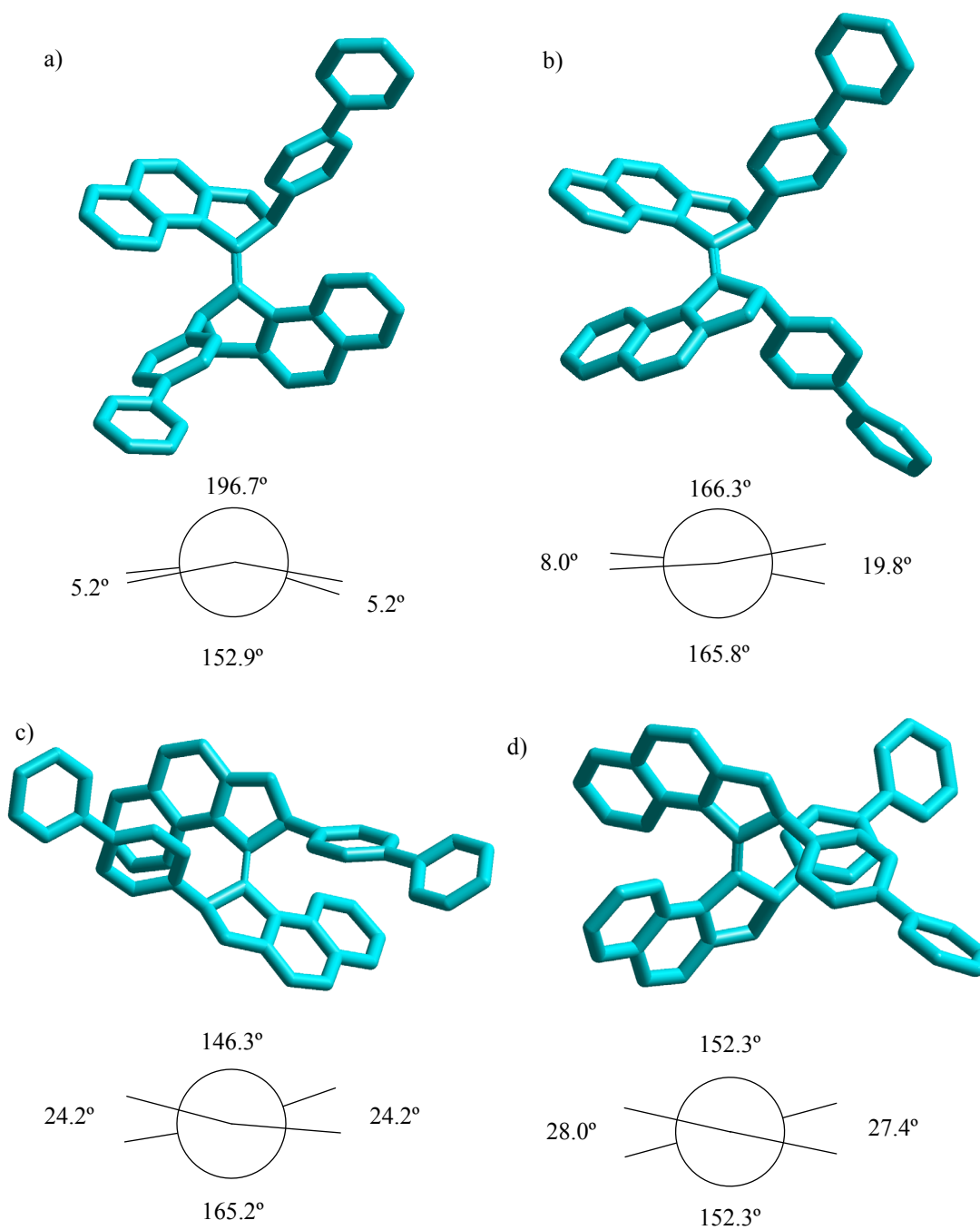
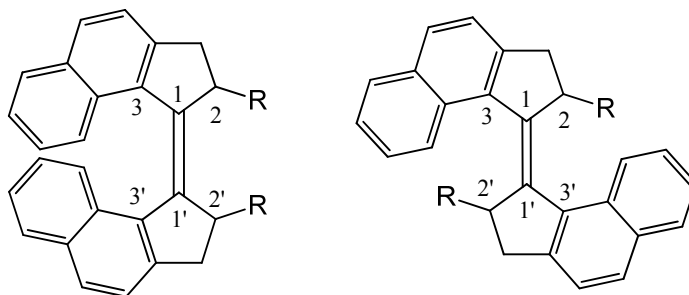


Figure 15: Structures and Newman projections of **6.3** calculated at the DFT B3LYP 6-31G(d,p) level of theory. a) stable *trans*; b) stable *cis*; c) unstable *trans*; d) unstable *cis*.



stable trans	R=-C₆H₄-C₆H₅ (6.3)	R=-C₆H₅ (6.1)	R=Me
211'2'	152.9	153.2	152.8
311'3'	163.3	163.1	159.9
211'3'	5.2	4.9	3.5
311'2'	5.2	4.9	3.5
average	13.5	13.4	13.6
1-1'	1.36	1.36	1.36

stable cis	R=-C₆H₄-C₆H₅ (6.3)	R=-C₆H₅ (6.1)	R=Me
211'2'	19.8	19.8	17.2
311'3'	8.0	7.8	4.2
211'3'	165.8	166.2	169.3
311'2'	166.3	166.2	169.3
average	13.9	13.8	10.7
1-1'	1.36	1.36	1.36

unstable trans	R=-C₆H₄-C₆H₅ (6.3)	R=-C₆H₅ (6.1)	R=Me
211'2'	146.3	146.5	142.2
311'3'	165.2	165.0	162.5
211'3'	24.2	24.2	27.7
311'2'	24.2	24.2	27.7
average	24.2	24.2	27.7
1-1'	1.37	1.37	1.37

unstable cis	R=-C₆H₄-C₆H₅ (6.3)	R=-C₆H₅ (6.1)	R=Me
211'2'	27.4	26.9	31.4
311'3'	28.0	27.0	25.3
211'3'	152.3	153.0	151.7
311'2'	152.3	153.0	151.7
average	27.7	27.0	28.3
1-1'	1.37	1.37	1.37

Table 9: Geometrical parameters calculated for the four isomers of motor **6.3**, motor **6.1** and for the five-five membered ring methyl motor (dihedral angles in degrees and lengths in Angstroms).

It can be seen that the length of the central double bond in motor **6.3** does not present a difference with that of motor **6.1** and with the 5-5 membered ring methyl motor in any of the four isomers.

Also, on the basis of the reported dihedral angles, the distortion of the double bond in motor **6.3** does not deviate significantly from the distortion of the double bond in motor **6.1** in any of the four isomers. This confirms that, as could already be expected, the addition of a further aryl group in the *para* position as present in **6.3** does not significantly change the geometry of the motor.

In conclusion, the same considerations for motor **6.1** stand also for motor **6.3**.

Additionally, DFT thermochemical analysis at 25°C was performed to calculate the energies of all the four stable isomers of motor **6.3**. Their relative values after zero point energy correction are shown in Figure 16.

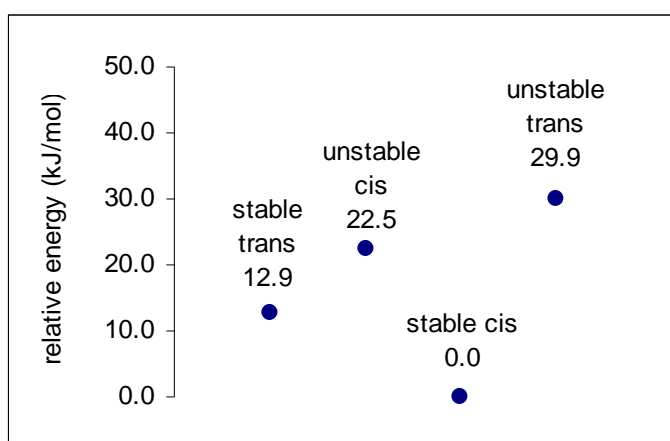


Figure 16: Relative energies (kJ/mol) of the four isomers of motor **6.3**, calculated by DFT thermochemical analysis at 25°C.

In this case calculations on the transition states were not performed. Therefore, conclusions on the expected half life of the two unstable forms can not be drawn.

6.4.4 $^1\text{H-NMR}$ measurements

The rotary cycle was followed with $^1\text{H-NMR}$ spectroscopy, in order to verify that it occurs in the expected unidirectional fashion.

In Figure 17a the region between 8.1 and 6.4 ppm of the $^1\text{H-NMR}$ spectrum of a sample of motor *trans* **6.3** in $\text{DCM-}d_2$ at -50°C is shown. All the absorptions of the naphthalene

moiety can be assigned by comparison with the data reported for motor **6.1** (*vide supra*). The absorption at 7.46 ppm, very broad at -50°C , appears like a sharp doublet at 25°C (inset), and is relative to two protons of the most internal ring of the biphenyl group (conclusion based on the coupling constants calculation). This suggests that the freedom of rotation of the biphenyl is significantly more limited at lower temperatures. The same result was observed for stable *trans* **6.1** (broad absorption at 7.2 ppm in Figure 3c).

The sample was irradiated with a 365 nm lamp for 4 h, while kept at -75°C in an ethanol bath. The spectrum was measured again at -50°C (Figure 17b) showing that every absorption shifted. The new isomer obtained can be identified as the unstable *cis* by considering that the aromatic protons of the naphthalene moieties absorb in the range of 6.6-7.8 ppm. No residual peaks of the initial stable *trans* are visible, indicating full photoconversion.

Subsequently, the sample was left in the dark at room temperature for 4 d, and then measured again at -50°C (Figure 17c). All the absorptions shifted once again. A comparison with previous results on motor **6.1** indicates that this new isomer is the *cis* stable (absorptions of the aromatic protons range from about 7.8 to 6.5 ppm). Interestingly, absorptions of stable *trans* isomer are now visible in an amount of ca. 5%. As in the photoisomerization step no residual stable *trans* was found, this indicates that the unstable *cis*, although the stable *cis* isomer remains the main product, can thermally convert also back to the stable *trans* isomer in a minor but detectable amount.

A second irradiation experiment was performed by irradiating the same sample with a 365 nm lamp for 4 h, while kept at -75°C in an ethanol bath. The $^1\text{H-NMR}$ was then measured again at -50°C (Figure 17d). Again, a shift of all the absorptions of the motor moiety was observed, implying conversion to a new isomer, which can be identified as the unstable *trans* by considering the absorption range of the aromatic protons (7.1-8.0 ppm) and comparing with previous results of motor **6.1**. The aryl group in the unstable *trans* isomer of motor **6.1** appeared to be blocked from free rotation, as demonstrated by the fact that all its five protons absorb at different frequencies (Figure 3b). In case of motor **6.3**, the same result is expected, but due to the overlap of the absorptions, it can not be verified.

On the basis of the integrals of the absorptions in the $^1\text{H-NMR}$ spectrum, the stable *cis*/unstable *trans* isomeric ratio at the PSS was calculated to be 15:85.

The sample was then warmed to 25°C for ca. 15 min, and subsequently another $^1\text{H-NMR}$ spectrum was acquired at -50°C (Figure 17e). This spectrum was identical to the one in Figure 17a (stable *trans* **6.3**), indicating that the second thermal step has occurred, and a full 360° cycle around the central double bond has been performed. The absorptions of the residual stable *cis* at the PSS are visible (for example at 6.50, 6.95, 7.48, 7.77 ppm). The absorptions of the unstable *cis* isomer from the photoisomerization of the residual *trans* isomer left after the first half of the cycle (for example at 6.64, 7.6, 7.67 ppm) are visible also.

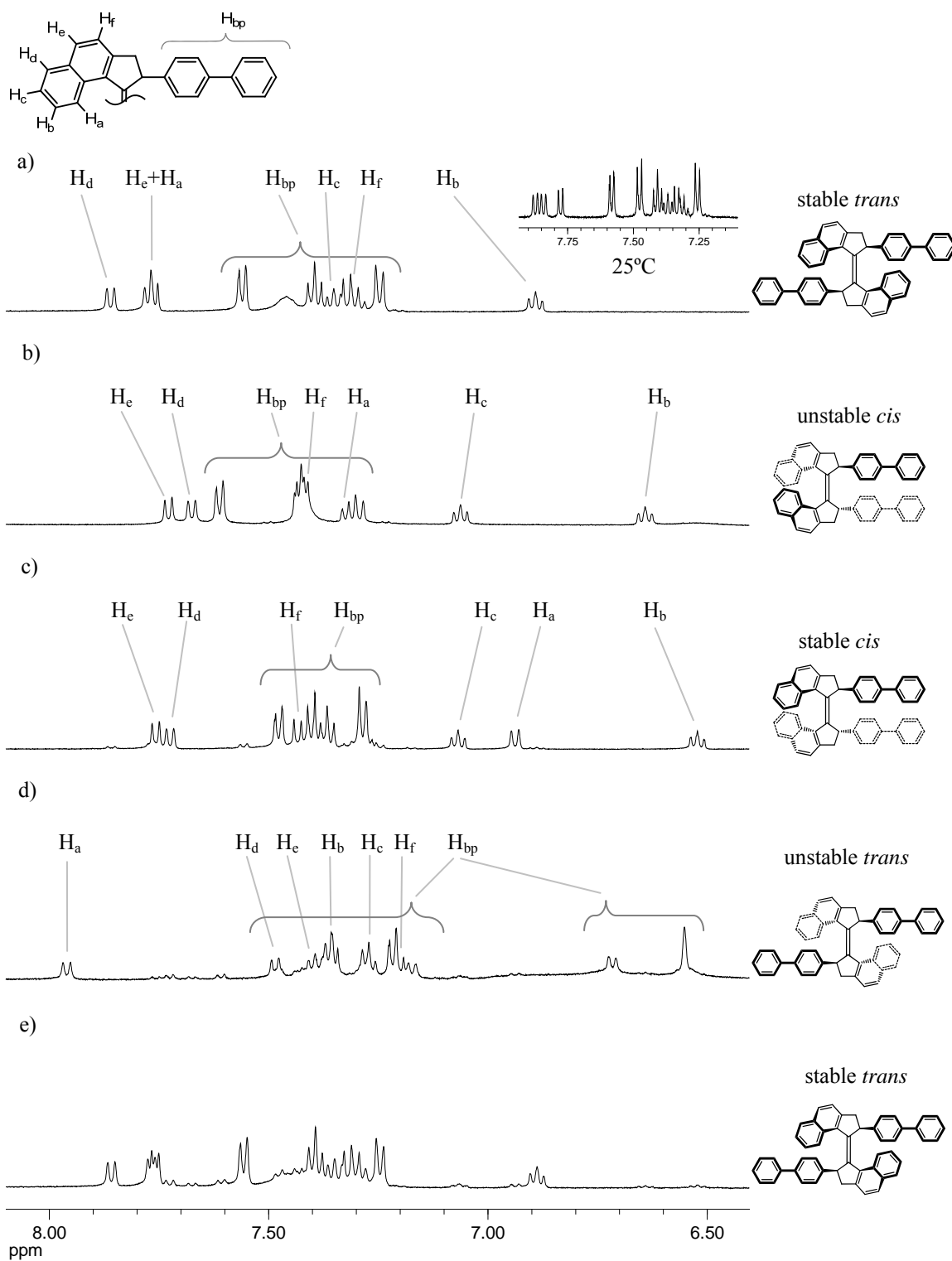
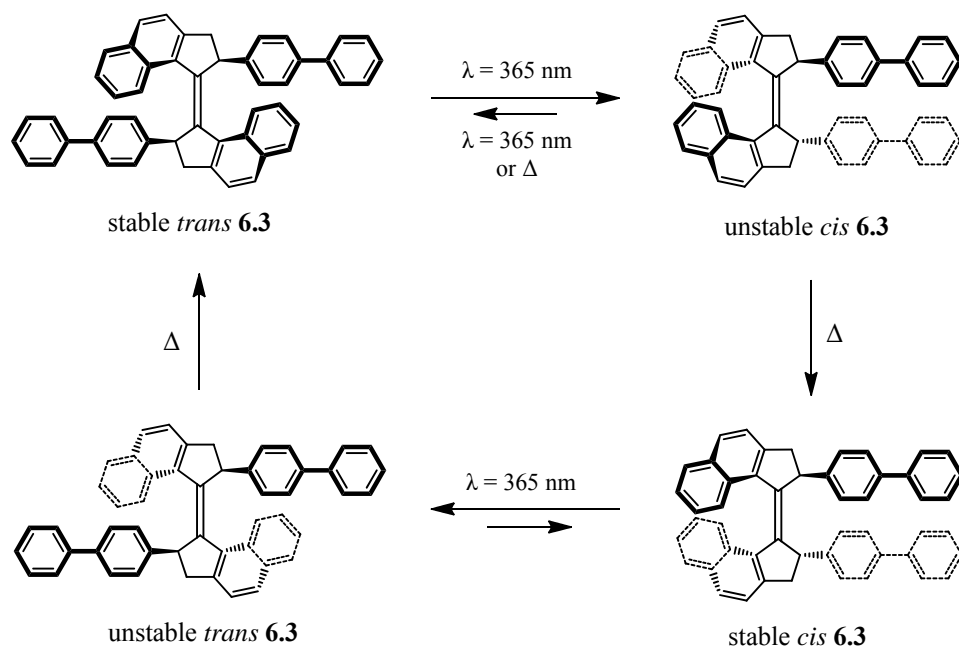


Figure 17: $^1\text{H-NMR}$ measurements of motor **6.3** in DCM-d_2 . a) stable *trans* (-50°C ; inset at 25°C); b) PSS after first irradiation ($\lambda = 365 \text{ nm}$): unstable *cis* (-50°C); c) first thermal step: stable *cis* (-50°C); d) PSS after second irradiation ($\lambda = 365 \text{ nm}$): unstable *trans* (-50°C); e) second thermal step: stable *trans* (-50°C).

It should be noted that the fact that the unstable *cis* can thermally lead to stable *trans* (even in a small amount) does not compromise the unidirectionality of the rotation, as the unstable to stable *cis* and the unstable to stable *trans* thermal steps are irreversible.

In a final analysis, we can conclude that molecule **6.3** functions as a controllable unidirectional rotor. The full rotary cycle is shown in Scheme 11.



Scheme 11: Rotary cycle of motor **6.3**.

6.4.5 UV/Vis measurements

A $1.3 \cdot 10^{-5} \text{ M}$ solution of motor *trans* **6.3** in dichloroethane was used for UV/Vis spectroscopic measurements. The UV/Vis spectra of the first half of the cycle are shown in Figure 18a. The spectrum at 0°C was acquired, presenting two maxima at 359 nm and 376 nm. The sample was kept at this temperature and irradiated with a 365 nm light until the PSS was reached. As in the NMR experiments a conversion of stable *trans* **6.3** of ca. 95% was observed after irradiation, and considering that the light used was the same employed in this experiment, a very similar conversion can be expected here. This means that the UV/Vis spectrum at the PSS is representative of the unstable *cis* **6.3** isomer. A bathochromic and hypochromic effect were observed, with a maximum at 405 nm. This

red-shift is consistent with the generation of a higher energy isomer, due to the increased strain on the central double bond. Increasing the temperature to 60°C for 20 min led the UV/Vis spectrum to change to give a maximum at 378 nm. This UV/Vis spectrum is characteristic of a stable *cis* isomer, and suggests therefore that the expected thermal rearrangement did occur.

The same sample was used for the study of the second half of the cycle; UV/Vis spectra are shown in Figure 18b. Light at 365 nm was used to irradiate at -30°C the previously obtained *cis* **6.3**. When the PSS was reached, a UV/Vis spectrum was acquired at -30°C. According to the ¹H-NMR experiments, it is expected that ca. 85% of the compound is now present as the unstable *trans* isomer. Also in this case a bathochromic effect, with two maxima at 390 and 407 nm, is clearly visible (indicating the formation of a higher energy isomer), together with an increase of absorption.

After performing the second thermal step by increasing the temperature to -10°C, the resulting UV/Vis spectrum obtained was found to be similar to the spectrum of the initial isomer stable *trans* **6.3**. The slight difference in the UV/Vis of stable *trans* **6.3** in the final spectrum after one cycle compared with the one of the initial stable *trans* **6.3** is expected since the two PSS are not quantitative, and after completing one cycle the amount of *trans* is <100%, with some of the sample being in the *cis* state.

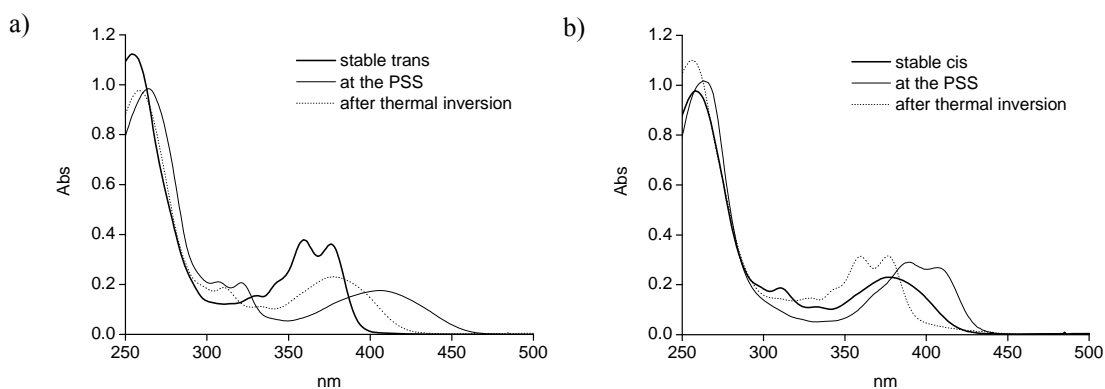


Figure 18: UV/Vis study of molecule **6.3** ($1.3 \cdot 10^{-5}$ M in DCM). a) first half of the cycle: stable *trans* (thick line), PSS after irradiation (main product: unstable *cis*, thin line), after thermal inversion (main product: stable *cis*, dotted line); b) second half of the cycle: sample after the first thermal inversion (thick line, main product: stable *cis*), PSS after irradiation (main product: unstable *trans*, thin line), after thermal inversion (main product: stable *trans*, dotted line).

In order to demonstrate the unimolecularity of each of the four steps of the cycle and show then the evidence of the four steps of the unidirectional rotation, the presence of isobestic points was verified for each of the four steps. The results are shown in Figure 19. Figure 19a and Figure 19c refer to the photochemical steps, and were obtained at regular

intervals during irradiation; Figure 19b and Figure 19d refer to the thermal steps, and were obtained at regular intervals of time during the thermal inversions.

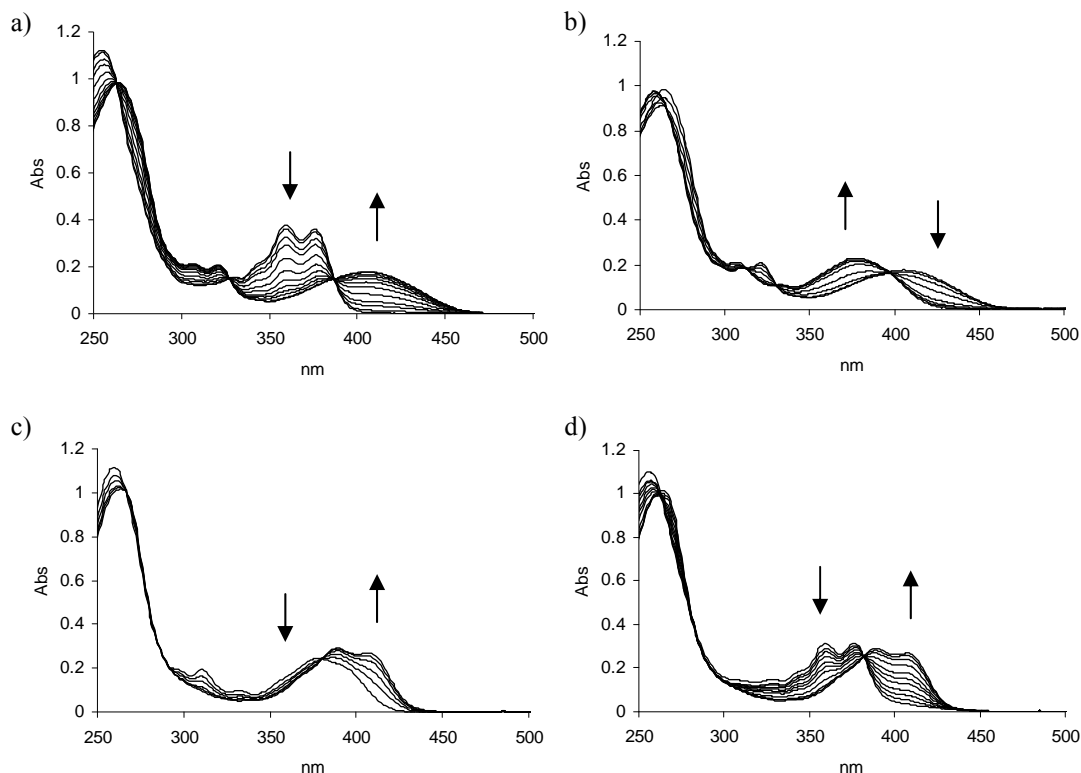


Figure 19: UV/Vis irradiation and thermal inversion experiments for **6.3** ($1.3 \cdot 10^{-5}$ M in DCM). a) photochemical step from stable *trans* to unstable *cis* ($\lambda = 365$ nm); b) thermal step from unstable *cis* to stable *cis* ($T = 30^\circ\text{C}$); c) photochemical step from stable *cis* to unstable *trans* ($\lambda = 365$ nm); d) thermal step from unstable *trans* to stable *trans* ($-10^\circ\text{C} < T < 10^\circ\text{C}$).

6.4.6 Kinetic study

UV/Vis spectroscopic measurements were also performed to study the kinetics of the two thermal steps. A 300 nm filter was mounted on the exit of the UV/Vis light source to cut off high energy light that might otherwise induce unwanted photochemistry during the thermal conversion. The changes in UV/Vis absorption spectrum as a function of time due to the thermal inversion at the specific wavelengths at different temperatures (35, 45, 55 and 65°C for the thermal step of unstable *cis* **6.3** to stable *cis* **6.3** and -15 , -5 , 0 , and 5°C for the thermal step of unstable *trans* **6.3** to stable *trans* **6.3**) were measured. From these data the rate constants (k) for the first-order thermal helix inversion processes at the different

temperatures were obtained. The enthalpy of activation ($\Delta^\ddagger H^\circ$) and entropy of activation ($\Delta^\ddagger S^\circ$) were determined from the rate constant by means of the Eyring plot, and from this, the Gibbs free energy of activation ($\Delta^\ddagger G_{20^\circ\text{C}}$) and the half life ($t_{1/2}^{20^\circ\text{C}}$) at room temperature (20°C) were calculated. The Eyring plots of the first thermal step (unstable *cis* to stable *cis*) and of the second thermal step (unstable *trans* to stable *trans*) are shown in Figure 20a and Figure 20b, respectively. The thermodynamic results are shown in Table 10.

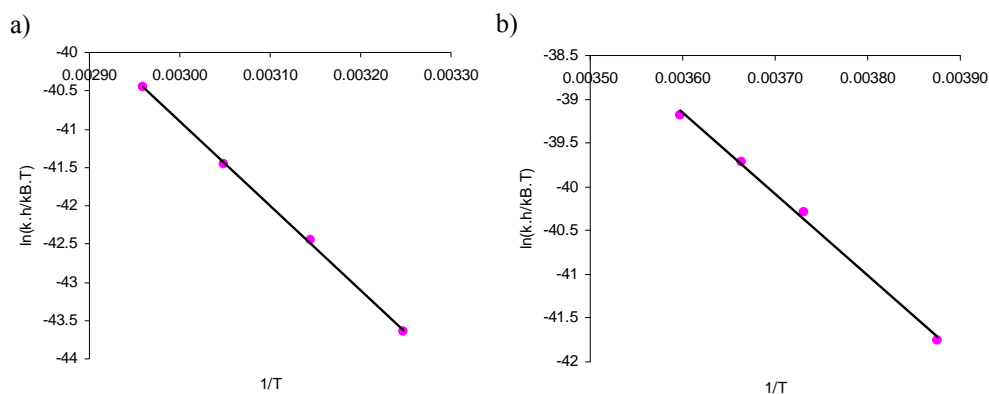


Figure 20: Eyring plot of motor **6.3**, relative to: a) the first thermal step (unstable to stable *cis*), and b) the second thermal step (unstable to stable *trans*).

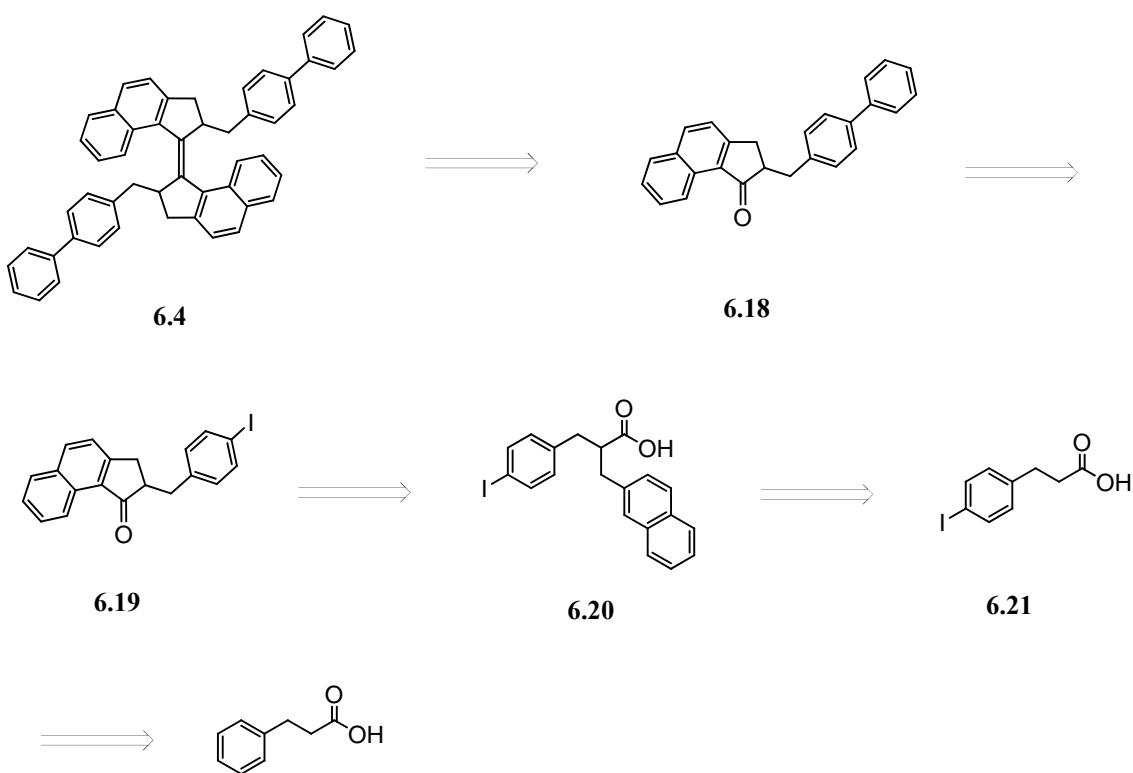
	unstable to stable <i>trans</i>	unstable to stable <i>cis</i>
$k^{20^\circ\text{C}}$	$3.6 \cdot 10^{-2} \text{ s}^{-1}$	$9.6 \cdot 10^{-6} \text{ s}^{-1}$
$\Delta^\ddagger H^\circ$	$79 \text{ kJ} \cdot \text{mol}^{-1}$	$97 \text{ kJ} \cdot \text{mol}^{-1}$
$\Delta^\ddagger S^\circ$	$-4.1 \text{ J} \cdot \text{K}^{-1} \cdot \text{mol}^{-1}$	$-8.6 \text{ J} \cdot \text{K}^{-1} \cdot \text{mol}^{-1}$
$\Delta^\ddagger G_{20^\circ\text{C}}$	$80 \text{ kJ} \cdot \text{mol}^{-1}$	$100 \text{ kJ} \cdot \text{mol}^{-1}$
$t_{1/2}^{20^\circ\text{C}}$	19 s	20 h

Table 10: Thermodynamic data for motor **6.3**.

6.5 p-Phenyl-benzyl motor

6.5.1 Retrosynthetic analysis

The retrosynthesis of motor **6.4** is shown in Scheme 12. Motor **6.4** can be prepared with a McMurry coupling from ketone **6.18**. The biphenyl group can be made via Suzuki coupling from ketone **6.19**, which can be obtained by Friedel-Crafts intramolecular acylation of acid **6.20**. Acid **6.20** can be obtained from the ester of 3-(4-iodophenyl)propanoic acid **6.21** by means of α -alkylation with 2-(bromomethyl)naphthalene. Finally, acid **6.21** can be prepared from 3-phenylpropanoic acid according to the method for the iodination of aromatic compounds.²⁸



Scheme 12: Retrosynthetic analysis of motor **6.4**.

6.5.2 Synthesis

The synthesis of motor **6.4** is shown in Scheme 13²⁹. Iodination of 3-phenylpropanoic acid²⁸ gave product **6.21** in good yield. Next, methoxy ester **6.22** was prepared, and subsequently treated with freshly prepared lithium diisopropylamide (LDA). The obtained enolate was immediately allowed to react with 2-(bromomethyl)naphthalene, which gave product **6.23** in 70% yields. The ester group was hydrolyzed, and the obtained carboxylic group was activated with thionylchloride, to form the acylchloride **6.24**. This product was immediately treated with aluminum trichloride to perform a ring closure *via* intramolecular Friedel-Crafts acylation, which gave ketone **6.19** in 69% yield. Next, a Suzuki coupling with benzenboronic acid was performed to obtain ketone **6.18** in 90% yield. The key step in the synthesis was the homocoupling of ketone **6.18** in presence of low valent titanium (McMurry coupling), which gave product **6.4** as a mixture of *trans* and *cis* isomer, in a *trans/cis* ratio of 3:1, and an overall yield of 59%. The two isomers were distinguished on the basis of their ¹H-NMR in the aromatic region, as in the *cis* isomer, due to the interaction between the two naphthalene moieties, the shifts of the naphthalene protons are more upfield than in the *trans* (see Figure 23a and c).

Separation of *trans*-**6.4** and *cis*-**6.4** was achieved with flash column chromatography on silica gel only with addition of 10% silver nitrite.²³

6.5.3 Molecular modeling

For a better insight in the molecular structure of motor **6.4**, computer modeling was performed on all the four isomers of the rotary cycle.

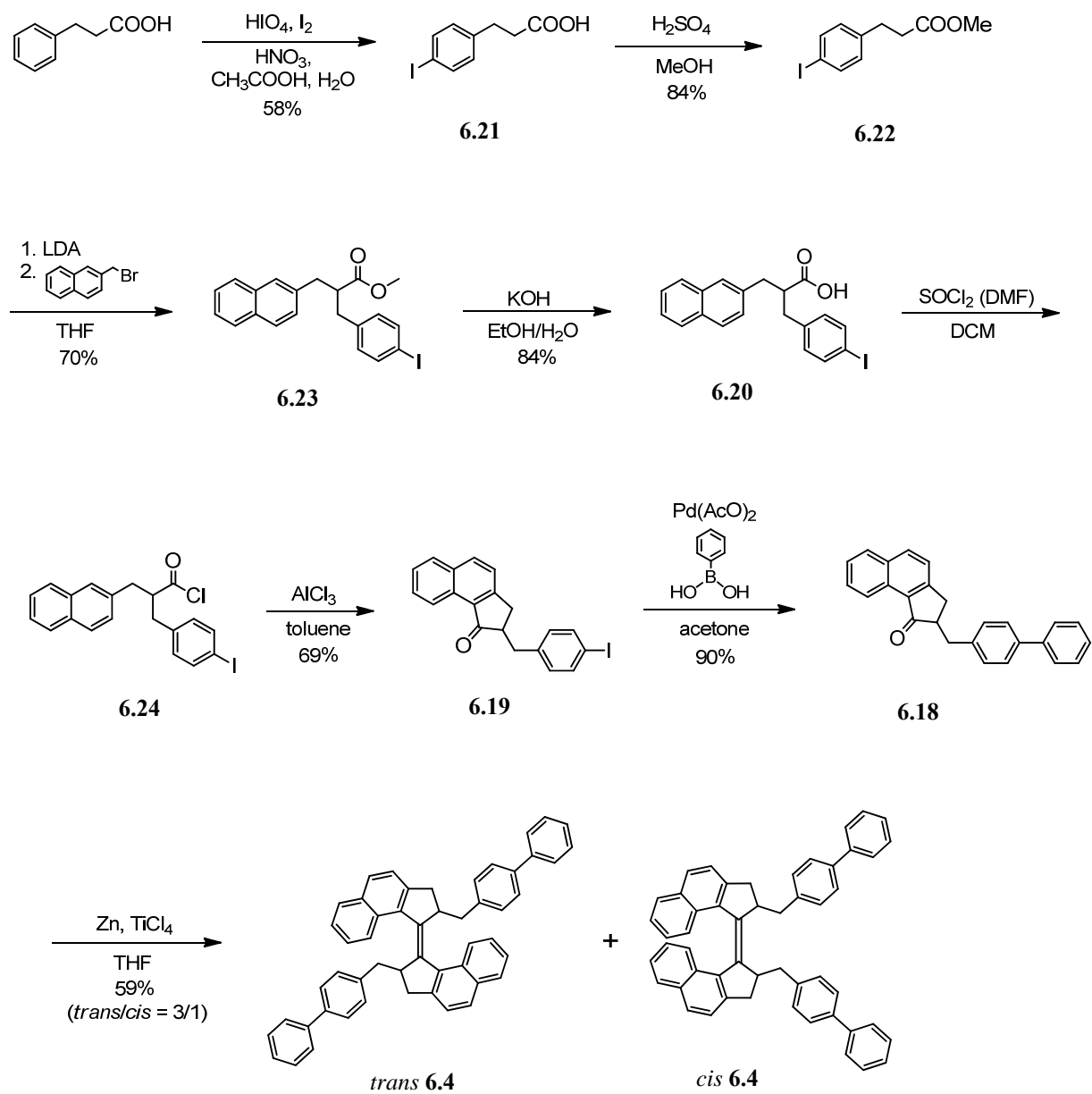
The structures were drawn adding an aryl group to the previously calculated structures of motor **6.2**. The optimizations were performed at the DFT B3-LYP 6-31G(d,p) level of theory with the Gaussian 03W software package.¹⁰ The final DFT optimized structures of the four isomers are shown in Figure 21.

It can be seen that the length of the central double bond in motor **6.4** does not present any difference with motor **6.2** and with the 5-5 membered ring methyl motor in any of the four isomers.

Also, on the basis of the reported dihedral angles, the distortion of the double bond in motor **6.4** does not deviate significantly from the distortion of the double bond in motor **6.2** in any of the four isomers. This confirms that, as could already be expected, the addition of a further aryl group in the *para* position does not significantly change the geometry of the motor. In conclusion, the same considerations for motor **6.2** stand also for motor **6.4**.

Additionally, DFT thermochemical analysis at 25°C was performed to calculate the energies of all the four stable isomers of motor **6.4**. Their relative values after zero point energy correction are shown in Figure 22.

Chapter 6



Scheme 13: Synthesis of motor 6.4.

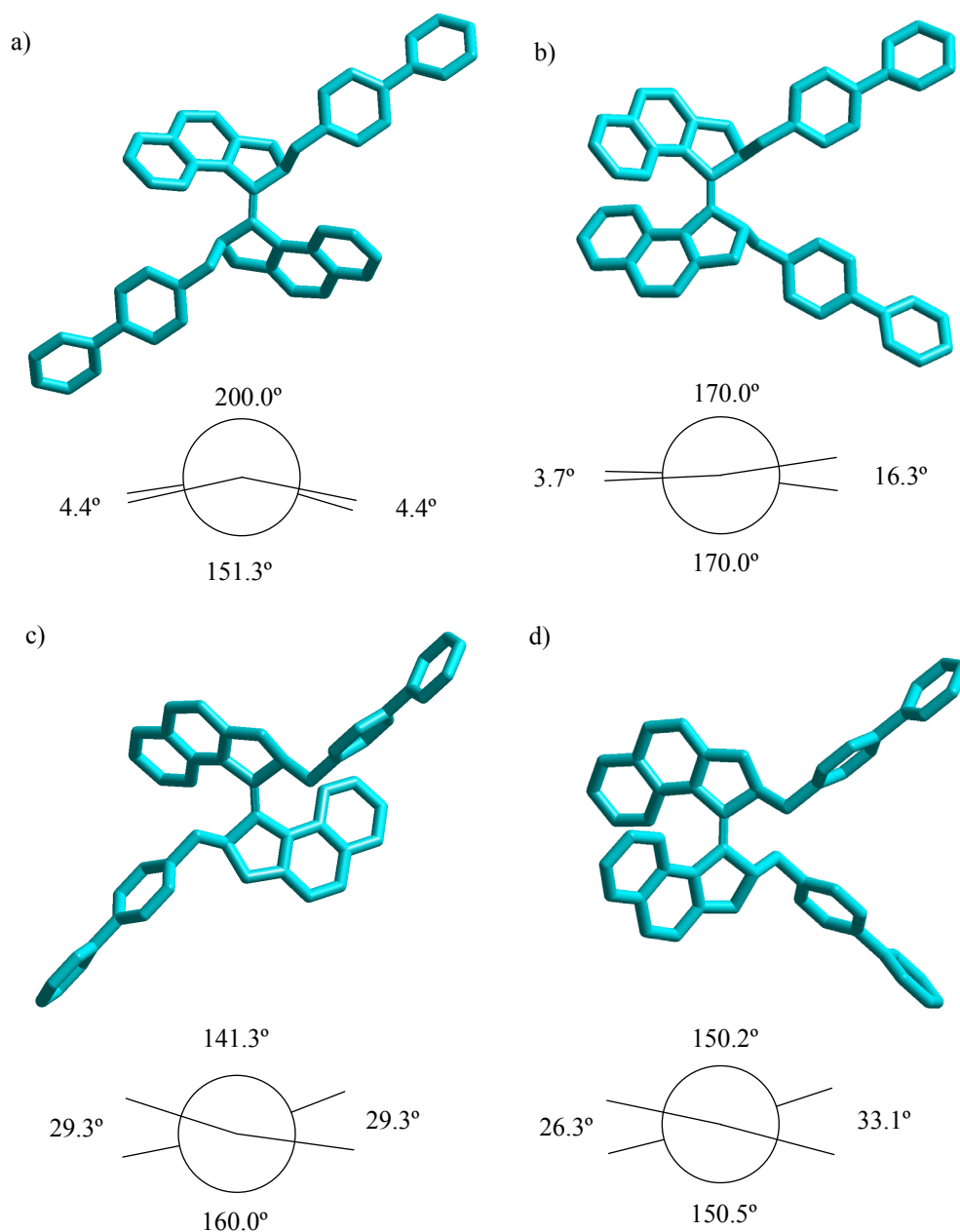
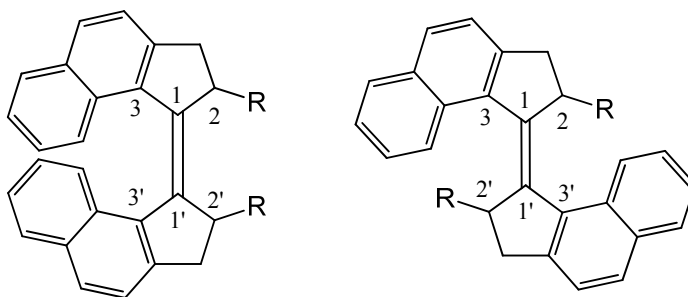


Figure 21: Structures and Newman projections of **6.4** calculated at the DFT B3LYP 6-31G(d,p) level of theory. a) stable *trans*; b) stable *cis*; c) unstable *trans*; d) unstable *cis*.

In Table 11 the most important geometrical features of motor **6.4** are summarized, together with those of motor **6.2** and of the 5-5 membered ring methyl motor (see Chapter 2) for comparison. Specifically, are shown the double bond length, and the four dihedral torsion angles formed by the two olefinic carbons and the four carbons connected to them; an average of the deviation from ideality (0° or 180°) of these four dihedral angles is also indicated.



stable trans	R=-CH₂-C₆H₄-C₆H₅ (6.4)	R=-CH₂-C₆H₅ (6.2)	R=Me
211'2'	151.3	151.1	152.8
311'3'	160.0	160.2	159.9
211'3'	4.4	4.5	3.5
311'2'	4.4	4.5	3.5
average	14.4	14.4	13.6
1-1'	1.36	1.36	1.36
stable cis	R=-CH₂-C₆H₄-C₆H₅ (6.4)	R=-CH₂-C₆H₅ (6.2)	R=Me
211'2'	16.3	16.8	17.2
311'3'	3.7	3.8	4.2
211'3'	170.0	169.7	169.3
311'2'	170.0	169.7	169.3
average	10.0	10.3	10.7
1-1'	1.36	1.36	1.36
unstable trans	R=-CH₂-C₆H₄-C₆H₅ (6.4)	R=-CH₂-C₆H₅ (6.2)	R=Me
211'2'	141.3	141.3	142.2
311'3'	160.0	159.7	162.5
211'3'	29.3	29.5	27.7
311'2'	29.3	29.5	27.7
average	29.3	29.5	27.7
1-1'	1.37	1.37	1.37
unstable cis	R=-CH₂-C₆H₄-C₆H₅ (6.4)	R=-CH₂-C₆H₅ (6.2)	R=Me
211'2'	33.0	32.2	31.4
311'3'	26.3	25.7	25.3
211'3'	150.2	151.0	151.7
311'2'	150.5	151.0	151.7
average	29.7	29.0	28.3
1-1'	1.37	1.37	1.37

Table 11: Geometrical parameters calculated for the four isomers of motor **6.4**, motor **6.2** and for the five-membered ring methyl motor. (dihedral angles in degrees and lengths in Angstroms).

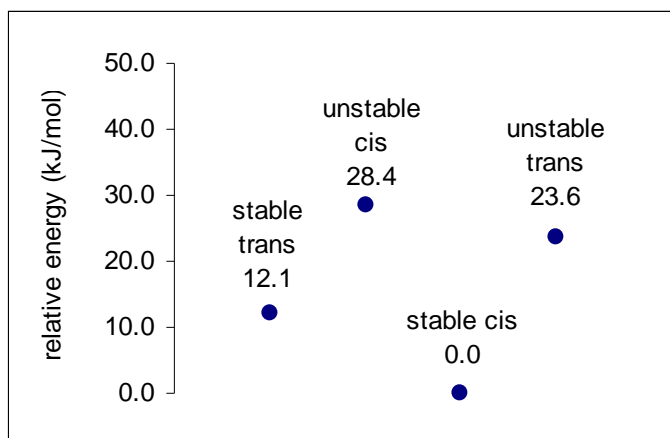


Figure 22: Relative energies (kJ/mol) of the four isomers of motor **6.4**, calculated by DFT thermochemical analysis at 25°C.

Also in this case, calculations on the transition states were not performed. Therefore, conclusions on the expected half lives of the two unstable forms can not be drawn.

6.5.4 $^1\text{H-NMR}$ measurements

In Figure 23a the region between 9 and 6 ppm of the $^1\text{H-NMR}$ spectrum of a sample of motor *trans* **6.4** in $\text{DCM-}d_2$ at -50°C is shown. All the absorptions in the aromatic region can be assigned by comparison with the data reported for motor **6.2** (*vide supra*) and in chapter 2 for the five-five membered ring motor (the absorptions left without assignment belong to the protons of the biphenyl group).

The sample was irradiated with a 365 nm lamp for 4 h, while kept at -75°C in an ethanol bath. The color changed from slightly yellow to more intense yellow. The spectrum was then measured again at -50°C (Figure 23b) and a shift of every absorption is observed. The new isomer obtained can be identified as the unstable *cis* by considering that the aromatic protons of the naphthalene moieties absorb in the range of 6.5-7.7 ppm, and the absorptions could be assigned by comparison with the data reported for motor **6.2** (*vide supra*). A lower range in absorption for the naphthalene moiety is indeed consistent with a *cis* conformation, as the two naphthalene moieties are in closer proximity. No residual stable *trans* is detectable, implying a quantitative photoconversion on $^1\text{H-NMR}$ scale.

Subsequently, the temperature of the sample was increased to 30°C for about 15 min. The color of the sample changed for less intense yellow. The spectrum was then measured again at -50°C (Figure 23c). All the absorptions resulted shifted once again. A comparison with previous results on motor **6.2** (*vide supra*) and on the five-five membered ring motor

Chapter 6

measured in the same solvent (chapter 2) indicates that this new isomer is the stable *cis* (range of the absorptions of the aromatic protons from about 6.3 to 7.8 ppm).

Interestingly, absorptions of stable *trans* isomer are now visible in an amount of ca. 5% (see region between 7.8 and 8.5 ppm). As in the photoisomerization step no residual stable *trans* was found, which indicates that the unstable *cis*, although the stable *cis* isomer remains the main product, can thermally convert also back to the stable *trans* isomer in a minor but detectable amount.

A second irradiation experiment was performed on the same sample with a 365 nm light for 4 h, while kept at -75°C in an ethanol bath. The ¹H-NMR spectrum was then measured at -50°C (Figure 23d). A shift of all the absorptions of the protons of the motor moiety was observed, implying full conversion to a new isomer, which can be identified as the unstable *trans* by considering the absorption range of the aromatic protons of the naphthalene moiety (7.2-8.2 ppm) and comparing with previous results (chapter 2 and motor **6.2**). Also in this case, the yellow color of the sample became more intense. Residual stable *cis* is not detected, implying a quantitative photoconversion with the limit of ¹H-NMR spectroscopic detection.

The sample was then warmed to room temperature for ca. 2 min, and subsequently another ¹H-NMR was acquired at -50°C (Figure 23e). This spectrum was identical to the one in Figure 23a (stable *trans* **6.4**), indicating that the second thermal step has occurred, and a full 360° cycle around the central double bond has been performed.

It is remarkable that at the PSS the conversion from the stable to the unstable isomer appeared to be higher than 95% in both photochemical steps.

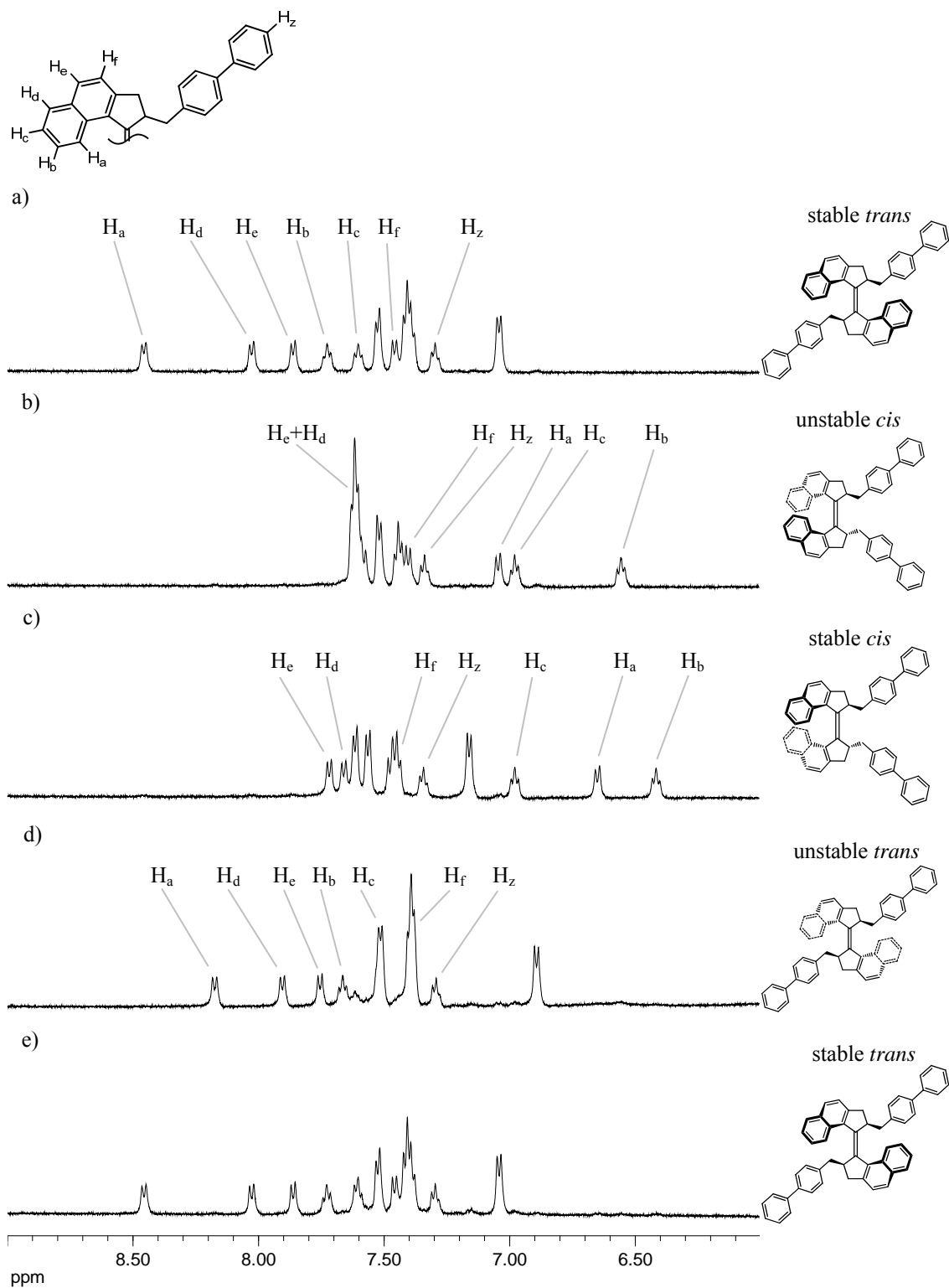
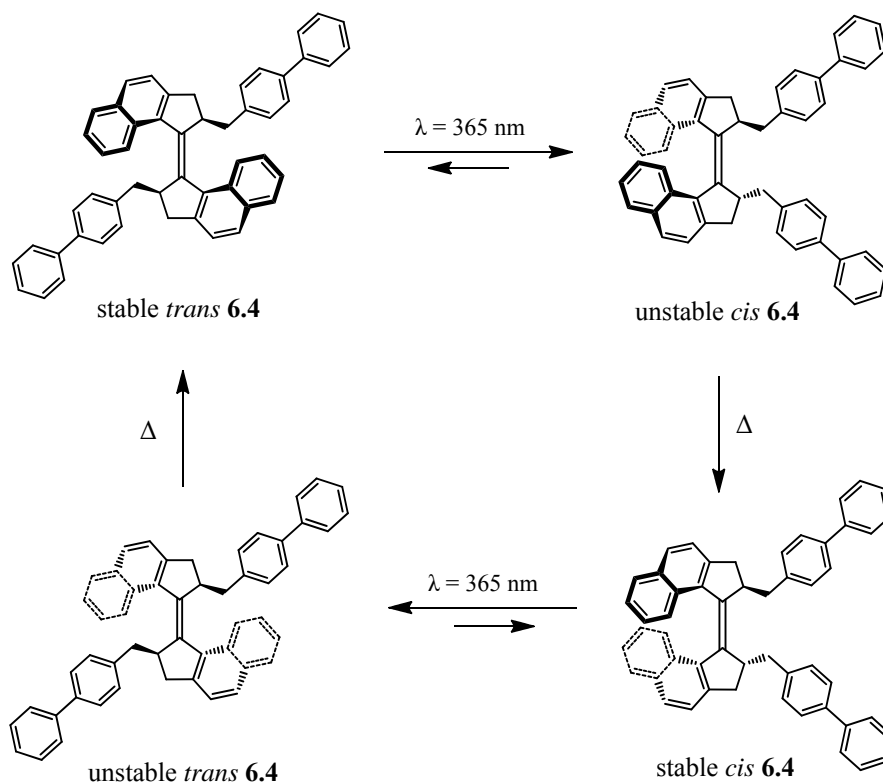


Figure 23: ¹H-NMR measurements of motor 6.4 in DCM-d₂. a) stable *trans*; b) PSS after first irradiation (λ = 365 nm): unstable *cis*; c) first thermal step: stable *cis*; d) PSS after second irradiation (λ = 365 nm): unstable *trans*; e) second thermal step: stable *trans*. (All the spectra were acquired at -50°C).

Based on the spectroscopic data, we can conclude that molecule **6.4** functions as a controllable unidirectional rotor. The full rotary cycle is shown in Scheme 14.



Scheme 14: Rotary cycle of motor **6.4**.

6.5.5 UV/Vis measurements

A $1.4 \cdot 10^{-5}$ M solution of motor *trans* **6.4** in dichloromethane was used for UV/Vis spectroscopic measurements. The UV/Vis spectra of the first half of the cycle are shown in Figure 24a. The spectrum at -15°C was acquired, presenting two maxima at 356 nm and 372 nm. The sample was kept at this temperature and irradiated with 365 nm light until the PSS was reached. As in the $^1\text{H-NMR}$ experiments a conversion of stable *trans* **6.4** higher than 95% was observed after irradiation, and considering that the solvent and the light used were the same employed in this experiment, the same conversion can be expected here. This means that the UV/Vis spectrum at the PSS is well representative of the unstable *cis*

6.4 isomer. A bathochromic and hypochromic effect was observed, with a maximum at 404 nm. This red-shift is consistent with the generation of a higher energy isomer, due to the increased strain of the central double bond. Increasing the temperature to 30°C for about 60 min led the UV/Vis spectrum to change to give a maximum at 372 nm. This UV/Vis spectrum is characteristic of a stable *cis* isomer, and indicates therefore that the expected thermal rearrangement did occur.

The same sample was used for the study of the second half of the cycle; UV/Vis spectra are shown in Figure 24b. First, the spectrum of the obtained stable *cis* **6.4** was reacquired at -40°C. The sample was then irradiated with a 365 nm light while kept at this temperature, until the PSS was reached. As in the NMR experiments a conversion of stable *cis* **6.4** higher than 95% was observed after irradiation, and considering that the solvent and the light used were the same employed in this experiment, the same conversion can be expected here. This means that the UV/Vis spectrum at the PSS is representative of the unstable *trans* **6.4** isomer. A bathochromic and hyperchromic effect were observed, with a maximum at 402 nm. As before, this red-shift is consistent with the generation of a higher energy isomer, due to the increased strain of the central double bond. Increasing the temperature to 20°C for 10 min led the UV/Vis spectrum to change to give two maxima at 356 and 373 nm. This UV/Vis spectrum was found to be identical to the spectrum of the initial isomer stable *trans* **6.4** (Figure 24a). The slight difference in the UV/Vis of stable *trans* **6.4** in the final spectrum after one cycle compared with the one of the initial stable *trans* **6.4** (the two maxima slightly lower, the region after 400 nm slightly higher) can be expected since the conversion at the two PSS is higher than 95% but less than 100% (see ¹H-NMR spectroscopic experiments). Therefore, after completing one cycle of rotation, the amount of motor in the *trans* isomer is nearly 100%, with a minor amount of the sample being in the *cis* configuration (< 5%).

In order to demonstrate the unimolecularity of each of the four steps of the cycle and support the 360° unidirectional rotation ability of the motor, the presence of isosbestic points was verified for each of the four steps. The results are shown in Figure 25. Figure 25a and Figure 25c refer to the photochemical steps, and were obtained at regular intervals during irradiation; Figure 25b and Figure 25d refer to the thermal steps, and were obtained at regular intervals of time during the thermal inversions.

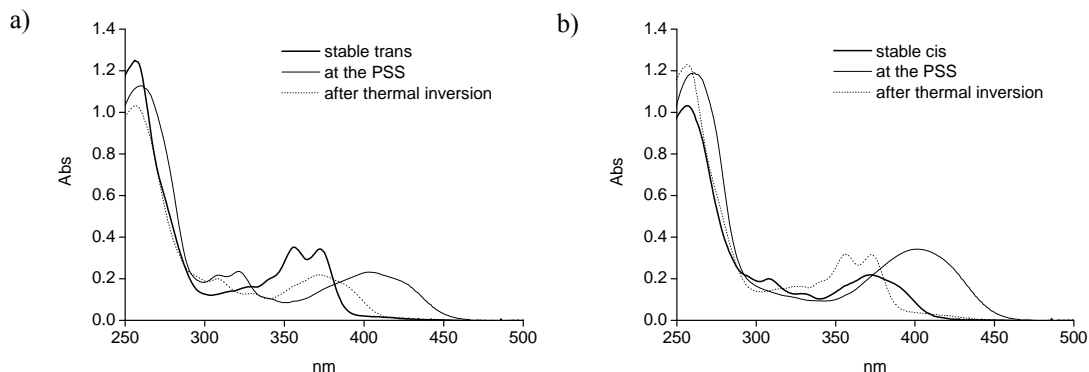


Figure 24: UV/Vis study of molecule **6.4** ($1.4 \cdot 10^{-5}$ M in DCM). a) first half of the cycle: stable *trans* (thick line), PSS after irradiation (main product: unstable *cis*, thin line), after thermal inversion (main product: stable *cis*, dotted line); b) second half of the cycle: sample after the first thermal inversion (thick line, main product: stable *cis*), PSS after irradiation (main product: unstable *trans*, thin line), after thermal inversion (main product: stable *trans*, dotted line).

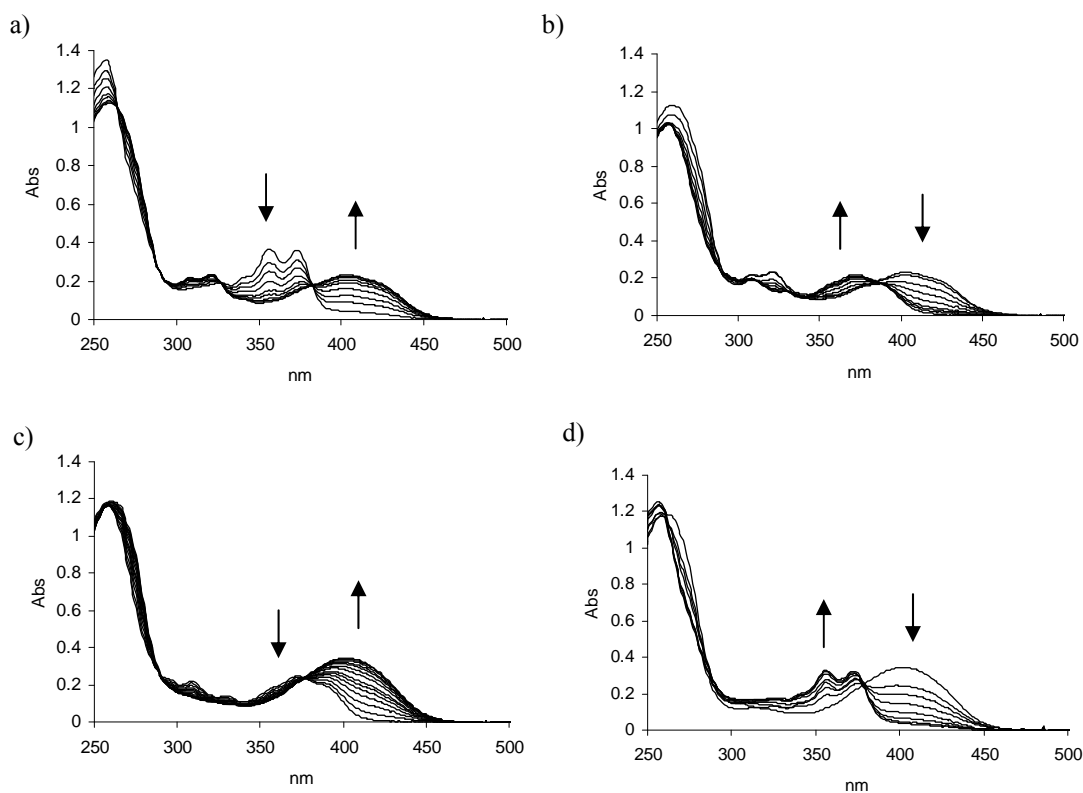


Figure 25: UV/Vis irradiation and thermal inversion experiments for **6.4** ($1.4 \cdot 10^{-5}$ M in DCM). a) photochemical step from stable *trans* to unstable *cis* ($\lambda = 365$ nm); b) thermal step from unstable *cis* to stable *cis* ($T = 60^\circ\text{C}$); c) photochemical step from stable *cis* to unstable *trans* ($\lambda = 365$ nm); d) thermal step from unstable *trans* to stable *trans* ($-10^\circ\text{C} < T < 0^\circ\text{C}$).

6.5.6 Kinetic study

UV/Vis spectroscopic measurements were also performed to study the kinetics of the two thermal steps. A 300 nm filter was mounted on the exit of the UV/Vis light source to cut off high energy light that might otherwise induce unwanted photochemistry during the thermal conversion. The changes in UV/Vis absorption spectrum as a function of time due to the thermal inversion at the specific wavelengths at different temperatures (10, 20, 25 and 30°C for the thermal step of unstable *cis* **6.4** to stable *cis* **6.4** and -5, 0, 5 and 10°C for the thermal step of unstable *trans* **6.4** to stable *trans* **6.4**) were measured. From these data the rate constants (k) for the first-order thermal helix inversion processes at the different temperatures were obtained. The enthalpy of activation ($\Delta^\ddagger H^\circ$) and entropy of activation ($\Delta^\ddagger S^\circ$) were determined from the rate constant by means of the Eyring plot, and from this, the Gibbs free energy of activation ($\Delta^\ddagger G_{20^\circ\text{C}}$) and the half life ($t_{1/2}^{20^\circ\text{C}}$) at room temperature (20°C) were calculated. The Eyring plots of the first thermal step (unstable *cis* to stable *cis*) and of the second thermal step (unstable *trans* to stable *trans*) are shown in Figure 20a and Figure 20b, respectively. The thermodynamic results are shown in Table 12.

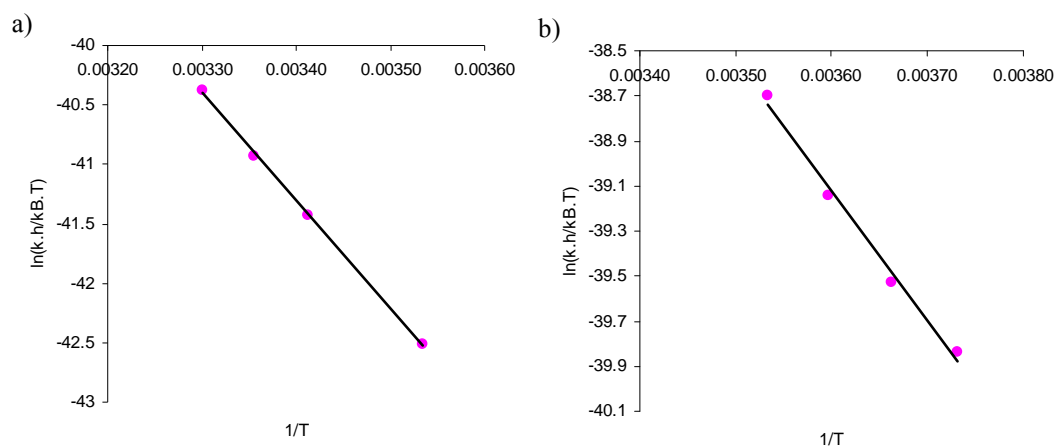


Figure 26: Eyring plot of motor **6.4**, relative to: a) the first thermal step (unstable to stable *cis*), and b) the second thermal step (unstable to stable *trans*).

	unstable to stable <i>trans</i>	unstable to stable <i>cis</i>
$k^{20^\circ\text{C}}$	$2.0 \cdot 10^{-2} \text{ s}^{-1}$	$6.1 \cdot 10^{-4} \text{ s}^{-1}$
$\Delta^\ddagger H^\circ$	$51 \text{ kJ} \cdot \text{mol}^{-1}$	$67 \text{ kJ} \cdot \text{mol}^{-1}$
$\Delta^\ddagger S^\circ$	$-103 \text{ J} \cdot \text{K}^{-1} \cdot \text{mol}^{-1}$	$-78 \text{ J} \cdot \text{K}^{-1} \cdot \text{mol}^{-1}$
$\Delta^\ddagger G_{20^\circ\text{C}}$	$93 \text{ kJ} \cdot \text{mol}^{-1}$	$90 \text{ kJ} \cdot \text{mol}^{-1}$
$t_{1/2}^{20^\circ\text{C}}$	34 s	18 min

Table 12: Thermodynamic data for motor **6.4**.

6.6 Conclusions and discussions

Four new first generation molecular motors **6.1**, **6.2**, **6.3** and **6.4**, where the methyl group at the stereogenic center has been changed for aromatic or benzylic substituents, have been successfully synthesized. Their unidirectional rotary function was studied by ^1H -NMR and UV/Vis spectroscopies, and confirmed in all cases.

In case of motor **6.1**, a slow competing photoconversion from the stable *cis* isomer directly to the stable *trans* has been observed as a minor pathway.

In case of motor **6.3**, a ca. 5% thermal conversion of the unstable *cis* back to the stable *trans* has been observed. Remarkably, this does not compromise the unidirectionality of the rotation, as the unstable to stable *cis* and the unstable to stable *trans* thermal isomerization steps are irreversible.

Moreover, based on temperature dependent ^1H -NMR data in motor **6.1** the free rotation of the phenyl group has been found to be blocked in the unstable *trans* isomer, due to the considerable steric hindrance with the naphthalene moiety. Therefore, motor **6.1** can be seen as a rotation-on-rotation-off switching system concomitant with the switching between the stable *cis* and the unstable *trans* isomers.¹⁷

The same is expected for motor **6.3**. However, due to the overlap of the absorptions of the arylphenyl protons in the ^1H -NMR spectroscopic measurements, this could not be verified.

In Table 13 the kinetic data of some of the currently reported five-five membered ring first and second generation molecular motors are shown. Considering first and second generation motors with the same substituent at the stereogenic center (entries 1 and 2, 3 and 4, and 8 and 9), it can be concluded that the $t_{1/2}$'s values associated with of the second generation model are always in between the $t_{1/2}$'s of the unstable-stable *trans* and the unstable-stable *cis* thermal isomerization of the first generation analogous.

A correlation between the substituent at the stereogenic center and speed of the thermal isomerization for the second generation motors has already been observed.¹ Some conclusions can be also drawn for first generation molecular motors regarding the unstable-stable *trans* thermal isomerization step, where the naphthalene moiety has to pass over the (more or less bulky) substituent at the stereogenic centers.

Motors **6.2** and **6.4** (entries 5 and 7, respectively) have groups connected to the stereogenic centers the flexibility of which is comparable, as bonded to the stereogenic centers are benzylic groups in both cases. This also implies that comparable steric hindrance is offered.

The half lives of motors **6.2** and **6.4** do not differ significantly from each other. Therefore, one further aromatic ring connected in *para* to the benzylic group in motor **6.4**, does not affect significantly the speed of the thermal inversions.

On the contrary, considering motors **6.1** and **6.3** (entries 3 and 6, respectively) where the aromatic groups are directly connected to the stereogenic centers, half lives about twice as long were found for motor **6.3** compared with **6.1**. Therefore, the presence of a group which gives more flexibility to the structure (benzylic carbon in motors **6.2** and **6.4**) does play a role in determining the speed of the rotation.

These connection between structure and speed must be taken into account in a further functionalization of molecular motors for future applications in nanotechnology.

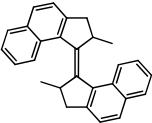
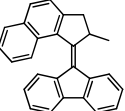
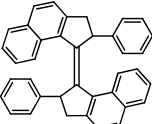
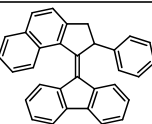
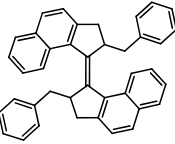
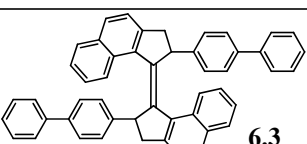
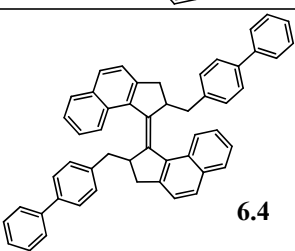
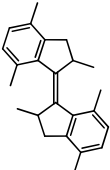
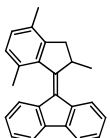
entry	motor	unstable-stable <i>trans</i>		unstable-stable <i>cis</i>	
		$t_{1/2}^{20^\circ\text{C}}$	$\Delta^\ddagger G_{20^\circ\text{C}}$ (kJ/mol)	$t_{1/2}^{20^\circ\text{C}}$	$\Delta^\ddagger G_{20^\circ\text{C}}$ (kJ/mol)
1 (ref. 3)		18 s	80	74 min	93
2 (ref. 1)		190 s	85		
3	 6.1	9 s	78	8 h	98
4 (ref. 1)		587 s	88		
5	 6.2	33 s	81	13 min	89
6	 6.3	21 s	80	18 h	100
7	 6.4	38 s	81	18 min	90
8 (ref. 30)		1.2 s	71	>1.5 d	101
9 (ref. 30)		15 s	79		

Table 13: Summary of half lives for reported five-five membered ring first and second generation molecular motors.

6.7 Experimental section

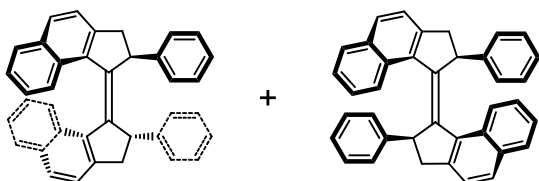
6.7.1 General remarks

For general informations, see general remarks in the experimental section of Chapter 2.

6.7.2 Computational details

The Hyperchem v.7.52 software package²⁴ was first used for a semiempirical PM3 preoptimization of all the structures. Subsequently, the Gaussian 03W (rev. B.03) software package¹⁰ was used for all the other calculations. The PM3 structures were used for a further optimization at the DFT B3-LYP/6-31G(d,p) level.³¹ To verify that they were at energy minima, a frequency analysis was performed, which gave only positive eigenvalues in all cases.

For the ¹H-NMR calculations, the DFT structures were reoptimized at the same level including the solvent effect of dichloromethane using the integral equation formalism of the polarizable continuum model (IEFPCM).¹⁵ The shielding constants were calculated with the gauge-including-atomic-orbital (GIAO) method¹⁴ at the DFT B3-PW91/6-31G(2d,p) level of theory,^{31b,32} also applying the IEFPCM formalism for dichloromethane. The values obtained for the shielding constants were converted in a ppm scale by subtracting the value obtained for TMS calculated in the same way. This not only makes the comparison with experimental data easier, but also compensates to some extent for the error due to correlation effects.³³



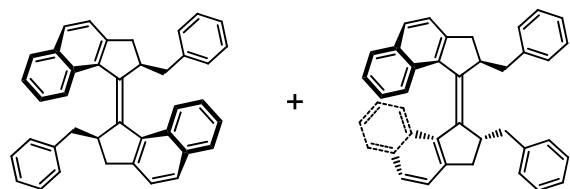
(2*R,2'*R**)-(*P**,*P**)-*trans*-(±)- and (2*R**,2'*R**)-(*P**,*P**)-*cis*-(±)-2,2'-diphenyl-2,2',3,3'-tetrahydro-1,1'-bicyclopenta[*a*]naphthalenyliene** (this structure does not express the absolute stereochemistry of the molecule) (**6.1**):

Titanium tetrachloride (170 μl, 1.5 mmol) was added dropwise to a suspension of zinc powder (203 mg, 3.1 mmol) in 10 ml of dry THF under vigorous stirring at 0°C. After refluxing for 2 h, ketone **6.5** (200 mg, 0.8 mmol) was added, and the solution was heated at

reflux overnight. The reaction was quenched with sat. aq. NH_4Cl (5 ml), and the mixture was extracted 4 times with 15 ml of ethyl acetate. The organic layers were collected, dried with MgSO_4 , filtered, and the solvent was eliminated under vacuum. Flash column chromatography on silica gel using heptane with a 0 to 3% gradient of toluene as eluent (*trans*: $R_f = 0.21$, *cis*: $R_f = 0.14$ in heptane/toluene 90:10) gave the *trans* as a pale yellow solid (22 mg, 0.045 mmol, 11%), and the *cis* isomer as a yellow solid (9 mg, 0.019 mmol, 5%). Further purification could be achieved by recrystallizing the *trans* **6.1** from DCM/MeOH at 5°C, and the *cis* **6.1** from DCM/MeOH at room temperature.

trans: ^1H NMR (400 MHz, CDCl_3) δ ppm 7.84 (d, $J = 8.0$ Hz, 2H), 7.73 (d, $J = 8.1$ Hz, 4H), 7.37-7.32 (m, 2H), 7.27 (d, $J = 8.4$ Hz, 2H), 7.22-7.11 (m, 10H), 6.87 (t, $J = 7.6$ Hz, 2H), 4.29 (d, $J = 6.5$ Hz, 2H), 3.51 (dd, $J = 15.0, 6.6$ Hz, 2H), 2.79 (d, $J = 14.9$ Hz, 2H). ^1H NMR (500 MHz, CD_2Cl_2 , -10°C) δ ppm 7.84 (d, $J = 8.3$ Hz, 2H), 7.74 (d, $J = 8.1$ Hz, 2H), 7.71 (d, $J = 8.3$ Hz, 2H), 7.34 (t, $J = 7.6$ Hz, 2H), 7.29 (d, $J = 8.1$ Hz, 2H), 7.22-7.14 (m, 10H), 6.82 (t, $J = 7.7$ Hz, 2H), 4.27 (d, $J = 6.5$ Hz, 2H), 3.51 (dd, $J = 14.8, 6.5$ Hz, 2H), 2.78 (d, $J = 15.1$ Hz, 2H). ^{13}C NMR (101 MHz, CDCl_3) δ ppm 145.4, 140.8, 140.2, 139.4, 133.0, 128.9, 128.7, 128.2, 128.1, 128.1, 127.8, 125.8, 125.4, 124.9, 123.7, 54.1, 43.3.

cis: ^1H NMR (400 MHz, CDCl_3) δ ppm 7.77-7.66 (m, 4H), 7.38 (d, $J = 8.2$ Hz, 2H), 7.21-7.13 (m, 12H), 7.04 (t, $J = 7.5$ Hz, 2H), 6.84 (d, $J = 8.4$ Hz, 2H), 6.48 (t, $J = 7.6$ Hz, 2H), 4.51 (d, $J = 7.1$ Hz, 2H), 3.86 (dd, $J = 15.6, 7.2$ Hz, 2H), 2.97 (d, $J = 15.6$ Hz, 2H). ^1H NMR (500 MHz, CD_2Cl_2) δ ppm 7.75 (d, $J = 8.2$ Hz, 2H), 7.71 (d, $J = 8.3$ Hz, 2H), 7.42 (d, $J = 8.1$ Hz, 2H), 7.21-7.12 (m, 10H), 7.04 (t, $J = 7.6$ Hz, 2H), 6.88 (d, $J = 8.0$ Hz, 2H), 6.49 (t, $J = 7.7$ Hz, 2H), 4.50 (d, $J = 7.0$ Hz, 2H), 3.88 (dd, $J = 15.4, 7.2$ Hz, 2H), 2.99 (d, $J = 15.5$ Hz, 2H). ^{13}C NMR (101 MHz, CDCl_3) δ ppm 145.6, 143.9, 139.0, 138.1, 132.4, 129.2, 129.1, 128.4, 127.8, 127.2, 126.6, 126.1, 124.5, 124.4, 123.2, 52.9, 42.4. HRMS: calcd. for $\text{C}_{38}\text{H}_{28}$: 484.2185, found 484.2164.



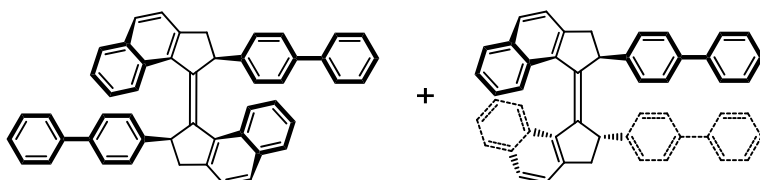
(2*R,2'*R**)-(*P**,*P**)-*trans*-(±)- and (2*R**,2'*R**)-(*P**,*P**)-*cis*-(±)-2,2'-dibenzyl-2,2',3,3'-tetrahydro-1,1'-bicyclopenta[a]naphthalenyldiene** (this structure does not express the absolute stereochemistry of the molecule) (**6.2**):

Titanium tetrachloride (482 μl , 4.4 mmol) was added dropwise to a suspension of zinc powder (571 mg, 8.7 mmol) in 30 ml of dry THF under vigorous stirring at 0°C. After refluxing for 2 h, a solution of ketone **6.9** (595 mg, 2.2 mmol) in dry THF (7 ml) was added, and the solution was heated at reflux overnight. The reaction was quenched with sat. aq. NH_4Cl (5 ml), the volatiles were removed under reduced pressure, and the mixture was extracted 4 times with 30 ml of ethyl acetate. The organic layers were collected, dried

with MgSO_4 , filtered, and the solvent was removed under vacuum. Flash column chromatography on silica gel using heptane with a 20 to 50% gradient of toluene as eluent ($R_f = 0.45$ in heptane/toluene 80:20 and $R_f = 0.75$ in heptane/toluene 50:50) gave a mixture of *cis* and *trans* in a 1:1 isomeric ratio (243 mg, 0.47 mmol, 43%). Separation between *cis* and *trans* was achieved with flash column chromatography on silica gel with 5% AgNO_3 ²³ using pentane with a 5 to 80% gradient of toluene as eluent (*trans*: $R_f = 0.36$, *cis*: $R_f = 0.22$ in pentane/toluene 80:20; *trans*: $R_f = 0.60$, *cis*: $R_f = 0.42$ in pentane/toluene 50:50), which gave *trans* **6.2** as pale yellow solid and *cis* **6.2** as a yellow solid. For both the isomers, further purification could be achieved by recrystallizing from chloroform/heptane.

trans: m.p. = 194.4-195.0°C. ^1H NMR (400 MHz, CDCl_3) δ ppm 8.48 (d, $J = 8.1$ Hz, 2H), 8.03 (d, $J = 8.1$ Hz, 2H), 7.86 (d, $J = 8.1$ Hz, 2H), 7.67 (t, $J = 7.2$ Hz, 2H), 7.60 (t, $J = 7.4$ Hz, 2H), 7.44 (d, $J = 8.1$ Hz, 2H), 7.24-7.13 (m, 6H), 7.01 (d, $J = 7.6$ Hz, 4H), 3.63 (d, $J = 13.8$ Hz, 2H), 3.34-3.26 (m, 2H), 2.74 (dd, $J = 15.1, 5.3$ Hz, 2H), 2.57 (dd, $J = 13.9, 11.8$ Hz, 2H), 2.48 (d, $J = 15.1$ Hz, 2H). ^1H NMR (500 MHz, CD_2Cl_2) δ ppm 8.42 (d, $J = 8.5$ Hz, 2H), 8.00 (d, $J = 8.7$ Hz, 2H), 7.84 (d, $J = 8.1$ Hz, 2H), 7.64 (t, $J = 7.6$ Hz, 2H), 7.56 (t, $J = 7.5$ Hz, 2H), 7.42 (d, $J = 8.1$ Hz, 2H), 7.19-7.10 (m, 6H), 6.98-6.96 (m, 4H), 3.6 (d, $J = 14.05$ Hz, 2H), 3.24-3.19 (m, 2H), 2.70 (dd, $J = 14.9, 5.7$ Hz, 2H), 2.51 (dd, $J = 14.2, 11.5$ Hz, 2H), 2.44 (d, $J = 15.1$ Hz, 2H). ^{13}C NMR (101 MHz, CDCl_3) δ ppm 141.6, 140.9, 140.6, 139.0, 133.1, 130.1, 129.3, 128.8, 128.1, 128.1, 126.5, 125.9, 124.9, 124.1, 50.1, 37.9, 36.7. HRMS: calcd. for $\text{C}_{40}\text{H}_{32}$: 512.25040, found 512.24825. Elem. anal. (%): calcd. for $\text{C}_{40}\text{H}_{32}$: C, 93.71; H, 6.29; found C, 93.20; H, 6.24.

cis: m.p. = 195.1-195.7°C. ^1H NMR (400 MHz, CDCl_3) δ ppm 7.73 (d, $J = 8.1$ Hz, 2H), 7.67 (d, $J = 8.2$ Hz, 2H), 7.46 (d, $J = 8.1$ Hz, 2H), 7.36-7.30 (m, 4H), 7.25-7.22 (m, 2H), 7.12 (d, $J = 6.8$ Hz, 4H), 6.99 (t, $J = 7.5$ Hz, 2H), 6.62 (d, $J = 8.4$ Hz, 2H), 6.43 (t, $J = 7.6$ Hz, 2H), 3.16-3.03 (m, 2H), 2.70 (dd, $J = 13.3, 7.8$ Hz, 2H), 2.61-2.53 (m, 2H). ^1H NMR (500 MHz, CD_2Cl_2) δ ppm 7.72 (d, $J = 8.0$ Hz, 2H), 7.66 (d, $J = 8.1$ Hz, 2H), 7.47 (d, $J = 8.1$ Hz, 2H), 7.32-7.28 (m, 4H), 7.24-7.20 (m, 2H), 7.11 (d, $J = 6.8$ Hz, 4H), 6.97 (t, $J = 7.5$ Hz, 2H), 6.63 (d, $J = 8.5$ Hz, 2H), 6.41 (t, $J = 7.7$ Hz, 2H), 3.16-3.04 (m, 4H), 2.68 (dd, $J = 13.5, 7.6$ Hz, 2H), 2.57 (d, $J = 14.9$ Hz, 2H), 2.55 (dd, $J = 13.3, 7.4$ Hz, 2H). ^{13}C NMR (101 MHz, CDCl_3) δ ppm 143.9, 141.0, 139.1, 137.3, 132.2, 129.7, 129.5, 128.5, 128.1, 127.7, 126.3, 126.0, 124.2, 124.1, 123.4, 50.1, 40.8, 38.5.

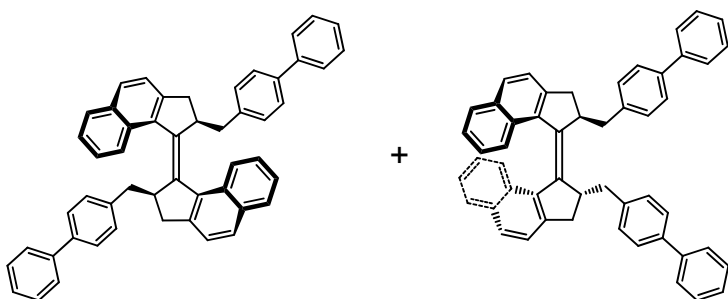


($2R^*, 2'R^*$)-(P^*, P^*)-*trans*-(\pm)- and ($2R^*, 2'R^*$)-(P^*, P^*)-*cis*-(\pm)-2,2'-di(diphenyl)-2,2',3,3'-tetrahydro-1,1'-bicyclopenta[a]naphthalenyldene (this structure does not express the absolute stereochemistry of the molecule) (**6.3**):

Titanium tetrachloride (90 μ l, 0.82 mmol) was added dropwise to a suspension of zinc powder (107 mg, 1.6 mmol) in 5 ml of dry THF under vigorous stirring at 0°C. After refluxing for 2 h, a solution of ketone **6.13** (595 mg, 2.2 mmol) in dry THF (2 ml) was added, and the solution was heated at reflux overnight. The reaction was quenched with sat. aq. NH_4Cl (2 ml), the volatiles were removed under reduced pressure, and the mixture was extracted 3 times with 15 ml of ethyl acetate. The organic layers were collected, dried with MgSO_4 , filtered, and the solvent was eliminated under vacuum. Flash column chromatography on silica gel using heptane with a 0 to 50% gradient of toluene as eluent ($R_f = 0.20$ in heptane/toluene 80:20) gave a mixture of *cis* and *trans* in a 2:5 isomeric ratio (total: 31 mg, 0.49 mmol, 24%). A recrystallization of this mixture by slow diffusion of pentane into dichloromethane, gave *trans* **6.3** as a white solid.

trans: m.p. = 208.6-209.3°C. ^1H NMR (400 MHz, CDCl_3) δ ppm 7.87 (d, $J = 8.2$ Hz, 2H), 7.82 (d, $J = 8.3$ Hz, 2H), 7.77 (d, $J = 8.2$ Hz, 2H), 7.61-7.55 (m, 4H), 7.48-7.29 (m, 14H), 7.22 (d, $J = 8.3$ Hz, 4H), 6.93 (t, $J = 7.6$ Hz, 2H), 4.35 (d, $J = 6.5$ Hz, 2H), 3.56 (dd, $J = 15.0, 6.6$ Hz, 2H), 2.85 (d, $J = 15.0$ Hz, 2H). ^1H NMR (500 MHz, CD_2Cl_2) δ ppm 7.87 (d, $J = 8.2$ Hz, 2H), 7.84 (d, $J = 8.3$ Hz, 2H), 7.78 (d, $J = 8.1$ Hz, 2H), 7.6 (d, $J = 7.5$ Hz, 4H), 7.48 (d, $J = 8.2$ Hz, 4H), 7.41 (t, $J = 7.7$ Hz, 4H), 7.38 (t, $J = 7.4$ Hz, 2H), 7.34 (d, $J = 8.3$ Hz, 2H), 7.30 (t, $J = 7.4$ Hz, 2H), 7.26 (d, $J = 8.2$ Hz, 4H), 6.93 (t, $J = 7.6$ Hz, 2H), 4.35 (d, $J = 6.4$ Hz, 2H), 3.57 (dd, $J = 15.1, 6.5$ Hz, 2H), 2.85 (d, $J = 15.0$ Hz, 2H). ^{13}C NMR (101 MHz, CDCl_3) δ ppm 144.6, 140.9, 140.8, 140.3, 139.4, 138.5, 133.0, 128.9, 128.8, 128.6, 128.6, 128.2, 127.7, 126.9, 126.8, 126.8, 125.5, 125.0, 123.7, 53.8, 43.3. HRMS: calcd. for $\text{C}_{50}\text{H}_{37}$: 637.28898, found 637.28009.

cis: ^1H NMR (400 MHz, CDCl_3) δ ppm 7.77 (d, $J = 8.2$ Hz, 2H), 7.74 (d, $J = 8.3$ Hz, 2H), 7.54 (d, $J = 7.3$ Hz, 4H), 7.50-7.28 (m, 16H), 7.08 (t, $J = 7.5$ Hz, 2H), 6.97-6.92 (m, 2H), 6.53 (t, $J = 7.6$ Hz, 2H), 4.63 (d, $J = 7.1$ Hz, 2H), 3.94 (dd, $J = 15.5, 7.2$ Hz, 2H), 3.05 (d, $J = 15.6$ Hz, 2H). ^1H NMR (500 MHz, CD_2Cl_2) δ ppm 7.78 (d, $J = 8.1$ Hz, 2H), 7.73 (d, $J = 8.2$ Hz, 2H), 7.52 (d, $J = 7.5$ Hz, 4H), 7.47-7.42 (m, 6H), 7.38 (t, $J = 7.6$ Hz, 4H), 7.30 (d, $J = 8.2$ Hz, 4H), 7.06 (t, $J = 7.6$ Hz, 2H), 6.92 (d, $J = 8.5$ Hz, 2H), 6.53 (t, $J = 7.3$ Hz, 2H), 4.61 (d, $J = 6.9$ Hz, 2H), 3.94 (dd, $J = 15.6, 6.9$ Hz, 2H), 3.05 (d, $J = 15.5$ Hz, 2H). ^{13}C NMR (101 MHz, CDCl_3) δ ppm 144.8, 144.0, 140.9, 139.0, 138.1, 132.4, 129.3, 129.1, 128.6, 127.9, 127.6, 127.2, 126.9, 126.9, 126.8, 126.6, 124.6, 124.4, 123.2, 52.7, 42.5.

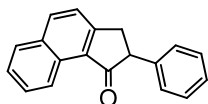


(2*R,2'*R**)-(*P**,*P**)-*trans*-(±)- and (2*R**,2'*R**)-(*P**,*P**)-*cis*-(±)-2,2'-di(4-arylbenzyl)-2,2',3,3'-tetrahydro-1,1'-bicyclopenta[*a*]naphthalenylidene** (this structure does not express the absolute stereochemistry of the molecule) (**6.4**):

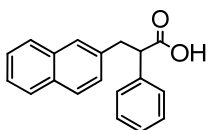
Titanium tetrachloride (157 μ l, 1.4 mmol) was added dropwise to a suspension of zinc powder (186 mg, 2.8 mmol) in 10 ml of dry THF under vigorous stirring at 0°C. After refluxing for 2 h, a solution of ketone **6.18** (248 mg, 0.71 mmol) in dry THF (2 ml) was added, and the solution was heated at reflux overnight. The reaction was quenched with sat. aq. NH_4Cl (5 ml), the volatiles were removed under reduced pressure, and the mixture was extracted 4 times with 25 ml of ethyl acetate. The organic layers were collected, dried with MgSO_4 , filtered, and the solvent was eliminated under vacuum. Flash column chromatography on silica gel using heptane with a 10 to 75% gradient of toluene as eluent ($R_f = 0.46$ in heptane/toluene 80:20 and $R_f = 0.62$ in heptane/toluene 50:50) gave a mixture of *cis* and *trans* in a 2:3 isomeric ratio (140 mg, 0.21 mmol, 59%). Separation of the *trans* could be achieved *via* additional flash column chromatography on silica gel with 10% AgNO_3 ²³ using heptane with a 20 to 100% gradient of toluene as eluent (*trans*: $R_f = 0.42$, *cis*: $R_f = 0.22$ in pentane/toluene 50:50), which gave fractions containing the *trans* only, and fractions still containing a mixture of *cis* and *trans*. Further purification for *trans* **6.4** was achieved by recrystallizing from toluene/heptane.

trans: ^1H NMR (400 MHz, CDCl_3) δ ppm 8.49 (d, $J = 8.0$ Hz, 2H), 8.03 (d, $J = 8.2$ Hz, 2H), 7.87 (d, $J = 8.1$ Hz, 2H), 7.69 (t, $J = 7.2$ Hz, 2H), 7.63-7.52 (m, 6H), 7.49-7.30 (m, 12H), 7.06 (d, $J = 7.9$ Hz, 4H), 3.64 (d, $J = 14.7$ Hz, 2H), 3.37-3.29 (m, 2H), 2.77 (dd, $J = 15.1, 5.3$ Hz, 2H), 2.62 (dd, $J = 13.9, 11.7$ Hz, 2H), 2.52 (d, $J = 15.1$ Hz, 2H). ^1H NMR (500 MHz, CD_2Cl_2) δ ppm 8.46 (d, $J = 8.9$ Hz, 2H), 8.02 (d, $J = 7.9$ Hz, 2H), 7.9 (d, $J = 8.1$ Hz, 2H), 7.68 (t, $J = 7.1$ Hz, 2H), 7.58 (t, $J = 7.5$ Hz, 2H), 7.54 (d, $J = 7.1$ Hz, 4H), 7.48-7.36 (m, 10H), 7.30 (t, $J = 7.0$ Hz, 2H), 7.06 (d, $J = 7.9$ Hz, 4H), 3.61 (d, $J = 14.3$ Hz, 2H), 3.30-3.24 (m, 2H), 2.76 (dd, $J = 14.7, 5.6$ Hz, 2H), 2.59 (dd, $J = 13.6, 11.7$ Hz, 2H), 2.51 (d, $J = 15.1$ Hz, 2H). ^{13}C NMR (101 MHz, CDCl_3) δ ppm 141.6, 140.9, 139.7, 139.0, 138.8, 133.1, 130.1, 129.7, 128.8, 128.6, 128.2, 126.9, 126.8, 126.5, 125.9, 124.9, 124.2, 124.1, 50.1, 37.6, 36.8, 29.7. HRMS: calcd. for $\text{C}_{52}\text{H}_{41}$: 665.32028, found 665.31974.

cis: ^1H NMR (500 MHz, CD_2Cl_2) δ ppm 7.73 (d, $J = 8.1$ Hz, 2H), 7.66 (d, $J = 7.4$ Hz, 2H), 7.61 (d, $J = 8.0$ Hz, 4H), 7.56 (d, $J = 8.1$ Hz, 4H), 7.48 (d, $J = 8.4$ Hz, 2H), 7.45 (t, $J = 7.4$ Hz, 4H), 7.35 (t, $J = 7.3$ Hz, 2H), 7.19 (d, $J = 8.1$ Hz, 4H), 6.98 (t, $J = 6.5$ Hz, 2H), 6.66 (d, $J = 8.2$ Hz, 2H), 6.42 (t, $J = 7.1$ Hz, 2H), 3.19-3.08 (m, 4H), 2.73-2.65 (m, 2H), 2.64-2.56 (m, 4H).

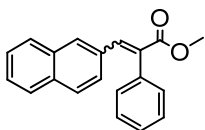


2-Phenyl-2,3-dihydro-cyclopenta[a]naphthalen-1-one (6.5): a solution of 3-naphthalen-2-yl-2-phenyl-propionic acid **6.6** (8.28 g, 30 mmol), SOCl_2 (20 ml) and DMF (2 drops) in CH_2Cl_2 (90 ml) was heated at reflux for 1 h. All volatiles were removed under reduced pressure, giving the crude acid chloride, which was dissolved in $\text{ClCH}_2\text{CH}_2\text{Cl}$ and cooled to 0°C . To the solution AlCl_3 (7.98 g, 60 mmol) was added quickly and the reaction mixture was stirred at 0°C for 30 min. The reaction was quenched with a saturated aqueous solution of NaHCO_3 (300 ml) and extracted with CH_2Cl_2 . After drying of the organic solvent over MgSO_4 the solvent was removed under low pressure. The crude residue was purified by column chromatography (SiO_2 , pentane:ether = 5:1), affording 5.65 g (73 %) of the ketone **6.5** as a white solid. ^1H NMR (400 MHz, CDCl_3) δ ppm 3.37 (dd, $J = 3.3$ Hz, $J = 18.0$ Hz, 1H), 3.78 (dd, $J = 7.7$ Hz, $J = 18.0$ Hz, 1H), 4.01 (dd, $J = 7.7$ Hz, $J = 3.3$ Hz, 1H), 7.24-7.30 (m, 3H), 7.34-7.37 (m, 2H), 7.58-7.61 (m, 2H), 7.69 (m, 1H), 7.94 (d, $J = 8.1$ Hz, 1H), 8.12 (d, $J = 7.3$ Hz, 1H), 9.17 (d, $J = 7.3$ Hz, 1H). ^{13}C NMR (75 MHz, CDCl_3) δ ppm 35.7, 53.5, 123.5, 123.7, 126.4, 126.6, 127.6, 127.9, 128.5, 128.7, 129.3, 129.7, 132.5, 135.8, 139.7, 156.8, 206.0. HRMS: calcd. for $\text{C}_{19}\text{H}_{14}\text{O}$: 258.105, found 258.104.



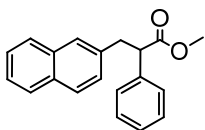
3-Naphthalen-2-yl-2-phenyl-propionic acid (6.6): a solution of methyl 3-naphthalen-2-yl-2-phenyl-propionate (**6.8**) (9.66 g, 35 mmol) and KOH (4.49 g, 80 mmol) in H_2O /EtOH 1:1 (100 ml) was stirred overnight under reflux. The reaction mixture was then acidified with HCl to pH = 1 and EtOH was removed under vacuum. The resulting aqueous mixture was extracted with CH_2Cl_2 (2×200 ml) and the combined organic layers were dried over MgSO_4 and concentrated under vacuum. The resulting solid was crystallized from Et_2O , affording 8.59 g (89%) of the acid **6.6** as a white solid.

^1H NMR (400 MHz, CDCl_3) δ ppm 3.12 (dd, $J = 7.3$, 13.6 Hz, 1H), 3.50 (dd, $J = 8.1$, 13.6 Hz, 1H), 3.90 (dd, $J = 8.1$, 7.3 Hz, 1H), 7.15-7.31 (m, 6H), 7.34-7.38 (m, 2H), 7.49 (s, 1H), 7.62-7.66 (m, 2H), 7.70 (m, 1H). ^{13}C NMR (75 MHz, CDCl_3) δ ppm 38.9, 53.6, 125.1, 125.6, 127.0, 127.1, 127.2, 127.3, 127.6, 127.8, 128.4, 131.8, 133.1, 135.8, 137.5, 179.1. HRMS: calcd. for $\text{C}_{19}\text{H}_{16}\text{O}_2$: 276.115, found 276.116. Elem. anal. (%): calcd. for $\text{C}_{19}\text{H}_{16}\text{O}_2$: C, 82.58; H, 5.84; O, 11.58; found C, 82.63; H, 5.81; O, 11.61.



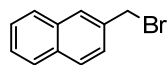
Methyl 3-naphthalen-2-yl-2-phenyl-acrylate (6.7): sodium hydroxyde was added in portions to a solution (diethoxyphosphoryl)- phenyl-acetic acid methyl ester (15.73 g, 55 mmol) in DME (150 ml) at 0°C. When the evolution of H₂ ceased, the reaction mixture was stirred at room temperature for 30 min and neat 2-naphthaldehyde (7.80 g, 50 mmol) was added. The solution was stirred at room temperature for 3 h and a saturated aq. solution of NH₄Cl was then added. The resulting mixture was extracted with CH₂Cl₂ (2 × 200 ml), the organics dried over MgSO₄ and concentrated under vacuum. The crude residue was purified by column chromatography (SiO₂, pentane:ether = 5:1), affording 11.10 g (77 %) of a mixture of alkenes *Z/E* (25:75) as a white solid.

¹H NMR (400 MHz, CDCl₃) δ 3.75 (s, 3H, CH₃ *Z*), 3.77 (s, 3H, CH₃ *E*), 6.93 (dd, *J* = 6.9, 1.6 Hz 1H, *E*), 7.16 (s, 1H, *Z*), 7.21-7.24 (m, 1H *E* and 1H *Z*), 7.33-7.50 (m, 3H *E* and 3H *Z*), 7.59-7.62 (m, 2H *Z*), 7.66 (d, *J* = 6.9 Hz, 1H, *Z*), 7.76-7.81 (m, 2H *E*), 7.98 (s, 1H, *E*).
¹³C NMR (75 MHz, CDCl₃) δ 52.1, (CH₃, *Z*), 52.3 (CH₃, *E*), 125.3 (CH *Z*), 126.2 (CH *E*), 126.3 (CH, *E*), 126.4 (CH *Z*), 126.7 (CH *Z*), 126.9 (CH *E*), 127.3 (CH *E*), 127.4 (CH *Z*), 127.5 (CH, *Z*), 127.8 (CH, *E*), 127.9 (CH *E*), 128.0 (CH *Z*), 128.1 (CH *Z*), 128.3 (CH *Z*), 128.4 (CH *E*), 128.5 2CH *E*), 128.6 (2CH *Z*), 129.8 (2CH *E* and 2CH *Z*), 131.4 (C *E*), 131.5 (C *Z*), 132.1 (C *E*), 132.4 (C *Z*), 132.8 (C *Z*), 132.9 (C *E*), 133.0 (C *Z*), 133.1 (C *E*), 134.9 (C *E*), 135.8 (C *Z*), 140.5 (CH *E*), 168.2 (C=O, *E*), 170.1 (C=O, *Z*). HRMS: calcd. for C₂₀H₁₆O₂: 288.116, found 288.115. Elem. anal. (%): calcd. for C₂₀H₁₆O₂: C, 83.31; H, 5.59; O, 11.10, found C, 83.37; H, 5.62; O, 11.08.



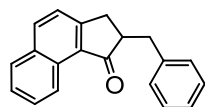
Methyl 3-naphthalen-2-yl-2-phenyl-propionate (6.8): a solution of methyl 3-naphthalen-2-yl-2-phenylacrylate (6.7) (10.94 g, 38 mmol) in MeOH (120 ml) was stirred overnight δ 10 % Pd on carbon (0.200 g) under a H₂ atmosphere. The reaction mixture was then filtered through celite and the solution was concentrated under vacuum. The crude residue was purified by crystallization from EtOH, affording 10.01 g (91 %) of the hydrogenated compound as a white solid.

¹H NMR (400 MHz, CDCl₃) δ 3.14 (dd, *J* = 6.6 Hz, *J* = 13.6 Hz, 1H), 3.54 (dd, *J* = 8.8, 13.6 Hz, 1H), 3.55 (s, 3H), 3.92 (dd, *J* = 6.6, 8.8 Hz, 1H), 7.20-7.31 (m, 6H), 7.35-7.42 (m, 2H), 7.53 (s, 1H), 7.67-7.75 (m, 3H). ¹³C NMR (75 MHz, CDCl₃) δ 39.9, 52.0, 53.5, 125.3, 125.8, 127.3, 127.4, 127.5, 127.6, 127.8, 127.9, 128.6, 132.1, 133.4, 136.5, 138.5, 173.7. HRMS: calcd. for C₂₀H₁₈O₂: 290.131, found 290.131. Elem. anal. (%): calcd. for C₂₀H₁₈O₂: C, 82.73; H, 6.25; O, 11.02; found C, 82.67; H, 6.22; O, 10.98.



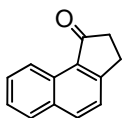
2-(Bromomethyl)naphthalene:³⁴ a solution of 2-methylnaphthalene (25 g, 176 mmol), NBS (31.3 g, 176 mmol) and dibenzoylperoxide (0.2 g, 0.8 mmol) in CCl_4 (200 ml) was heated at reflux for 18 h. The cooled solution was filtered and the solvent removed under reduced pressure. The brown solid was absorbed on silica and eluted with pentane ($R_f = 0.4$), to give the title compound as a white solid (26.3 g, 119 mmol, 68%). Alternatively, a recrystallization from pentane can also be performed, even if traces of succinimide were found to be more difficult to remove with this method.

^1H NMR (300 MHz, CDCl_3) δ 4.68 (s, 2H), 7.48-7.53 (m, 3H), 7.81-7.86 (m, 4H). ^{13}C NMR (101 MHz, CDCl_3) δ ppm 135.0, 133.1, 133.0, 128.7, 127.9, 127.8, 127.7, 126.7, 126.5, 126.4, 34.0.



2-Benzyl-2,3-dihydro-1H-cyclopenta[a]naphthalen-1-one (6.9): ketone **6.10** (2 g, 11.0 mmol) was dissolved in a 2:1 mixture of THF/DMPU.²² Next, NaH (0.53 g of a 50% oil mixture, 11.0 mmol) was added portionwise at 0°C while stirring. The temperature was allowed to raise to 20°C over night, while the solution kept under a nitrogen atmosphere. The obtained brown solution was added dropwise *via* cannula onto freshly distilled benzylbromide (4 ml, 33 mmol) to which NaI (5 mol%) was previously added. The mixture was stirred 1 d at room temperature. Subsequently, the reaction mixture was quenched with 4 ml of methanol. The volatiles were eliminated under reduced pressure, water (30 ml) was added, and the mixture was extracted three times with Et_2O (30 ml). The combined organic layers were dried over MgSO_4 and concentrated under vacuum. Purification was achieved by flash column chromatography on silica gel using heptane with a 20-30% gradient of toluene as eluent ($R_f = 0.25$ in toluene/heptane 1:1). Starting material (ketone **6.10**) was recovered in an amount of 42%. Product **6.9** was isolated as a very viscous yellow oil (599 mg, 2.2 mmol, 20%).

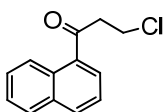
m.p. = 74.5-75.2°C. ^1H NMR (400 MHz, CDCl_3) δ ppm 9.22 (d, $J = 8.3$ Hz, 1H), 8.02 (d, $J = 8.4$ Hz, 1H), 7.89 (d, $J = 8.1$ Hz, 1H), 7.70 (t, $J = 7.6$ Hz, 1H), 7.57 (t, $J = 7.5$ Hz, 1H), 7.44 (d, $J = 8.4$ Hz, 1H), 7.38-7.27 (m, 5H), 3.50 (dd, $J = 14.0, 4.2$ Hz, 1H), 3.24 (dd, $J = 17.5, 7.3$ Hz, 1H), 3.15-3.07 (m, 1H), 2.95 (dd, $J = 17.5, 3.3$ Hz, 1H), 2.74 (dd, $J = 13.9, 10.5$ Hz, 1H). ^{13}C NMR (101 MHz, CDCl_3) δ ppm 208.2, 156.8, 139.7, 135.8, 132.6, 130.4, 129.4, 128.9, 128.9, 128.5, 128.1, 126.5, 126.5, 124.0, 123.9, 49.3, 37.2, 32.6. Elem. anal. (%): calcd. for $\text{C}_{20}\text{H}_{16}\text{O}$: C, 88.20; H, 5.92; found C, 88.08; H, 5.93.



2,3-Dihydro-1H-cyclopenta[a]naphthalen-1-one (6.10):²¹ compound **3.27** (32 g, 147 mmol) was poured onto stirring concentrated sulfuric acid (150 ml) over a period of 30 min. The mixture was warmed to 90°C for 2 h. Subsequently, the reaction mixture was poured onto ice, and extracted 4 times with 80 ml of DCM. After removal of the volatiles under vacuum, the residual brown oil was purified by flash column chromatography on silica gel, using toluene as eluent ($R_f = 0.21$). The product was isolated as a yellow solid (16.1 g, 88 mmol, 60%). Further purification can be achieved by recrystallization from ethyl acetate/heptane. The pure compound precipitates as yellow needles.

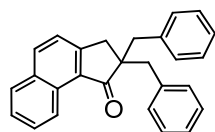
The spectroscopic data were in agreement with the data reported in literature.³⁵

m.p. = 105.0-105.2°C. ¹H NMR (400 MHz, $CDCl_3$) δ ppm 2.80 (m, 2H), 3.21 (m, 2H), 7.51 (d, $J = 8.5$ Hz, 1H), 7.54 (ddd, $J = 8.1, 6.9, 1.3$ Hz, 1H), 7.65 (ddd, $J = 8.3, 6.9, 1.3$ Hz, 1H), 7.88 (d, $J = 8.4$ Hz, 1H), 8.03 (d, $J = 8.4$ Hz, 1H), 9.16 (d, $J = 8.5$ Hz, 1H); ¹³C NMR (101 MHz, $CDCl_3$) δ ppm 207.6, 158.5, 135.7, 132.5, 131.0, 129.4, 128.9, 128.1, 126.6, 124.1, 124.0, 36.9, 26.2; IR (neat) ν 3055, 3030, 2924, 2861, 1692 cm^{-1} ; HRMS: calcd. for $C_{13}H_{10}O$ (M^+) 182.0732, found 182.0739.



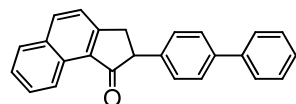
3-Chloro-1-(naphthalen-1-yl)propan-1-one (6.11):²⁰ a stirred slurry of $AlCl_3$ (70 g, 0.52 mol) in freshly distilled DCM (600 ml) was cooled to 0°C with an ice bath. 3-Chloro propionyl chloride (40 ml, 0.42 mol) was added, where up the $AlCl_3$ dissolved completely. Subsequently, naphthalene (51.5 g, 0.40 mol) was added portionwise over a period of half an hour. When the addition was completed, the ice bath was removed, and the solution was allowed to stir overnight. The solvent was removed by rotary evaporation, and the residual brown oil was purified by flash column chromatography on silica gel using as eluent a mixture of heptane and 5% of ethyl acetate ($R_f = 0.30$). The product was obtained as a yellow oil, and used for the next reaction without further purification (72 g, 0.329 mol, 82%).

¹H NMR (500 MHz, $CDCl_3$): δ ppm 3.51 (t, $J = 6.6$ Hz, 2H), 3.97 (t, $J = 6.6$ Hz, 2H), 7.49 (dd, $J = 7.3, 8.2$ Hz, 1H), 7.53 (ddd, $J = 1.2, 6.9, 8.1$ Hz, 1H), 7.59 (ddd, $J = 1.4, 6.7, 8.7$ Hz, 1H), 7.86 (d, $J = 7.6$ Hz, 2H), 7.99 (d, $J = 8.2$ Hz, 1H), 8.66 (d, $J = 8.2$ Hz, 1H). ¹³C NMR (126 MHz, $CDCl_3$): δ ppm 39.3, 44.4, 124.5, 125.9, 126.8, 128.2, 128.4, 128.6, 130.2, 133.5, 134.1, 135.1, 200.6. IR (neat): 3050 (w), 2968 (w), 1682 (s), 1593 (m), 1573 (m), 1508 (s), 1337 (s), 1236 (s), 1099 (s), 944 (m), 801 (s), 776 (s) cm^{-1} . HRMS: calcd. for $C_{13}H_{11}ClO$: 218.0498, found 218.0495.



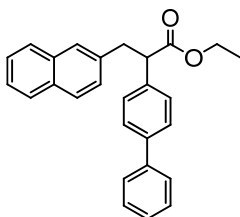
2,2-Dibenzyl-2,3-dihydro-1H-cyclopenta[a]naphthalen-1-one (6.12): this product was obtained as sideproduct from the reaction to provide ketone **6.9** ($R_f = 0.28$ in toluene/heptane 1:1). It was isolated as pale yellow solid (794mg, 2.2 mmol, 20%). It was recrystallized from DCM, giving colorless prismatic crystals.

m.p. = 109.8-110.5°C. $^1\text{H NMR}$ (400 MHz, CDCl_3) δ ppm 9.26 (d, $J = 8.4$ Hz, 1H), 7.81 (d, $J = 8.4$ Hz, 1H), 7.77 (d, $J = 8.1$ Hz, 1H), 7.70 (t, $J = 7.1$ Hz, 1H), 7.52 (t, $J = 7.0$ Hz, 1H), 7.23-7.04 (m, 11H), 3.35 (d, $J = 13.3$ Hz, 2H), 3.17 (s, 2H), 2.95 (d, $J = 13.3$ Hz, 2H). $^{13}\text{C NMR}$ (101 MHz, CDCl_3): δ ppm 210.6, 156.3, 137.2, 135.5, 132.3, 130.8, 130.1, 129.1, 128.7, 127.9, 127.9, 126.3, 126.2, 123.8, 123.4, 55.2, 43.6, 34.8. HRMS: calcd. for $\text{C}_{27}\text{H}_{22}\text{O}$: 362.16706, found 362.16596. Elem. anal. (%): calcd. for $\text{C}_{27}\text{H}_{22}\text{O}$: C, 89.47; H, 6.12; found C, 89.80; H, 6.14.



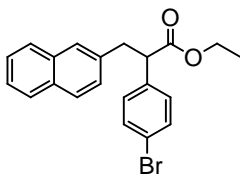
2-(Biphenyl-4-yl)-2,3-dihydro-1H-cyclopenta[a]naphthalen-1-one (6.13): acid **6.16** (630 mg, 1.8 mmol) was dissolved in dry DCM (20 ml) and the solution was cooled with an ice bath. Oxalylchloride (230 μl , 2.7 mmol) was slowly added while stirring, followed by 4 droplets of DMF. The ice bath was removed, and the mixture was stirred 2 h at room temperature. Subsequently, the volatiles were removed by rotary evaporation, and 30 ml of dry DCM were added to the oily residue of the acyl chloride **6.17**. Next, AlCl_3 (477 mg, 3.58 mmol) was added portionwise at 0°C while vigorously stirring. After 5 min at 0°C, the temperature was allowed to raise to room temperature, and stirring was continued for 6 h. Next, the reaction was quenched by adding 15 ml of water, and the product was extracted with ethylacetate (3×40 ml). The combined organic layers were dried over MgSO_4 and concentrated under vacuum. The product was purified with flash column chromatography on silica gel using heptane with a 0-80% gradient of toluene ($R_f = 0.23$ in heptane/toluene 1:1), after which it was recovered as a pale yellow solid (370 mg, 1.1 mmol, 62%). Further purification could be achieved with recrystallization from toluene/heptane, which gave product **6.13** as white needles.

m.p. = > 167°C (dec). $^1\text{H NMR}$ (400 MHz, CDCl_3) δ ppm 9.18 (d, $J = 8.3$ Hz, 1H), 8.13 (d, $J = 8.4$ Hz, 1H), 7.94 (d, $J = 8.2$ Hz, 1H), 7.70 (t, $J = 7.8$ Hz, 1H), 7.63-7.55 (m, 6H), 7.47-7.41 (m, 2H), 7.37-7.30 (m, 3H), 4.05 (dd, $J = 7.9, 3.5$ Hz, 1H), 3.81 (dd, $J = 17.9, 7.9$ Hz, 1H), 3.42 (dd, $J = 17.9, 7.9$ Hz, 1H). $^{13}\text{C NMR}$ (101 MHz, CDCl_3): δ ppm 206.3, 157.0, 140.8, 139.9, 138.9, 136.2, 132.9, 130.1, 129.7, 129.1, 128.7, 128.2, 128.1, 127.6, 127.1, 127.0, 126.7, 124.1, 123.7, 53.5, 36.1. HRMS: calcd. for $\text{C}_{25}\text{H}_{19}\text{O}$: 335.1430 (MH^+), found 335.1430. Elem. anal. (%): calcd. for $\text{C}_{25}\text{H}_{18}\text{O}$: C, 89.79; H, 5.43; found C, 89.81; H, 5.43.



Ethyl 2-(biphenyl-4-yl)-3-(naphthalen-2-yl)propanoate (6.14):²⁷ ester **6.15** (1 g, 2.6 mmol), phenylboronic acid (349 mg, 2.86 mmol) and potassium fluoride (697 mg, 5.72 mmol) were dissolved in 10 ml of a water/toluene mixture 1:1. Subsequently, tetrakis(triphenylphosphine)palladium (99.4 mg, 0.086 mmol, 3 mol%) was added while stirring. The mixture was heated at reflux for 7 h. Further 5 ml of water were added, and the product was extracted with ethylacetate (3 × 15 ml). The combined organic layers were dried over anhydrous Na₂SO₄, filtered and concentrated under vacuum. Flash column chromatography on silica gel using as eluent a gradient from 100-0% to 0-100% heptane/toluene (*R_f* = 0.23 in heptane/toluene, and 0.54 in neat toluene) gave product **6.14** as a white solid (0,809 g, 2.1 mmol, 81%). Further purification could be achieved by recrystallization from heptane.

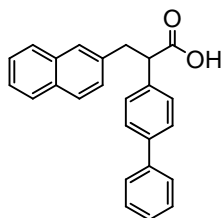
m.p. = 116.2-117.0°C. ¹H NMR (400 MHz, CDCl₃) δ ppm 7.87-7.77 (m, 3H), 7.70-7.58 (m, 5H), 7.53-7.44 (m, 6H), 7.42-7.34 (m, 2H), 4.21-4.02 (m, 3H), 3.68 (dd, *J* = 13.8, 9.1 Hz, 1H), 3.29 (dd, *J* = 13.7, 6.5 Hz, 1H), 1.17 (t, *J* = 7.1 Hz, 3H). ¹³C NMR (101 MHz, CDCl₃): δ ppm 173.2, 140.6, 140.2, 137.7, 136.5, 133.4, 132.1, 128.7, 128.3, 127.9, 127.5, 127.4, 127.3, 127.2, 126.9, 125.8, 125.3, 60.8, 53.2, 39.9, 14.0. HRMS: calcd. for C₂₇H₂₅O₂ (MH⁺): 381.18491, found 381.18488. Elem. anal. (%): calcd. for C₂₇H₂₄O₂: C, 85.23; H, 6.36; found C, 85.05; H, 6.35.



Ethyl 2-(4-bromophenyl)-3-(naphthalen-2-yl)propanoate (6.15):²⁶ ethyl 2-(4-bromophenyl)acetate (1 g, 4.1 mmol) were dissolved in 10 ml of dry DMF. Potassium hexamethyldisilazane (KHMDS) (9 ml of a 0.5 M solution, 4.5 mmol) was added slowly with stirring at room temperature, and the color of the solution changes from yellow to orange. After 20 min, 2-(bromomethyl)naphthalene (906.5 mg, 4.5 mmol) was added in one portion, and the color changed again to dark brown. Stirring was continued for 3 h. Subsequently, the reaction was quenched with sat. aq. NH₄Cl (4 ml), which was followed by a color change to light yellow. The product was extracted with ethylacetate (4 × 30 ml). The combined organic layers were dried over MgSO₄ and concentrated under vacuum. The volatiles were evaporated under reduced pressure. The residue was purified with flash column chromatography on silica gel using as eluent heptane with a 10-100% gradient of

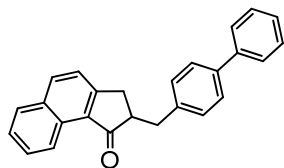
toluene ($R_f = 0.60$ in heptane/toluene 80:20), which gave product **6.15** as a white solid (1.19 g, 3.1 mmol, 75%). Further purification could be achieved by recrystallization from ethylacetate/heptane at -12°C .

m.p. = $89.9\text{--}90.4^\circ\text{C}$. ^1H NMR (400 MHz, CDCl_3) δ ppm 7.84–7.73 (m, 3H), 7.61 (s, 1H), 7.50–7.42 (m, 4H), 7.30–7.22 (m, 3H), 4.17–4.02 (m, 2H), 3.96 (dd, $J = 8.5, 7.0$ Hz, 1H), 3.59 (dd, $J = 13.7, 8.6$ Hz, 1H), 3.19 (dd, $J = 13.7, 6.9$ Hz, 1H), 1.13 (t, $J = 7.1$ Hz, 3H). ^{13}C NMR (101 MHz, CDCl_3): δ ppm 172.8, 137.5, 136.0, 133.3, 132.1, 131.6, 129.6, 127.9, 127.5, 127.4, 127.3, 127.2, 125.9, 125.4, 121.2, 60.9, 52.9, 39.7, 13.9. HRMS: calcd. for $\text{C}_{21}\text{H}_{19}\text{BrO}_2\text{Na}$: 405.0461 (MNa^+), found 405.0467. Elem. anal. (%): calcd. for $\text{C}_{21}\text{H}_{19}\text{BrO}_2$: C, 65.81; H, 5.00; found C, 65.70; H, 4.96.



2-(Biphenyl-4-yl)-3-(naphthalen-2-yl)propanoic acid (6.16): ester **6.14** (800 mg, 2.1 mmol) was dissolved in a mixture of THF/MeOH 1:1 (16 ml) and under stirring, 3.5 ml of a 3 M NaOH aq. solution (10.5 mmol) was added. The mixture was stirred at room temperature over night. The organic solvents were removed by rotary evaporation, and aq. HCl 10% was added till pH 1. The mixture was extracted with ethylacetate (3×12 ml); the organic layers were collected, dried with MgSO_4 and filtered. A quick filtration over silica gel with toluene/ethylacetate 1:1 as eluent ($R_f = 0.55$ in this solvent) and rotary evaporation of the solvents gave a white solid, which was then recrystallised from chloroform/heptane to give acid **6.16** as a white solid.

m.p. = $201.9\text{--}202.2^\circ\text{C}$. ^1H NMR (400 MHz, CDCl_3) δ ppm 7.79–7.74 (m, 1H), 7.73–7.67 (m, 2H), 7.58–7.50 (m, 5H), 7.45–7.31 (m, 7H), 7.28–7.23 (m, 1H), 4.02 (t, $J = 7.66$ Hz, 1H), 3.60 (dd, $J = 13.9, 8.3$ Hz, 1H), 3.23 (dd, $J = 13.9, 7.0$ Hz, 1H). ^{13}C NMR (101 MHz, CDCl_3): δ ppm 178.8, 140.5, 140.5, 136.9, 136.1, 133.4, 132.2, 128.7, 128.6, 128.5, 128.0, 127.6, 127.6, 127.5, 127.4, 127.3, 127.0, 125.9, 125.4, 52.9, 39.3. HRMS: calcd. for $\text{C}_{25}\text{H}_{20}\text{O}_2\text{Na}$: 375.13555 (MNa^+), found 375.13510.

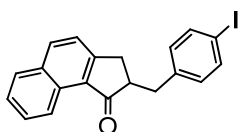


2-(Biphenyl-4-ylmethyl)-2,3-dihydro-1H-cyclopenta[a]naphthalen-1-one (6.18):³⁶ ketone **6.19** (124 mg, 0.31 mmol), phenylboronic acid (57 mg, 0.47 mmol) and potassium carbonate (0.78 ml of a 1 M aq. solution) were added to 1.5 ml of acetone. Palladium

acetate (catalytic amount) was added, and the mixture was degassed three times by freeze-pump-thaw technique. Next, the mixture was heated to reflux with stirring under a nitrogen atmosphere for 5 h. Subsequently, the volatiles were removed under reduced pressure, and the product was extracted with diethylether (3×10 ml). The combined organic layers were dried over anhydrous Na_2SO_4 , filtered and concentrated under vacuum. A filtration over silica gel using heptane/toluene 1:1 as eluent ($R_f = 0.30$ in this solvent mixture) gave product **6.18** as a white solid (99 mg, 0.28 mmol, 90%).

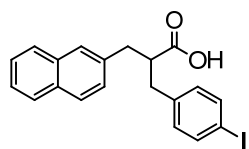
^1H NMR (400 MHz, CDCl_3) δ ppm 9.23 (d, $J = 8.3$ Hz, 1H), 8.03 (d, $J = 8.3$ Hz, 1H), 7.90 (d, $J = 8.1$ Hz, 1H), 7.71 (t, $J = 7.7$ Hz, 1H), 7.63-7.54 (m, 6H), 7.49-7.42 (m, 3H), 7.39-7.34 (m, 2H), 3.53 (dd, $J = 14.0, 4.2$ Hz, 1H), 3.29 (dd, $J = 17.5, 7.4$ Hz, 1H), 3.19-3.10 (m, 1H), 2.99 (dd, $J = 17.5, 3.4$ Hz, 1H), 2.78 (dd, $J = 14.0, 10.4$ Hz, 1H). ^{13}C NMR (101 MHz, CDCl_3): δ ppm 208.2, 156.9, 140.8, 139.1, 138.8, 135.8, 132.6, 130.4, 129.4, 129.3, 128.9, 128.7, 128.1, 127.1, 127.1, 126.9, 126.6, 123.9, 123.9, 49.2, 36.3, 32.6.

HRMS: calcd. for $\text{C}_{26}\text{H}_{20}\text{O}$: 348.15141, found 348.14978.



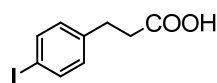
2-(4-Iodobenzyl)-2,3-dihydro-1H-cyclopenta[a]naphthalen-1-one (6.19): to a solution of acid **6.20** (7.63 g, 18.33 mmol) in 200 ml of dry DCM, SOCl_2 (10.5 ml, 140 mmol) was added while stirring, followed by DMF (6 drops), and the mixture was heated to reflux for 1 h. After evaporation of the volatiles by reduced pressure, the obtained acyl chloride (**6.24**) was dissolved in 200 ml of dry toluene. The solution was cooled at 0°C and AlCl_3 (4.93 g, 2 eq) was added rapidly with stirring, and the reaction mixture was kept at 0°C for 1 h. The reaction was quenched with a sat. aq. sol. of NaHCO_3 (100 ml), and the product extraction with ethylacetate (3×120 ml). The combined organic layers were dried over anhydrous MgSO_4 , filtered and concentrated under vacuum. The product was purified by recrystallisation from ethylacetate/heptane, giving a white powder (5.01 g, 12.6 mmol, 69%).

m.p. = 117.8 - 118.1°C . ^1H NMR (400 MHz, CDCl_3) δ 2.67-2.73 (m, 1H), 2.86-2.91 (m, 1H), 3.01-3.09 (m, 1H), 3.21-3.27 (m, 1H), 3.35-3.40 (m, 1H), 7.02-7.04 (d, $J = 8.1$ Hz, 2H), 7.43-7.45 (d, $J = 8.4$ Hz, 1H), 7.55-7.58 (t, $J = 7.7$ Hz, 1H), 7.60-7.62 (d, $J = 8.1$ Hz, 2H), 7.67-7.71 (t, $J = 7.3$ Hz, 1H), 7.88-7.90 (d, $J = 8.1$ Hz, 1H), 8.01-8.04 (d, $J = 8.4$ Hz, 1H), 9.15-9.17 (d, $J = 8.4$ Hz, 1H). ^{13}C NMR (101 MHz, CDCl_3) δ 32.4, 36.6, 48.9, 91.5, 123.8, 123.9, 126.6, 128.1, 128.9, 129.4, 130.3, 130.9, 132.7, 135.9, 137.5, 139.3, 156.7, 207.8. HRMS: calcd. for $\text{C}_{20}\text{H}_{15}\text{OI}$ 398.0168, found 398.0148.



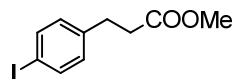
2-(4-Iodobenzyl)-3-(naphthalen-2-yl)propanoic acid (6.20): a mixture of ester **6.23** (10 g, 23.25 mmol), KOH (22 g, 392 mmol), ethanol (120 ml) and water (120 ml) was heated at reflux overnight with stirring. Subsequently, the mixture was acidified with aq. HCl (30 %) until pH = 3, and the product was extracted with ethylacetate (3 × 100 ml). The combined organic layers were washed with water, dried over anhydrous MgSO₄, filtered and concentrated under vacuum, to give product **6.20** as a white solid (8.13 g, 19.5 mmol, 84%).

¹H NMR (400 MHz, CDCl₃) δ 2.74-2.79 (m, 1H), 2.90-2.96 (m, 2H), 3.01-3.09 (m, 1H), 3.13-3.18 (m, 1H), 6.89-6.91 (d, *J* = 8.1 Hz, 2H), 7.27-7.29 (d, *J* = 8.4 Hz, 1H), 7.43-7.45 (m, 2H), 7.56-7.61 (m, 3H), 7.76-7.82 (m, 3H). ¹³C NMR (101 MHz, CDCl₃) δ 37.0, 37.9, 48.8, 91.9, 125.6, 126.1, 127.0, 127.5, 127.5, 127.6, 128.2, 130.9, 132.2, 133.4, 135.8, 137.5, 138.3, 180.2. HRMS: calcd. for C₂₀H₁₇IO₂ 416.0273, found 416.0275.



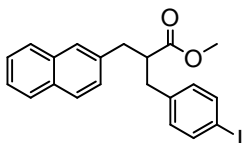
3-(4-Iodophenyl)propanoic acid (6.21): a solution composed of HNO₃ (1.8 ml), acetic acid (60 ml) and H₂O (12 ml) was added to a mixture of 3-phenylpropionic acid (9 g, 60 mmol), periodic acid (3 g, 12.9 mmol), and iodine (6 g, 24 mmol) with stirring. The resulting purple solution was heated at 65-70°C with stirring overnight. The reaction mixture was then diluted with water, the resulting precipitate was filtered and recrystallised in heptane to give product **6.21** as a white powder (9.60 g, 34.8 mmol, 58%).

¹H NMR (400 MHz, CDCl₃) δ 2.63-2.67 (t, *J* = 8 Hz, 2H), 2.87-2.91 (t, *J* = 8 Hz, 2H), 4.77 (br. s, 1H), 6.95-6.97 (d, *J* = 8 Hz, 2H), 7.60-7.62 (d, *J* = 8 Hz, 2H).



Methyl 3-(4-iodophenyl)propanoate (6.22): a solution of 34 g (123.16 mmol) of 3-(4-iodophenyl)propanoic acid (**6.21**) and 20 ml of conc. H₂SO₄ in 350 ml of MeOH was heated at reflux overnight with stirring. After cooling, the MeOH was partially evaporated under reduced pressure. The residue was dissolved in 200 ml of diethylether, washed with water till pH = 7, dried over MgSO₄, filtered, and the solvent removed under reduced pressure, to give the title ester as a white solid (30 g, 103 mmol, 84%).

¹H NMR (400 MHz, CDCl₃) δ 2.58-2.62 (t, *J* = 8 Hz, 2H), 2.87-2.91 (t, *J* = 8 Hz, 2H), 3.66 (s, 3H), 6.94-6.96 (d, *J* = 8 Hz, 2H), 7.59-7.61 (d, *J* = 8 Hz, 2H). ¹³C NMR (101 MHz, CDCl₃) δ 30.2, 35.1, 51.6, 91.3, 130.2, 137.3, 139.9, 172.8. HRMS: calcd. for C₁₀H₁₁O₂I: 289.9804, found 289.9792.



Methyl 2-(4-iodobenzyl)-3-(naphthalen-2-yl)propanoate (6.23): an LDA solution in dry THF (150 ml) was prepared at -50°C by adding n-BuLi (19 ml of a 1.6 M solution, 30.45 mmol) to diisopropylamine (4.28 ml, 30.45 mmol) with stirring. After 15 min at -50°C , methyl 3-(4-iodophenyl)propanoate (**6.22**) (5 g, 16.4 mmol) was added dropwise at -60°C and the resulting mixture was stirred for 1 h at approximately -60°C . Subsequently, 2-(bromomethyl)naphthalene (6.73 g, 30.45 mmol) dissolved in THF (40 ml) was added slowly and the reaction mixture was allowed to warm to room temperature overnight with stirring. The reaction was quenched with sat. aq. NH_4Cl (200 ml) and the product was extracted with diethylether (3×100 ml). The organic layers were combined, dried over anhydrous MgSO_4 , filtered and concentrated under vacuum. Further purification with flash column chromatography (SiO_2 , heptane/AcOEt 9:1) gave product **6.23** as a colorless oil (4.94 g, 11.5 mmol, 70%).

The compound was used directly for the next reaction.

¹ J. Vicario, M. Walko, A. Meetsma, B. L. Feringa, *J. Am. Chem. Soc.* **2006**, *128*; 5127-5135.

² M. K. J. ter Wiel, R. A. van Delden, A. Meetsma, B. L. Feringa; *J. Am. Chem. Soc.* **2005**, *127*, 14208-14222.

³ M. K. J. ter Wiel, R. A. van Delden, A. Meetsma, B. L. Feringa; *J. Am. Chem. Soc.* **2003**, *125*, 15076.

⁴ G. Caroli, M. G. Kwit, B. L. Feringa; *Tetrahedron*, **2008** Volume 64, Issue 25, 5956-5962.

⁵ M. K. J. ter Wiel, M. G. Kwit, A. Meetsma, B. L. Feringa; *Org. Biomol. Chem.*, **2007**, *5*, 87-96.

⁶ a) C. Ruslim, K. Ichimura, *J. Mat. Chem.* **2002**, *12*, 3377; b) S. Pieraccini, G. Gottarelli, R. Labruto, S. Masiero, O. Pandoli, G.P. Spada *Chem. Eur. J.* **2004**, *10*, 5632; c) N. Tamaoki, *Adv. Mater.* **2001**, *13*, 1135.

⁷ R. A. van Delden, N. Koumura, N. Harada, and B. L. Feringa, *PNAS* **2002**, *vol. 99, no. 8*, 4945-4949; R. Eelkema, M.M. Pollard, J. Vicario, N. Katsonis, B. Serrano Ramon, C.W.M. Bastiaansen, D. J. Broer, B.L. Feringa, *Nature*, **2006**, *440*, 163.

⁸ M. G. M. Jongejan, PhD thesis, University of Groningen, 2010.

⁹ The synthesis of ketone **6.5** was performed by J. Vicario, as described in ref. 1.

¹⁰ M. J. Frisch, G. W. Trucks, H. B. Schlegel, G. E. Scuseria, M. A. Robb, J. R. Cheeseman, J. A. Montgomery, T. Vreven, K. N. Kudin, J. C. Burant, J. M. Millam, S. S. Iyengar, J. Tomasi, V. Barone, B. Mennucci, M. Cossi, G. Scalmani, N. Rega, G. A. Petersson, H. Nakatsuji, M. Hada, M. Ehara, K. Toyota, R. Fukuda, J. Hasegawa, M. Ishida, T. Nakajima, Y. Honda, O. Kitao, H. Nakai, M. Klene, X. Li, J. E. Knox, H. P. Hratchian, J. B. Cross, V. Bakken, C. Adamo, J. Jaramillo, R. Gomperts, R. E. Stratmann, O. Yazyev, A. J. Austin, R. Cammi, C. Pomelli, J. W. Ochterski, P. Y. Ayala, K. Morokuma, G. A. Voth, P. Salvador, J. J. Dannenberg, V. G. Zakrzewski, S. Dapprich, A. D. Daniels, M. C. Strain, O. Farkas, D. K. Malick, A. D. Rabuck, K. Raghavachari, J. B. Foresman, J. V. Ortiz, Q. Cui, A. G. Baboul, S. Clifford, J. Cioslowski, B. B.

Stefanov, G. Liu, A. Liashenko, P. Piskorz, I. Komaromi, R. L. Martin, D. J. Fox, T. Keith, M. A. Al-Laham, C. Y. Peng, A. Nanayakkara, M. Challacombe, P. M. W. Gill, B. Johnson, W. Chen, M. W. Wong, C. Gonzalez, and J. A. Pople, Gaussian 03, Revision B.03. 340 Quinpiac St Bldg 40: Gaussian, Inc., 2004.

¹¹ M. M. Pollard, M. Klok, D. Pijper, B. L. Feringa, *Adv. Funct. Mater.* **2007**, *17*, 718-729.

¹² This is in agreement with that reported for the analogous second generation molecular motor in ref. 1, where, however, no assignment is proposed for protons H_q and H_r.

¹³ The Gaussian 03W software package was used (ref. 10). The ¹H-NMR calculation was performed with the GIAO method at the DFT B3-PW91/6-31G(2d,p) level, including the solvent effects (dichloromethane) using the IEFPCM model. For more details, see the computational details in the experimental session.

For the GIAO method see ref. 14.

For the IEFPCM model see ref. 15.

¹⁴ R. Ditchfield, *Mol. Phys.* **1974**, *27*, 789-807.

¹⁵ M. T. Cancès, B. Mennucci, and J. Tomasi, *J. Chem. Phys.* **1997**, *107*, 3032; B. Mennucci and J. Tomasi, *J. Chem. Phys.* **1997**, *106*, 5151; B. Mennucci, E. Cancès, and J. Tomasi, *J. Phys. Chem. B* **1997**, *101*, 10506; J. Tomasi, B. Mennucci, and E. Cancès, *J. Mol. Struct. (Theochem)* **1999**, *464*, 211.

¹⁶ No kinetic analysis was carried out to determine whether the phenyl groups in the unstable *trans* isomer are completely blocked or their rotation only slowed down. Herein, with "rotation-off" we refer to either of the two possibilities without distinction, for simplicity.

¹⁷ For further studies on similar systems, see A. Lubbe, bachelor thesis, University of Groningen, 2010.

¹⁸ The results would probably improve if scaled following the procedure proposed by Forsyth and Sebag (D. A. Forsyth, A. B. Sebag; *J. Am. Chem. Soc.* **1997**, *119*, 9483-9494).

¹⁹ The ³J_{H-H} constant has been calculated on line, on <http://www.stenutz.eu/conf/jhh.html>, where the the couplings constant are calculated according to C.A.G. Haasnoot, F.A.A.M. DeLeeuw and C. Altona; *Tetrahedron* **1980**, *36*, 2783-2792.

²⁰ M. M. -C. Lo, G. C. Fu, *Tetrahedron* **2001**, *57*, 2621-2634. All the analytical data were in agreement.

²¹ Prepared according the literature procedure reported in T. J. Katz, A. Sudhakar, M. F. Teasley, A. M. Gilbert, W. E. Geiger, M. P. Robben, M. Wuensch, M. D. Ward; *J. Am. Chem. Soc.* **1993**, *115*, 3182-3198

²² T. Mukhopadhyay, D. Seebach, *Helv. Chim. Acta*, **1982**, *Volume 65, Issue 1*, 385-391.

²³ C. M. Williams, L. N. Mander, *Tetrahedron*, **2001**, 425-447.

²⁴ HyperChem(TM) v. 7.5, Hypercube, Inc., 1115 NW 4th Street, Gainesville, Florida 32601, USA.

²⁵ J. Wang, A. Kulago, W. R. Browne, B. L. Feringa, *J. Am. Chem. Soc.* **2010**, *132*, 4191-4196.

²⁶ T. E. Nielsen, M. Meldal, *J. Org. Chem.* **2004**, *69*, 3765-3773.

²⁷ S. W. Wright, D. L. Hageman, L. D. McClure, *J. Org. Chem.* **1994**, *59*, 6095-6097.

²⁸ a) H. Suzuki, *Org. Synth., Coll. Vol. 6*, p. 700-703 (**1988**); *Vol. 51*, p. 94-97 (**1971**). b) J. T. Platti, W. H. Strain, S. L. Warren, *J. Am. Chem. Soc.*, **1943**, *65*, 1273-1274. c) N. Kawasaki, M. Goto, S. Kawabata, T. Kometani, *Tetrahedron Asymmetry*, **2001**, *12*, 585-596.

²⁹ The reactions up to compound **6.21** were performed by Dr. F. Dumur.

³⁰ M. M. Pollard, A. Meetsma, B. L. Feringa; *Org. Biomol. Chem.*, **2008**, *6*, 507-512.

³¹ a) C. Lee, W. Yang, R. G. Parr, *Phys. Rev. B* **1988**, *37*, 785-789. b) A. D. Becke, *J. Chem. Phys.* **1993**, *98*, 5648-5652. c) P. J. Stephens, F. J. Devlin, C. F. Chabalowski, M. J. Frisch, *J. Phys. Chem.* **1994**, *98*, 11623-11627.

³² J. P. Perdew, in *Electronic Structure of Solids '91*, Ed. P. Ziesche and H. Eschrig (Akademie Verlag, Berlin, 1991) 11.

³³ J. Gauss, *J. Chem. Phys.* **1993**, *99*, 3629-3643.

³⁴ W. Adcock, M. J. S. Dewar, R. Golden, M. A. Zeb, *J. Am. Chem. Soc.* **1975**, *97*, 2198-2205.

³⁵ J. Wisniewski Grissom, D. Klingberg, S. Meyenburg, B. L. Stallman *J. Org. Chem.*, **1994**, *59* (25), 7876-7888.

³⁶ F. E. Goodson, T. I. Wallow, and B. M. Novak, *Org. Synth., Coll. Vol. 10*, p.501-506 (**2004**); *Vol. 75*, p.61-66 (**1998**).